2020

Effects of Cellulose Nano-fiber as an Additive on Performance of Asphalt Binders and Mixes

Marco Paulo Pereira Castro
South Dakota State University

EFFECTS OF CELLULOSE NANO-FIBER AS AN ADDITIVE ON PERFORMANCE OF ASPHALT BINDERS AND MIXES

BY

MARCO PAULO PEREIRA CASTRO

A thesis submitted in partial fulfillment of the requirements for the

Master of Science

Major in Civil Engineering

South Dakota State University

2020

THESIS ACCEPTANCE PAGE

Marco Paulo Pereira Castro

This thesis is approved as a creditable and independent investigation by a candidate for the master's degree and is acceptable for meeting the thesis requirements for this degree. Acceptance of this does not imply that the conclusions reached by the candidate are necessarily the conclusions of the major department.

Rouzbeh Ghabchi
Advisor Date

Nadim Wehbe
Department Head Date

Dean, Graduate School Date

This thesis is dedicated to my beloved parents and sister.

ACKNOWLEDGEMENTS

I would like to start by thanking my mentor and advisor Dr. Rouzbeh Ghabchi for providing me the opportunity to be a part of this study. I would like to sincerely appreciate his guidance, support, and encouragement to complete this study. I would like to express my gratitude to Dr. Ghabchi for his valuable suggestions and comments helped improve my knowledge, research and writing skills. I am grateful to his mentorship and leadership that were instrumental to making this thesis work successful.

Besides my advisor, I would like to thank Dr. Anamika Prasad for all her support and providing me access to her lab during my study. Also, I am thankful to Mr. Buddhika Prasad Rajapaksha, Mr. Ruhit Sinha, and Mr. Mukesh Kumar Roy for helping me in the lab. I would like to acknowledge my professors, Dr. Suzette Burckhard and Dr. Michael Pawlovich for sharing their knowledge with me during the coursework. I am also thankful for all the staff at the Department of Civil and Environmental Engineering, Graduate College, International Affairs in South Dakota State University.

I would like to thank my family, Mrs. Maria Cristina Souza Pereira Castro, Mr. Celson de Castro, and Ms. Maria Júlia Pereira Castro, my mom, dad, and sister respectively, for the continuous support they have given me throughout my time in school; I could not have done it without them. They are the ultimate role model and I am very lucky to have them always by my side supporting me even from another country. Also, I would like to thank my dear girlfriend Ms. Maria Laura Velazco Fasce for all the love, comfort, and guidance she has given me during my years in college.

The work presented in this thesis was conducted with support from South Dakota State University, North Central Regional Sun Grant Center (NCRSGC) Seed Grant Program at South Dakota State University and the Mountain-Plains Consortium, a University Transportation Center funded by the U.S. Department of Transportation. The contents of this thesis reflect the views of the author, who is responsible for the facts and accuracy of the information presented.

TABLE OF CONTENTS

ABBREVIATIONS

AASHTO	American Association of State Highways and Transportation Officials
ABTS	Average Bond Tensile Strength
ASTM	American Society for Testing and Materials
AKA	Also Known As
BBS	Binder Bond Strength
CA	Cellulose Acetate
CNF	Cellulose Nanofiber
COV	Coefficient of Variation
CR	Crumb Rubber
DOT	Department of Transportation
DM	Dynamic Modulus
DMAc	Dimethylacetamide
EVA	Ethylene Vinyl Acetate
FHWA	Federal Highway Administration
GPC	Gel Permeation Chromatography
HMA	Hot Mix Asphalt
HWT	Hamburg Wheel Tracking
IA	Iowa
J_c	Critical Strain Energy Release Rate
LTPP	Long Term Pavement Performance
LSM	Laser Scan Microscopy
MO	Missouri
N	Newton
N/A	Not Applicable

NAPA	National Asphalt Pavement Association
NMAS	Nominal Maximum Aggregate Size
PATTI	Pneumatic Adhesion Tensile Testing Instrument
PG	Performance Grade
POTS	Pull-off Tensile Strength
PPA	Polyphosphoric Acid
RAP	Reclaimed Asphalt Pavement
RV	Rotational Viscometer
SCB	Semi Circular Bend
SD	South Dakota
SD	Standard Deviation
SDSU	South Dakota State University
SEBS	Styrene Ethylene Butylene Styrene
SEM	Scanning Electron Microscopy
SFE	Surface Free Energy
SIP	Stripping Inflection Point
TSR	Tensile Strength Ratio

LIST OF FIGURES

LIST OF TABLES

ABSTRACT

EFFECTS OF CELLULOSE NANO-FIBER AS AN ADDITIVE ON THE PERFORMANCE OF ASPHALT BINDERS AND MIXES

MARCO PAULO PEREIRA CASTRO

2020

Findings of a study conducted on asphalt binders and mixes modified by addition of cellulose nanofiber (CNF) to evaluate the feasibility of them as an additive is presented in the current thesis. Cellulose Acetate (CA) is an ester of cellulose and is obtained by the reaction of cellulose with acetic anhydride and acetic acid in the presence of sulfuric acid. Due to its high temperature sensitivity, high ductility, large surface area, high strain resistance, and low electrical resistivity, cellulose acetate can be used for several application. The question is if CNF can be used as an additive in the asphalt, with the goal of improving the pavement properties. Asphalt binder and asphalt mix properties, including adhesion, resistance to cracking by measurement of energy absorption, viscosity, moisture induced damage, fatigue resistance, and rutting were evaluated by conducting rotation viscometer (RV) test, Izod impact strength test, binder bond strength (BBS) test, tensile strength ratio (TSR) test, semi-circular bend (SCB) test, and Hamburg wheel tracking (HWT) test.

Cellulose nanofiber (CNF) production and evaluation, asphalt binders containing cellulose nanofiber evaluation, and asphalt mixes containing cellulose nanofiber evalujation are the three major parts of the study. For the CNF production and evaluation, two different electrospinning techniques as well as five different solutions were evaluated to find out which technique and solution produced the nanofiber suitable for the study.

CNF fibers were produced with two different electrospinning techniques, namely static and rotating electrospinning. Produced fibers' morphology, microstructure and strength properties were evaluated by conducting laser scan microscopy (LSM), scanning electron microscopy (SEM), and tensile strength test. After fiber production and evaluation, the CNF produced with the suitable technique was selected and was mixed with asphalt binder and asphalt mix for further evaluation. Three different asphalt binders, namely PG 58-28, PG 64-34, and PG 70-28 were used for the asphalt binder evaluation. For the asphalt mix evaluation, a hot mix asphalt (HMA) containing 20% reclaimed asphalt pavement (RAP) was used.

From the fiber production and evaluation, it was found that fibers produced using static electrospinning from a solution containing CA plus the solvent system acetone/water (Solution 5) and tested at a non-production direction had the highest average tensile strength. It was found that the average tensile strength for Solution 5 was 9.05 N, the highest among other alternatives. In addition to the average tensile strength of the produced fiber, the roughness and the average dimeter were evaluated using LSM and SEM techniques, respectively. It was found from these tests that the selected CNF had the roughest texture and the highest average diameter (1.756 μm). Overall, electrospun CNF produced using the abovementioned solution and technique was the roughest, the thickest and the strongest among all the tested fibers. Based on that it was the selected CNF to be used as an asphalt additive to improve the mechanical properties of asphalt binders and asphalt mixes.

For the asphalt binder evaluation, blends of three different binders, namely PG 58-28, PG 64-34, and PG 70-28 were mixed with different concentrations of CNF (0%, 0.2%, 0.3%, 0.5% and 0.7% by the weight of binder). For RV and BBS tests, binder blends containing 0%, 0.3%, and 0.7% CNF were used. For Izod impact strength binder blends containing 0%, 0.2%, 0.3%, 0.5% and 0.7% CNF by the weight of binder were used. It was found that the addition of CNF to asphalt binders resulted in an increase in viscosity of the asphalt binders, the higher the concentration of added CNF the higher the viscosity of the binder. A similar trend of variation in fracture toughness values with the increase in CNF concentration was also observed from Izod impact strength test. Furthermore, the BBS test results showed that for the majority of the cases addition of 0.7% CNF resulted in a higher BBS ratio compared to other combinations. It was found that for all the tested aggregates, granite, quartzite, and gravel, in contact with a PG 58-28 had the highest BBS ratio. For quartzite and gravel the addition of 0.3% CNF resulted in a reduction or no chance in BBS ratio values compared to binders without any CNF. However, for granite the addition of 0.3% and 0.7% CNF resulted in almost the same increase in BBS ratio value compared to the neat binder. The highest BBS ratio found was for PG 70-28 +0.7 CNF when tested in gravel.

For the asphalt mix evaluation, three different concentration of fibers on the RAP 20 Mix were evaluated (RAP 20 containing 0%, 0.3%, and 0.7% cellulose acetate nanofibers). For SCB test, used to evaluate the cracking resistance through determining the critical strain energy release rate (J_c), the addition of fibers improved the J_c value. It was found that the higher amount of added fibers resulted in the higher J_c value. Since the SCB test relates the J_c value with the fatigue cracking resistance, RAP20+0.7% CNF had the

highest fatigue cracking resistance. For the TSR test, it was found that the addition of fibers decreases the TSR ratio. The TSR test evaluates the resistance to moisture-induced damage of the mix. Based only on the TSR ratio, the addition of CNF causes the mix to be more susceptible to moisture induced damage. However, it was found that even though the TRS ratio decreases the addition of 0.3% and 0.7% CNF improved the dry conditioned tensile strength and the addition of 0.7% CNF improved the moisture conditioned tensile strength. So, based on the abovementioned fact it can say that the addition of fibers improves the resistance to moisture induced damage. For the HWT test, used to evaluate the moisture induced damage through determining the rutting and the stripping point, the addition of 0.7% CNF improved the rutting and increased the stripping point value. However, the addition of 0.3% CNF caused the asphalt mix to perform worse than the control asphalt mix.

It was found that the results of HWT test, TSR test, and BBS test supports the idea that the addition of fibers improve the moisture induced damage of the asphalt. However, an optimum quantity of fibers needs to be added to the asphalt for it to start performing better. It was proved that 0.3% CNF was not enough for the asphalt to perform better, it caused the opposite, the asphalt performs worse. From the results of Izod impact strength test and SCB it was clear that the addition of any quantity of fiber improved the resistance to fatigue cracking. For the RV test it was proved that the addition of CNF will requires more compaction efforts while paving. Overall, the study promoted valuable information that will help the development of cellulose acetate nanofibers as additives in asphalt binder and asphalt mix. However, future research is necessary to further understand and master

the production of nanofibers and to allow a better selection of CNF to be added onto the asphalt.

CHAPTER ONE: INTRODUCTION

1.1 Background

In the United States around 2.4 million miles are paved with Hot Mix Asphalt (HMA). Hot Mix Asphalt is a viscoelastic material consisting of mineral aggregates and asphalt binder, it is commonly used for high traffic pavement, such as highways, racetracks and airfields. Asphalt binder is a viscoelastic and thermoplastic material obtained from the distillation of naturally occurring crude oil responsible for the binding and viscoelastic behavior of the mix (Anderson et al., 1994, Rashid et al., 2009). Many aspects of pavement performance such as resistance to permanent deformation (rutting), thermal cracking, fatigue life, stripping, and thermal susceptibility are known to be influenced significantly by the mechanical properties of the asphalt binder. Asphalt binders that were modified with polymers, chains of repeated small molecules, showed to improve the performance of the pavement (Yildirim, 2007).

Asphalt pavement in general faces serious distresses due to traffic and environmental conditions along its work life. Repeated vehicular loading is recurring on the pavement, causing accumulation and growth of micro and macro cracks. These, cracks, are called fatigue cracks, which is the primary form of structural damage in asphalt roads in the United States. Asphalt pavements have the ability to withstand repeated bending without fracturing (Moghadas Nejad et al., 2010, Nozouri and Richard Kim, 2017). However, with the increase in traffic loading the fatigue manifests in form of cracks, transforming the pavement in nonworkable pavement. The quest to improve the pavement performance has led to the evaluation, development and use of a wide range of asphalt binder and mix modifiers. Polymer modified asphalt binder is one alternative to improve the pavement

properties. However, the development and use of polymer modified asphalt binder is challenging due to its high cost when comparing to the unmodified asphalt binder. Also, the poor asphalt polymer compatibility (which influences the stability of the system), and the higher viscosities during asphalt processing and application make it difficult to use polymer modified asphalt binder (Becker et al., 2001).

During the last two decades, with the introduction of new asphalt technologies, new materials and methods are being developed as alternative sources to replace and reduce the petroleum-based asphalt used in Hot Mix Asphalt. New materials and methods are necessary to overcome the scarcity of natural resources, increase in the oil price, emerging environmental concerns, and necessity for sustainable materials that are renewable and environmentally friendly. Among those new alternatives, asphalt mixes containing reclaimed asphalt pavement (RAP) and the use of renewable material, such as Cellulose Acetate Nano-fibers to modify the asphalt mix and binder are being studied. These available alternatives are economically efficient and environmentally sustainable. The use of RAP may result in an increase in resistance of asphalt mix to rutting and improvement in fatigue life (Huang et al. 2004, Ghabchi et al., 2015). Also, the use of RAP in 2010 conserved approximately 20.5 million barrels of asphalt binder (NAPA 2011

Cellulose Acetate is an important ester of cellulose. It is obtained by the reaction of cellulose with acetic anhydride and acetic acid in the presence of sulfuric acid. It can be used for a variety of application, including fibers production. The cellulose acetate is soluble in acetone and acetic acid (Fischer et al., 2008). The use of CNF as a replacement of the polymers will result in a cost-effective and sustainable asphalt mixes. Due to its mechanical strength and biocompatibility, nanocrystalline cellulose has been used as

reinforcement polymer matrices for some applications. The goal is that asphalt binder containing CNF will be capable to change rheological properties of the asphalt binder which will improve the performance against pavement distresses (El-latief, 2018). However, due to the absence of a widely accepted standards for addition of CNF in asphalt binder and mixes and lack of laboratory results, Cellulose Acetate Nanofibers as additive is not explored in pavement industry.

The electrospinning of Cellulose Acetate Nanofibers has attracted a great deal of attention due to their good thermal stability, chemical resistance, and biodegradability. Electrospinning technique was used to produce the fibers used to modify the asphalt binder and mix. Electrospinning is a technique that utilizes electrical forces to produce polymer fibers with diameters ranging from 2nm to several micrometers using polymer solutions. It is a unique approach that uses electrostatic forces and a high voltage to produce fibers from polymer solutions (Bhardwaj and Kundu, 2010). Overall, is a robust and simple technique to produce nanofibers from a wide variety of polymers (Li and Xia, 2004). Fibers produced using the electrospinning technique has several advantages such as, an extremely high surface-to-volume ratio, tunable porosity, malleability to conform to a wide variety of sizes and shapes and the ability to control the nanofiber composition to achieve the desired results (Bhardwaj and Kundu, 2010). The basic setup of the electrospinning consists in a high voltage power supply, a spinneret (metallic needle) and a collector (grounded conductor) (Li and Xia, 2004).

Nano-reinforced materials hold the potential to redefine the pavement industry in terms of performance and sustainability. In many cases, asphalt binder properties need to be changed to enhance the asphalt grade allowing improvements on the performance of the

Hot Mix Asphalt (El-latief, 2018). Polymers are added to asphalt binder to allow those improvements. However, Polymers are non-renewable source and have a high cost, they are considered as unsustainable materials. The replacement of the conventional polymers for cellulose nanofiber will result in cost-effective and sustainable asphalt mixes. The addition of CNF into the asphalt is not being used due to the lack of standard production methods and lack of prove that the performance of the asphalt improves with the addition of fibers instead of the conventional polymer. The goal of the study is to show performance results and evaluate the feasibility of using the electrospun CNF as additives.

To promote the use of sustainable bio-materials and agricultural byproducts as the main feedstock for production of bio-asphalt binder, electrospun cellulose nanofiber were used as a substitute of the conventional polymers to improve the performance of asphalt mix. Cellulose Nanofibers has been shown to improve the binding capacity of asphalt mixes and after their dynamic properties (McDaniel, 2015). To evaluate the produced CNF a series of laboratory testing needs to be conducted to determine the fibers structure and the effects on the asphalt binder and mix. Laser Scan Microscopy and Scanning Electron Microscopy will be used to characterize the fibers size and morphological features. In order to characterize the resistance of asphalt mixes to fatigue cracking and rutting, Semi Circular Bend test will be conducted on the asphalt mix containing cellulose nanofiber using an asphalt standard tester according to AASHTO TP 105-13. Hamburg Wheel Tracking and Tensile Strength Ratio test will also be conducted on the samples to evaluate their resistance to rutting and moisture damage according to AASHTO T324-17 and AASHTO T283, standard methods, respectively. For the asphalt binder characterization Izod impact strength test will be conducted according to D256 – Test Method A to determine the impact

resistance of the asphalt binder containing cellulose nanofiber. Binder Bonding Strength test will be conducted to evaluate the adhesion between the asphalt binder containing cellulose nanofiber and different aggregates, in accordance with AASHTO TP-XX-11. Finally, the optimum plant mixing and compaction temperatures for asphalt binders will be determine by the Rotational Viscometer test, according to AASHTO T316-13 test method. These laboratory tests will provide important information regarding the limitations and advantages of designing mixes using CNF as additives.

1.2 Research Objectives

Specific objectives of this study are as follows:

1. Production of Cellulose Acetate Nano-fibers using static and rotating electrospinning fiber production technique;
2. Characterization of the Cellulose Nanofiber, which includes the identification of the optimum solvent, roughness, average diameter of the fiber, and tensile strength. Also, selection of the solution that will be used as additive in asphalt binder and asphalt mixes.
3. Evaluation of neat asphalt binders and CNF modified asphalt binder Identify the optimum concentration of the added CNF and evaluate the performance of the asphalt binder when CNF are added.
4. Evaluation of asphalt mix, which includes the feasibility of utilization of CNF as additives for pavement construction.

1.3 Significance of Study

The present study was pursued to generate useful test results of Cellulose Nanofibers used as additives in asphalt binder and asphalt mixes. The test results are expected to help the development of plant-based bio-asphalt binder to replace the petroleum-based binder to maximize the sustainability of ground transportation system and be more cost-effective. Cellulose has been shown to improve the binding capacity of asphalt mixes affecting their dynamic properties. The rutting performance, ability to resist fatigue cracking, and resistance to moisture damage are expected to be improved by using CNF as an additive. Also, the impact resistance of asphalt binder, adhesion to aggregates, and mixing temperature properties of the binder are expected to improve with the use of the CNF in the asphalt binder. The present study is an attempt to add information and reliable results on the usage of Cellulose Nanofibers as additives in asphalt binder to improve the performance of the pavement. In addition, the outcomes of this study are expected to help the pavement engineers gain an understanding on the effect of using Cellulose Nanofibers as additives on the performance of asphalt mixes commonly used in South Dakota. Resulting, in a reduced need for petroleum-based binder, leading to numerous environmental benefits.

1.4 Study Tasks

Specific tasks to be carried in the study are as follows:

1. Prepare five different solutions, mixing cellulose acetate powder with a solvent for future production of Cellulose Nanofibers;
2. Produce Cellulose Nanofibers from the previous prepared solutions using the static and rotating electrospinning technique;

3. Evaluate the roughness, entanglement, and the average diameter of the produced CNF using the Laser Scan Microscopy and the Scanning Electron Microscopy;
4. Evaluate the average tensile strength of the different produced CNF to select the optimum solution and electrospinning technique for the continuity of the study;
5. Collect three types of asphalt binders, namely PG 58-28, PG 64-34, and PG 70-28, and produce a modified binder by mixing the produced Cellulose Nanofibers on the collected asphalt binder;
6. Conduct Izod impact strength test in accordance with ASTM D256 – Test Method A using a pendulum machine on the neat asphalt binder and on the modified asphalt binder;
7. Conduct Rotational Viscometer test in accordance with AASHTOO T316 using a Brookfield Rotational Viscometer on the unmodified binder and on the CNF modified asphalt binder;
8. Conduct Binder Bond Strength tests in accordance with AASHTO TP-XX-11 using a pneumatic adhesion tensile testing instrument (PATTI) on unconditioned and moisture-conditioned asphalt binder-aggregate samples;
9. Collect an HMA mix containing PG 58-28 asphalt binder, mainly quartzite and granite-II aggregates, and 20% RAP with a nominal maximum aggregate size (NMAS) of 12.5 mm;
10. Produce a CNF modified asphalt mix with the collected asphalt for future laboratory testing;

11. Compact CNF asphalt mix and prepare the test specimen for TSR tests in accordance with AASHTO T 283 on unconditioned and moisture-conditioned specimens;
12. Compact CNF asphalt mix and prepare test specimens for SCB tests in accordance with AASHTO T283 on unconditioned and moisture-conditioned specimens;
13. Compact CNF asphalt mix and prepare test specimens for HWT tests in accordance with AASHTO T324;
14. Analyze the results from all the tests done on the neat and CNF modified asphalt binder and neat and CNF modified asphalt mix.
15. Evaluate the effect of the asphalt binder type, aggregate type, and percentage of fibers on adhesion of the asphalt binder with aggregates in moisture-conditioned and unconditioned states;
16. Evaluate the effectiveness of the addition of Cellulose Nanofibers on the asphalt mix from the results obtained from the TSR, SCB, and HWT tests. Evaluate the asphalt performance when no CNF are added and when CNF are added.

1.5 Thesis Organization

The presentation of the materials in this thesis is organized in the following order:

Chapter 1: Introduction – This chapter includes a background on the Cellulose Nanofibers, electrospinning technique, and conventional test methods available for characterizing

asphalt binders and asphalt mixes. The background is followed by the research objectives, significance of the study, study tasks and thesis organization.

Chapter 2: Literature Review – The first part of this chapter presents a summary of the literature review conducted with a focus on the rheological, mechanical and performance properties of RAP asphalt mixes and polymer-modified binders and non-polymer modified binders. This chapter also summarizes previous studies related to the conventional asphalt binder and asphalt mix characterization methods and their limitations. A review of literature focusing on the development, advantages, production, and implementation on asphalt binder and asphalt mix of the Cellulose Nanofibers is presented in the last part.

Chapter 3: Materials and Methods – This chapter describes the selection, collection and preparation of Cellulose Nanofibers, asphalt binder, and asphalt mix. Also, the laboratory testing used to evaluate the produced CNF, the neat and CNF modified asphalt binders and asphalt mixes. Descriptions laboratory test methods such as Tensile Strength Ratio (TSR), Semi Circular Bending (SCB), Hamburg Wheel Tracking (HWT), Izod impact strength test, Rotational Viscometer (RV), and Binder Bond Strength (BBS).

Chapter 4: Test Results of Produced Nano-Fibers: Evaluation and analyze of the roughness, entanglement, average diameter and tensile strength of the different produced CNF. Also, comparison between all electrospun CNF and selection of the optimum solution for production of CNF for the continuity of the study.

Chapter 5: Test Results of Asphalt Binders: Analyses of the Izod impact strength test, Rotational Viscometer test, and BBS test conducted on the different types of neat asphalt

binders and CNF modified binders. Also, comparison between the results obtained, the feasibility of the addition of the CNF on the asphalt binder and the evaluation on the performance of the asphalt binder when Cellulose Nanofibers are added.

Chapter 6: Test Results of Asphalt Mixes: Analyze of the HWT test, SCB test, and TSR test conducted on the asphalt mix with Cellulose Nanofibers and on asphalt mix without any CNF. Also, a comparison between the neat asphalt mix with the CNF modified asphalt mix. Evaluation of the performance of the asphalt mix when CNF are added.

Chapter 7: Conclusions and Recommendations– Important findings of this study and the recommendations based on these findings are presented in this chapter. The recommendations for future studies are also included in this chapter.

CHAPTER TWO: LITERUATURE REVIEW

2.1. Background

Cellulose Nanofibers are being studied to determine if it can be used as additives, to improve the performance of asphalt pavements. World-wide asphalt pavements are facing distress problems due to the rapidly increase in traffic loads (Nejad, et al 2010, Li et al. 2017). Industries are progressing rapidly and seeking the production of higher quality materials for construction, rehabilitation and maintenance operations (Toraldo and Mariani, 2014). In the United States around 96% of the roads, are paved with Hot Mix Aphalt (HMA). HMA is a viscoelastic material consisting of aggregates particles (coarse and fines) that are bonded together by asphalt binder, it is commonly used for high traffic pavement, such as highways, racetracks and airfields. (Wen et al.,2013). Its asphalt binder component is a viscoelastic thermoplastic material due to its time dependent response. It is composed of heavy hydrocarbons and soluble in carbon disulfide and it is obtained from the distillation of naturally occurring crude oil responsible for the binding and viscoelastic behavior of the mix (Aziz et at. 2016, Khattak et al, 2011, Anderson et al., 1994, Rashid et al., 2009). Because of the rising challenges faced by the asphalt pavement as well as the increasing price of petroleum and quest for sustainable materials the Cellulose Nanofibers are being study as a possible additive in the asphalt.

Asphalt pavement in general faces serious distresses along its work life. The ever-increasing traffic volume causes repeated loading on the pavement. The higher traffic load and cyclic loading causes shortness of life on the pavement. Asphalt pavements are designed to behave and withstand repeated bending without fail. Due to the constant increase of load the asphalt tends to fail. Fatigue cracks are an example of how the increase

in load can cause the pavement to fail. Resistance to fatigue cracking is only one example of the necessity of higher quality, safer, more reliable and more environmentally friendly asphalt pavement (Moghadas Nejad et al., 2010, Nozouri and Richard Kim, 2017, and Li at al., 2017).

The world is now taking actions to set up an is bio-based economy where renewable organic matter is the source of energy rather than natural fossil. Bio-based source of energy is renewable, efficient, cost effective, and environment friendly. Because of the limitation of petroleum, increase price and impact on the environment the pavement industry is following the same path. Therefore, to save the world from depletion of natural petroleum source, to save the environment from the pollution by bitumen and bitumen fume, to save the living being from the exposure of bitumen and develop a bio-based renewable economy for sustainable living introduction of an alternative source or additive for flexible pavement is necessary.

During the last decades, with the introduction of new asphalt technologies, new materials and methods the pavement industry came up with different ways to improve the performance of the pavement as well as contribute for sustainability. The studies focus in a few new materials and alternatives that the industry came up with, recycling asphalt pavement (RAP), polymer-modifed asphalt binder, and Cellulose Nanofibers (CNF) as asphalt binder additive. With the crude oil short supply for long term running, and the effort to reduce petroleum asphalt usage in an environmentally friendly manner, RAP is being used to reduce the usage of fresh asphalt (Yang et al., 2013). With the intention of improving the viscoelastic characteristics of the pavement without huge impact on the environment certain dosage of certain polymers are being used by the asphalt industry.

Cellulose Nanofibers, the main focus of the study, has attracted a great deal of attention due to its characteristics and potential to improve mechanical properties of asphalt binder and asphalt mixes.

2.2. Recycling Asphalt Pavement (RAP)

The use of recycling asphalt pavement has become an important part of the pavement construction practice in recent years due to environmental concerns, scarcity of high-quality aggregates and increased cost of virgin asphalt binder. With the growth of usage of RAP in asphalt pavement, it is estimated that over $2 billion was saved in fresh asphalt binder (Hansen and Copeland, 2013). A number of studies have been conducted to evaluate performance of asphalt binders with the addition of different amounts of RAP binder (Kim et al., 2009 and Colbert and You, 2012 and Reyes-Ortiz et al., 2012).

Kim et al. (2009) investigated the rutting and fatigue performances of RAP binder. The rutting and fatigue parameters were found to increase with an increase in the amount of RAP binder. The indirect tensile strength of asphalt mixes containing RAP was also found to increase with an increase in RAP content. All mixes containing RAP showed relatively low creep compliance values. It was also reported that a mix containing RAP may lead to a better resistance to fatigue cracking. Colbert and You (2012) studied the performance of the RAP binder blends using Superpave® binder characterization tests. Effects of short-term and long-term aging on the binders' viscosity and stiffness were evaluated. It was found from the Rotational Viscosity (RV) test results that the workability and pumping potential of the RAP binder blends reduced as the amount of RAP binder increased.

The rutting susceptibility of asphalt binders and asphalt mixes containing different polymer modifiers and RAP binder from different sources was evaluated by Bernier et al. (2012). West et al. (2009) evaluated the performance of asphalt mixes containing moderate (i.e., 20%) amounts of RAP. The test sections constructed using asphalt mixes containing RAP were found to perform well for rutting under heavy loading conditions. It was also concluded from the indirect tensile strength test results that the use of RAP improved the tensile strength of asphalt mixes.

Another study conducted by Hong et al. (2010) evaluated the long-term performance of HMA containing percentages of RAP. For this purpose, FHWA's Long-Term Pavement Performance (LTPP) test sections in Texas were investigated for transverse cracking, rut depth and ride quality over sixteen years. The asphalt mixes with 35% RAP were found to be more rut resistant than the asphalt mixes with virgin binders.

Ghabchi et al. (2014) evaluated the effect of addition of different amounts of RAP binder to virgin binders on the moisture-induced damage potential of the asphalt mixes using the Surface Free Energy (SFE) approach. Evaluating the energy parameters of the asphalt aggregate system, it was observed that the moisture-induced damage potential of the binder reduced with an increase in the RAP binder content. In a recent study, Ghabchi et al. (2016) evaluated the effects of RAP on the fatigue cracking, low-temperature cracking and stiffness of HMA mixes. The fatigue cracking was found to be a major concern among all the state DOTs while using RAP. The resistance to fatigue cracking, low-temperature cracking and stiffness of the asphalt mixes containing different amounts of RAP (0 to 30%) were evaluated in the laboratory using Four-point Bending Beam Fatigue, DM test, Creep Compliance, and Indirect Tensile Strength tests. The increase in

the fatigue life was observed. However, the increase was not as noticeable for the different amounts of RAP. On the other hand, the dynamic moduli of the asphalt mixes were observed to increase with the addition of RAP indicating a better rutting performance of mixes.

Ozer et al. (2016), and Singh et al. (2017) conducted SCB tests on asphalt mixes and found an increase in fracture resistance and a decrease in moisture-induced damage potential of asphalt mixes after addition of RAP. In another study, Ghabchi et al. (2016) evaluated the moisture- induced damage potential of the asphalt mixes containing RAP by HWT tests. From HWT test result it was found that moisture- induced damage decreased with an increase in the RAP content. In a study conducted by Cong et al. (2016), it was found that the both moisture-induced damage potential and rutting resistance of the asphalt mixes increased as a result of addition of RAP to mixes. Fakhri et al. (2017) after conducting wheel tracking test on the asphalt mixes found that moisture-induced damage potential decreases with addition of RAP in both aged and unaged asphalt mixes. In view of the benefits associated with incorporating RAP in asphalt mixes, the paving industry is in favor of using RAP in asphalt pavement construction. (Daniel et al., 2010 and Ghabchi et al., 2016 and Reyes-Ortiz et al., 2012).

2.3. Polymer Modified Asphalt Binder

The asphalt industry has used asphalt binder modification with polymers as an effective tool for producing mixes with better performance and improved service life. The recent circumstances, increasing traffic and axle load has led to the search for new types of asphalt

binders with better performance (Yildirim, 2007, Toraldo and Mariani, 2014 and Xiao et al., 2014).

Several studies have been conducted to characterize the viscoelastic properties and to evaluate performance of polymer-modified asphalt binders (Collins et al., 1991; Sargand and Kim, 2001; Chen et al., 2002). Plastics, elastomers, fibers and additives are the four major groups of polymers used for the modification of asphalt binders. Several studies have been conducted to determine the effect of modifiers on the rheological properties of asphalt binders and asphalt mixes (Read and Whiteoak, 2003; Airey, 2004). It has been observed that addition of polymers to asphalt binders helps mitigate major pavement distresses such as rutting at high temperature, low-temperature cracking, and fatigue cracking (Yildirim, 2007).

The effects of aging and polymer content on the performance of the binders were investigated by Elseifi et al. (2003). The rheological and physical changes associated with the modification of two elastomeric polymers, namely SBS linear block copolymers and Styrene Ethylene Butylene Styrene (SEBS) linear block copolymers, were analyzed. A significant improvement in the fatigue resistance was observed for SBS- modified binders at intermediate service temperatures. The low-temperature performance grade was found to remain unchanged after binder modification.

Kumar et al. (2010) studied the effect of addition of Crumb Rubber (CR), Ethylene Vinyl Acetate (EVA) and SBS modifiers to neat binder. It was observed that the temperature susceptibility of the binder decreased as the modifier content increased. SBS-modified binder was found to exhibit a lower viscosity temperature susceptibility than

EVA- and CR-modified binders. The EVA-modified binder was observed to show a higher rutting resistance value than SBS- and CR-modified binders, while adding each of the modifiers in the same amount. In addition, the SBS-modified binder exhibited maximum elastic recovery than the CR- and EVA-modified binders. The results of the Tensile Strength Ratio (TSR) of asphalt mixes exhibited that the asphalt mix containing EVA was more resistant to moisture-induced damage than any other modified binders. From wheel-tracking test results, the EVA- and SBS-modified asphalt mixes were found to exhibit a better resistance to rutting than mixes containing neat binder.

The high-temperature rheological properties of SBS-, oxidized polyethylene-, propylene-maleic anhydride-, and recycled crumb rubber-modified binders with and without PPA were investigated by Xiao et al. (2014). It was observed that the rubber-modified binder containing PPA showed greater viscosity than the binders modified using other compounds. The polymer-modified binders produced with oxidized polyethylene and propylene-maleic anhydride was found to exhibit the potential of reducing the energy demand during mixing and compaction of the mixes. Moreover, the results of viscosity, amplitude sweep, frequency sweep, creep and creep recovery, and relaxation spectrums of polymer-modified binders were found to get affected by polymer types, asphalt sources, and test temperatures.

Toraldo and Mariani (2014) studied the effects of polymers as additives for bituminous mixtures. Polymers were evaluated on the performance on the mixture at in service temperature by means of simulative tests concerning stiffness master curve, fatigue life, and rut resistance. In particular, mixtures containing polymers show a decrease in the dynamic modulus at high frequencies, implying low temperature in the field, according to

the time-temperature superposition principle. Results from fatigue tests indicate that polymer influence the mixture behavior as demonstrated by the increase in fatigue resistance (represented by the number of load cycles to failure) with higher polymer dosages. As far as rutting resistance is concerned, results showed that polymers greatly improve the mixtures performance, dependent, obviously, on the type and dosage.

In view of the benefits associated with incorporating polymer modified asphalt binder in asphalt mixes, the paving industry is in favor of using such materials in asphalt pavement construction. However, these materials are unstable, modified bitumen require refineries with high quality equipment for their manufacture (Toraldo and Mariani, 2014). Hence, the cost is high, and its production could have a great impact on the environment. Based on that new alternatives, like modification of asphalt binder with cellulose acetate Nano-fibers, are being developed by the pavement industry.

2.4. Cellulose Nanofibers

Among the new materials alternatives are the use of Cellulose Nanofibers to modify the asphalt mix and binder. This available alternative is economically efficient and environmentally sustainable. Nano-reinforced materials host the potential to redefine the field of traditional materials both in terms of performance and potential applications (Hussain et al., 2006 and Khattak et al., 2011). Nano materials are described as a material with at least on dimension within 1-100nm (Li et al. 2017). These types of materials exhibit high temperature sensitivity, high ductility, large surface area, high strain resistance, and low electrical resistivity (Li et al.,2017).

The goal behind the usage of CNF in asphalt binder and mix is that the CNF network may bridge across micro-cracks developed due to loading and environmental effects causing hindrance in their growth and consequently increasing the strength and fracture properties of the mixture. Ghile (2006) showed that Nanoclay modification improved some characteristics of asphalt binder and asphalt mixtures such as rutting. In addition to that, CNF has shown significant improvements in the mechanical properties of polymer composites (Khattak et al., 2011, Tandon et al., 2002), and Glasgow et al., 2004).

In Addition, Nanomaterial can enhance the performance properties of asphalt materials such as visco-elastic, high temperature property, and the resistance to aging, fatigue and moisture damage (Xiao et al.,2009 and Li et at., 2017). Several studies showed that asphalt binder modified with Nanomaterials like, Cellulose Nanofiber, Nanosilica, and Nanoclay, had up to 47% increase in rutting performance. Similarly, the modified asphalt binder with nanomaterials showed to have a prolonged fatigue life (up to 2-3 times) (Khattak, et at., 2012, Li et al., 2017).

Fatigue performance and moisture damage resistance of the Nanomaterial modified asphalt mix were also investigated by several researchers. Because of its high modulus and tensile strength, large aspect ratio and good network Cellulose Nanofibers would be beneficiary to hindrance the cracking development and consequently prolong fatigue life. (Li et al. 2017). Khattack showed that Carbon Nanofibers improved the fatigue life in 98%. Regarding the damage induced damage, Carbon Nanofibers showed to be an effective additive. Moisture damage occurs when the bonding between asphalt binder and aggregates is lost. Since the broken bonds between aggregates and asphalt binder occur in Nanoscale, Nanoscale materials could be the solution for improvement on that aspect. Tensile Strength

ratio (TSR) test was used to investigate the moisture damage resistance of nanomaterials modified binder. The TSR results showed that the moisture resistance of the new materials was superior than the base binders (Li et al., 2017, Khattak, et al. 2012, and Cheng et al.2011).

Several studies showed the positive impact on the addition of Nanomaterials in asphalt on its performance properties. Following the same path, Cellulose Nanofibers are being studied to also be considered a possible additive for the asphalt industry. Cellulose Acetate is one of the most important esters of cellulose (Fischer et al., 2008). It is the primary structural component of the cell wall of green plants and one of the most common biopolymers on earth (Tungprapa et al., 2007). It is abundant, and it is rapidly renewable polymer (Frey, 2008). The challenges of using Cellulose is that it does not melt, and it needs to be processed from a solution (Frey, 2008). So, together with the Cellulose, electrospinning technique was introduced to the asphalt industry for the production of nanofibers from a cellulose acetate solution.

2.5. Electrospinning Technique and its Solvents

The electrospinning technique has gained attention due to the versatility in spinning a wide variety of polymeric fibers but also due to its consistence in producing Nanofibers (Subbiah et al., 2005). The electrospinning of Cellulose Nanofibers has attracted a great deal of attention due to their good thermal stability, chemical resistance, and biodegradability. Also, CNF has the advantage of ready solubility in suitable electrospinning solvents and straightforward conversion to Cellulose (Frey, 2008). Electrospinning is a technique to produce fibers with average diameter in the range of

micrometers to nanometers (Tungprapa et al., 2007). Liu and Hsieh studied the range of Cellulose Acetate solvents for electrospinning including acetone, DMAc, and acetic acid in mixtures. Several researches have pursued a mixture of a Cellulose Acetate solvent, acetone, and a non-solvent, water. Electrospinning is a technique that utilizes electrical forces to produce polymer fibers using polymeric solution. The principle behind the electrospinning technique is: the solution of polymer flows out of the tip of a needle, where a droplet forms under the influence of surface tension of the solution. A high electric charge is applied to the solution, which causes repulsive electrostatic forces between polymer and solvent molecules to overcome the surface tension, and a jet of polymer shoots away from the needle towards a grounded collector (Smit, et al., 2005, Tungprapa et al., 2007, Subbiah et al., 2005, and Son et al. 2003). Overall, is a robust and simple technique to produce Nanofibers from a wide variety of polymers (Li and Xia, 2004).

Various studies were conducted on the effect of solvent composition for the electrospinning of Cellulose Acetate. Tungprapa et al. (2007) studied the effect of solvents on electrospun Cellulose Nanofibers. It was observed that Cellulose Acetate solution in acetone and water under acidic conditions produced larger fibers whereas use of the solution under a basic condition produced finer fibers. It was also observed that CA solution in acetone produced from finer fiber to flat fibers with smooth surface depending on que concentration of Cellulose Acetate. It was found that the solutions of acetone were difficult to electrospin due to the low boing point of acetone. The solution often clogged at the tip of the nozzle (Tunggprapa et al., 2007). Son et al. (2004) found that water helped the electrospinnability of solutions of Cellulose Acetate in acetone. Water decreased the overall evaporation rate in the electrospinning air gap, allowing sufficient time for fiber

draw-down and decreasing the clogging (Frey, 2008).

Other types of solvents were also evaluated by other studies. Han et al. (2008) studied the electrospinning of Cellulose Acetate solved in a various solvent system. A new solvent system, a mixed solvent of acetic acid/water was developed for the electrospinning of CNF (Han et al., 2008). It was reported that Cellulose Nanofibers could be electrospun from a mixed solvent system, acetic acid/water. The electrospinning of Cellulose Acetate using acetic acid as a solvent was investigated by Liu and Hsieh (2002). The researchers found that the solution could not be continuously electrospun. Based on that other mix solvent systems were tested. It was found that acetic acid/DMAc and acetic acid/acetone could be electrospun but, the results were fine fibers with large beads. It was also found that the viscosity of the solution increased with the increase of the acetic acid content. The viscosity is a factor affecting the diameter of CNF but, it is not a major one. It was recorded that the increased in viscosity caused thicker CNF to be electrospun (Han et al., 2008).

Important information was gathered form the several studies of CNF electrospinning. It was found that the average diameter of the electrospun CNF could be controlled by changing the composition of the solvent (Han et al., 2008). Also, water was found to be an environmentally safe co-solvent to delay the evaporation of acetone during the Cellulose Nanofibers electrospinning (Son et al., 2003). It was found that the desirable solvents for electrospinning are the ones with low surface tension (Liu and Hsieh, 2002).

Subbiah et al. (2004) studied the parameter of the electrospinning technique that affects the fiber morphology. It was found that the increase in voltage causes change in the shape of the jet initiating point, hence the structure and morphology of CNF. Generally, the higher the voltage the higher to deposition rate. In addition, that regardless the

concentration of the solution the lesser nozzle-collector distance the wetter and beaded are the CNF. The solution concentration playas and important role on CNF production. Low concentration solution forms droplets due to the influence of surface tension, while higher concentration prohibits fiber formation due to higher viscosity. On the other hand, the major concerns regarding the electrospinning technique are the challenge of producing align CNF and the scaling up of the process (Subbiah et al., 2004).

Electrospinning apparatus and procedure are very simple to be constructed and performed. However, the production rate is slow. To produce a high quantity of CNF days/ months would be necessary. Alternatives set up are being study to ease and increase the productivity of the Cellulose Nanofibers (Subbiah, et al., 2004, Warner et al., 1998, and Jaeger et al., 1998). Regarding the alignment of the CNF, various studies and approaches are being taken to obtain align fibers (Smit et al., 2005, Liu and Hsieh, 2002). The random orientation of the electrospun CNF in the typically non-woven webs is acceptable for some application (Smit et al., 2005). However, for other and for commercialization Nanofibers need to be obtained in a uniaxial form (Smit, et al., 2005). When taking into consideration a static collector, fibers diameter is generally observed to increase with an increase in solution concentration (Deitzel et al., 2001). The use of grounded electrode inside a water bath and a take up roller showed to be effective of producing aligned fibers with the typical fiber characterizations (Smit et al., 2005). Other methods also gave positive feedback on alignment of fibers. They are electrospinning onto a rotating drum (Doshi and Reneker, 1995), spinning onto a sharp edge of a thin rotating wheel (Zussmann et al., 2003), and using a metal frame as the collector (Dersch et al., 2003).

2.6. Moisture-Induced Damage

The tentative of production of uniaxial CNF could be the answer for the commercialization and usage on the pavement industry. The Cellulose Nanofibers could be the answer for one of the most important problem faced by the asphalt industry; Moisture-induced damage. Moisture-induced damage of asphalt mixture is the loss of adhesion at the aggregate-bitumen interface and/or the loss of cohesion within the bitumen film due to water (Zhang et al., 2016). The addition of Nanomaterials, potentially Cellulose Nanofibers, can remarkably enhance the performance properties of asphalt material such as visco-elasticity, high temperature property, and the resistance to fatigue and moisture damage (Li et al., 2017, Li et al., 2010, Amirkhanian et al., 2011, and Khattak et al., 2011).

Moisture enters the asphalt through the air voids and other discontinuities in the asphalt mix (Lu et al., 2007). Several forms of distresses like fatigue cracking, potholes, and rutting can be caused and/or accelerated by the moisture induced damage (Huang et al., 2010). Various researches have evaluated moisture- induced damage of HMA mixes by conducting TSR test in accordance with the conditioning method described in AASHTO T 283 (AASHTO, 2010) test method (Ahmad et al., 2014, Kakar et al., 2015, and Zhang et al., 2017). The tensile strength ratio obtained from TSR test was found to be less than one. Moisture- induced damage was found to decrease the tensile strength of the asphalt mixes. The HMA samples subjected to long-term conditioning were found to show further decrease in the tensile strength (e.g. Chen et al., 2008)

Researchers have conducted Hamburg wheel tracking test (HWT) test to evaluate moisture-induced damage potential of the asphalt mixes (Ghabchi et al., 2014; and Wen et

al., 2016). They have found that, after attaining stripping inflection point, the moisture-induced damage potential of the HMA samples increases as the creep slope decreases.

A number of laboratory and field studies have been carried out to evaluate the fracture resistance of the asphalt mixes (Mohammad et al., 2012 and Kim et al., 2015). However, only a few (e.g. Gong et al., 2012) have analyzed the moisture-induced damage potential of the asphalt mixes using fracture energy methods. They have found that fracture energy of the hot mix asphalt decreases after moisture conditioning. Kim (2011) found that SCB test is the most accurate laboratory test method for characterizing the fracture energy of the asphalt mixes. An increase in the strain energy release rate of HMA samples in SCB test was found to result in a reduction in fatigue cracking rate in the field (Mohammad et al., 2012).

The evaluation of moisture induced damage of asphalt that contain RAP was investigated by some researches (Ghabchi et al., 2014, Cong et al., 2016, and Ghabchi et al., 2016). It was found that the results can vary depending on several asphalt characteristics, like RAP source, aggregate type, and binder source (Ghabchi et al., 2014). Ozer et al. (2016), and Singh et al. (2017) conducted SCB tests on asphalt mixes and found an increase in fracture resistance and a decrease in moisture-induced damage potential of asphalt mixes after addition of RAP. In another study, Ghabchi et al. (2016) evaluated the moisture- induced damage potential of the asphalt mixes containing RAP by TSR and HWT tests. The TSR test results showed that addition of RAP increased the moisture-induced damage of the asphalt mixes. However, from HWT test result it was found that moisture- induced damage decreased with an increase in the RAP content.

Moisture induced damage also occurs on asphalt binder aggregate systems (Moraes et al., 2011 and Lu et al., 2017). Moraes et al. (2011) conducted BBS test on granite and limestone aggregates with modified asphalt binders and found that pull-off tensile strength (POTS) is higher in unconditioned samples and it decreases after moisture conditioning. The failure mode was found to change from the cohesive to adhesive due to the moisture-induced damage. The POTS values were found to be higher in the modified binders with increased adhesion with the aggregate and cohesion within binder. Lu et al. (2017) found that Limestone is a better aggregate than quartzite because it reduced the moisture induced damage potential due to the nonpolar-surface in the limestone and polar silica in the quartzite.

Overall, water can cause the asphalt pavement to failure in multiple ways, like fatigue cracking and rutting. The goal of having a Cellulose Nanofibers as additive on asphalt binder and asphalt mixes is a tentative to improve the properties of the asphalt minimizing the water action, hence improving the life of the asphalt. With the advancement of technologies and quest for environmentally friendly material the asphalt industry is now encouraged to pursue this line of study.

CHAPTER THREE: MATERIALS AND METHODS

3.1 Materials

This section presents an overview of the materials used and tested in the present study including their origin, collection, and properties.

3.1.1 Cellulose Acetate Nano-fiber

Cellulose is a naturally occurring polymer obtained from wood fibers. While Cellulose Acetate, is a synthetic compound derived from the acetylation of the plant substance cellulose. (Encyclopedia Britannica, 2009). For the fiber production cellulose acetate with density of 1.3 g/mL at 25 °C from Sigma Aldrich, Co., 3050 Spruce Street, St. Louis, MO (Figure 1) was used together with five different solvents. The solvents used were (i) acetic acid, (ii) acetone, (iii) acetone/water, (iv) acetic acid/water, and (v) acetic acid/acetone. The solution of cellulose acetate and the solvent used for the production of the Nanofiber was prepared by dissolving the required amounts of cellulose acetate in the solvents using a magnetic spinner at 50^{o}C for 20 minutes.

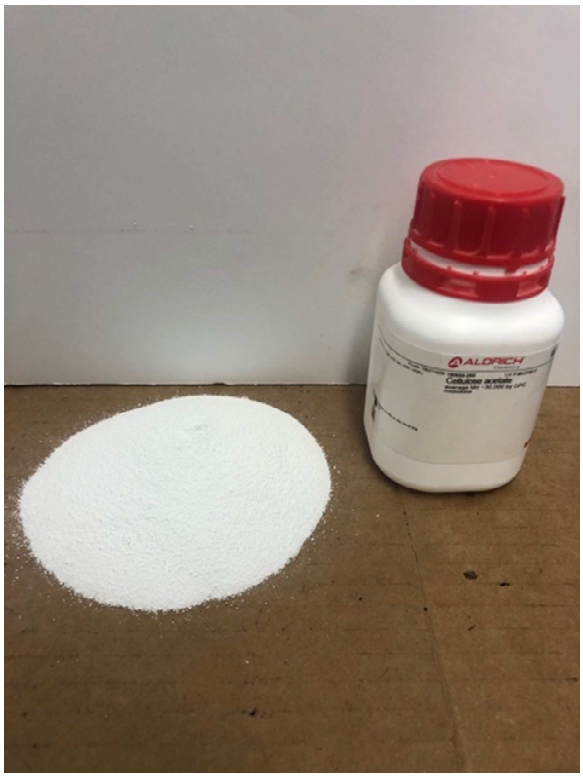

Figure 3.1: *Cellulose Acetate used for the production of the Cellulose Nanofibers.*

3.1.2 Asphalt Binder

Asphalt binder is a dark, black, and viscoelastic hydrocarbon residue obtained by distillation of the crude petroleum (HMA Construction, 2001). Asphalt binder is used as an adhesive to bond the aggregates to each other in the asphalt mix. Asphalt binder due to its viscoelastic nature has a time- and temperature-dependent mechanical behavior. Three different types of asphalt binders, namely PG 58-28, PG 64-34, and PG 70-28 were collected from Jebro Inc., Sioux City, IA. and were used for preparing the specimens for conducting the Izod impact strength test, Rotational Viscometer (RV) and Binder Bond Strength (BBS) tests. Figure 2 is showing one the asphalt binders used on the study, PG 64-34.

Figure 3.2: *PG 64-34 asphalt binder used on the study.*

3.1.3 Asphalt Mixes

Asphalt mix consists of a mixture of aggregates and asphalt binder prepared at high temperature. Superpave® volumetric mix design method is a widely-accepted mix design method in practice. Asphalt mix design consists of the selection of the appropriate asphalt binder type, aggregate gradation and determination of an optimum asphalt binder content while meeting the volumetric requirements based on traffic and climate data. The asphalt mix tested in the current study came from a pavement construction project in Brookings, SD. The collected mix were transported and stored on the asphalt lab at South Dakota State University (SDSU), then reheated, compacted and tested in laboratory. The asphalt mix collected consists of an HMA mix containing a PG 58-28 asphalt binder, mainly quartzite and granite-II aggregates, and 20% RAP (RAP20). Figure 3.3 shows the asphalt mix that was collected and used for the study. The asphalt mix had a nominal maximum aggregate size (NMAS) of 12.5mm. For the asphalt mix containing Cellulose Nanofiber, the RAP20 was reheated at 165 ºC for 1.5 hours then CNF were added gradually into the asphalt and

mixed by hand. The addition of CNF into the asphalt procedure was repeated every 15 minutes until all the CNF were incorporated into the RAP20 mix.

Figure 3.3: *Asphalt mix (RAP20) that was collected and used for the study.*

3.2 Methods

This section presents an overview of the methods used and in the present study including fiber production, fiber testing, and asphalt binder and mix laboratory testing.

3.2.1 Static and Rotating Electrospinning

Electrospinning is a process of electrostatic fiber formation by which uses electrical forces to produce polymer fibers from polymer solution, with nanometer-scale diameters (Ahn et al., 2006). For the production of Cellulose Nanofibers was used the static and the rotating electrospinning technique. These techniques differ only on where the produced CNF are being collected. For the static electrospinning the CNF were collected on a static plate covered in aluminum foil while the rotating electrospinning the CNF were collected onto a moving drum covered in aluminum foil. The electrospinning setup consisted of a

syringe and needle, a syringe pump, a ground electrode, a high voltage power supply, and a collector. Figure 3.4 illustrates the static electrospinning setup and Figure 3.5 illustrates the rotating electrospinning setup. The Cellulose plus polymers solutions were electrospum onto a static plate or a rotating drum covered in aluminum foil at a variating positive voltage of 15Kv, a tip-to-collector distance of 17cm and a varying collection time and flow rate. The solution composition used is presented in Table 3.1 and the characteristics of each electrospinning technique and the solutions tested can be found on Table 3.2 and Table 3.3. LSM and SEM were conducted to characterize the fibers produced using the static and rotating electrospinning.

Figure 3.4: *Static Electrospinning setup used for the production of the fibers.*

Figure 3.5: *Rotating Electrospinning setup used for the fiber production.*

Table 3.1: *Solution composition for electrospinning process.*

Solution	Polymer Type	Solvent Type	Concentration of Polymer by Weight (%)	Ratio of Solvent (%)	Total Weight (g)
1	Cellulose Acetate	Acetone	15	100	25
2	Cellulose Acetate	Acetic Acid	13	100	25
3	Cellulose Acetate	Acetic Acid/Water	17	75/25	25
4	Cellulose Acetate	Acetic Acid/Acetone	13	75/25	25
5	Cellulose Acetate	Acetone/Water	17	88/12	25

Table 3.2: *Electrospinning Times and discharge rate used for Solution 1 (CA and Acetone), Solution 2 (CA and Acetic Acid), Solution 3 (CA and Acetic Acid/Water), Solution 4 (CA and Acetic Acid/Acetone), and Solution 5 (CA and Acetone/Water).*

Sample #	Solution Type	Collection Time (min.)	Voltage (kV)	Discharge Rate (ml/min.)	Tip-to-Collector distance (cm)
1	1	2	15	0.01	17
2	1	2	15	0.01	17
3	1	5	15	0.01	17
4	1	5	15	0.01	17
5	1	10	15	0.01	17
6	1	10	15	0.01	17
7	1	20	15	0.01	17
8	1	20	15	0.01	17
9	1	60	15	0.01	17
10	1	60	15	0.01	17
11	2	2	15	0.01	17
12	2	2	15	0.01	17
13	2	5	15	0.01	17
14	2	5	15	0.01	17
15	2	10	15	0.01	17
16	2	10	15	0.01	17
17	2	20	15	0.01	17
18	2	20	15	0.01	17
19	2	60	15	0.01	17
20	2	60	15	0.01	17
21	3	2	15	0.01	17
22	3	2	15	0.01	17
23	3	5	15	0.01	17
24	3	5	15	0.01	17
25	3	10	15	0.01	17
26	3	10	15	0.01	17
27	3	20	15	0.01	17
28	3	20	15	0.01	17
29	3	60	15	0.01	17
30	3	60	15	0.01	17
31	4	2	15	0.01	17
32	4	2	15	0.01	17
33	4	5	15	0.01	17
34	4	5	15	0.01	17
35	4	10	15	0.01	17
36	4	10	15	0.01	17
37	4	20	15	0.01	17
38	4	20	15	0.01	17
39	4	60	15	0.01	17
40	4	60	15	0.01	17
41	5	2	15	0.5 to 1	17
42	5	5	15	0.5 to 1	17
43	5	2	15	0.5 to 1	12.5
44	5	5	15	0.5 to 1	12.5
45	5	2	15	0.5 to 1	7.5
46	5	5	15	0.5 to 1	7.5

Table 3.3: *Electrospinning Times and discharge rate used for Solution 1 (CA and Acetone), Solution 2 (CA and Acetic Acid), Solution 3 (CA and Acetic Acid/Water), Solution 4 (CA and Acetic Acid/Acetone), and Solution 5 (CA and Acetone/Water).*

Sample #	Solution Type	Collection Time (min.)	Voltage (kV)	Discharge Rate (ml/min.)	Tip-to-Collector distance (cm)
1.1	1	15	15	1	17
1.2	1	15	15	1	17
1.3	1	10	15	1	17
2.1	2	15	15	0.2	17
2.2	2	15	15	0.2	17
2.3	2	15	15	0.2	17
3.1	3	15	20	0.01	17
3.2	3	15	20	0.01	17
3.3	3	20	15	0.01	17
4.1	4	15	15	0.3	17
4.2	4	15	15	0.3	17
4.3	4	15	15	0.3	17
5.1	5	20	15	0.01	17
5.2	5	20	15	0.01	17
5.3	5	20	15	0.01	17

3.2.2 Laser Scam Microscopy (LSM)

Laser Scan Microscopy is an image tool capable of generate high-resolution images. For the purpose of the study the LSM images were used to analyze the roughness and entanglement of the produced fibers. A total of 5 samples (1 from each solution used form the production of CNF were chosen to be analyzed using LSM. Figure 3.6 shows a sample image of a Laser Scan Microscopy machine used in the study.

Figure 3.6: *A Laser Scan Microscope (Source: Nikon Instruments Inc.*, www.microscope.healthcare.nikon.com/about/news/nikon-develops-enhanced-c2-plus-confocal-microscope)

3.2.3 Scanning Electron Microscopy (SEM)

A scanning electron microscope (SEM) produces images of a sample by scanning the surface with a focused beam of electrons. The morphology of the electrospun CNF were observed by SEM after applying a gold coating to each sample. The electrons of the microscopy interact with the atoms of the sample producing images that contain information about the surface topography and composition of the sample. The images generated on the SEM were used to determine the fibers diameters. The diameters were determined by analyzing the SEM images with an image analysis program. ImagePro was the software chosen for determining the diameter of the electrospun CNF. A total of 5 samples (1 from each solution used form the production of cellulose nanofiber) were chosen to be analyzed using SEM. Figure 3.7 shows an sample image of the Scanning Electron Microscopy machine used in the study.

Figure 3.7: *A Scan Electron Microscope (Source: JEOL Ltd.*, www.jeol.co.jp/en/products/list_sem.html)

3.2.4 Fiber Tensile Strength Test

For the tensile strength test on the produced fibers the MTS® Insight 5 machine was used (Figure 3.6). A 250N load cell was used to determine the tensile strength of each tested fiber. The test was conducted on the total amount of CNF found on the collector and not on an individual nanofiber. Based on that the CNF needed to go through a sample preparation procedure. Prior testing, the produced fibers went through two different sample preparations. Because of the inconsistent collection of the fibers, it was necessary find a method to prepare similar sample with all the electrospun CNF. It was necessary to fold and cut the electrospun CNF in equal testing samples. The fibers were tested in two different directions, namely production direction, which is the direction that the fibers were produced and cross-production direction, which is the opposite direction that the fibers were produced. To start the sample preparation the produced fibers were peeled from the aluminum foil and folded three times according to the direction that the test demanded. After being folded the fibers were cut into identical sizes. The samples sizes were

determined to be 12 cm. After completing the folding and cutting procedures the fibers were ready to be placed in the MTS Insight 5 machine and tested. The testing length of the CNF fibers was determined to be 8 cm. The testing size was measured between the two clamps of the machine. A fiber holding clamp was used to avoid the slippage of the fibers during the test (Figure 3.7). The following diagrams show the produced fiber, the folding direction, and the testing direction. The Figure 3.8 shows the test set up, with the machine used for the test, the clamps and the fiber in place before testing.

⇒ Production direction:

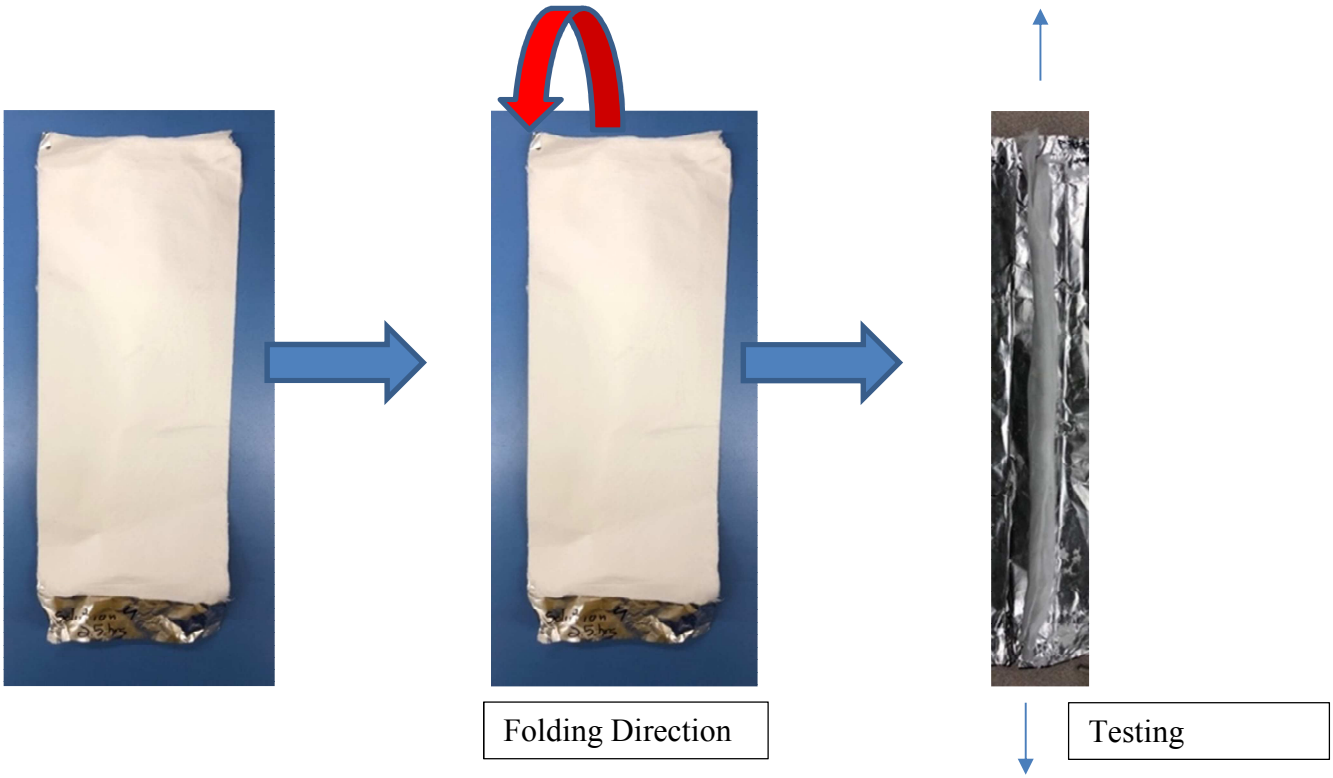

⇒ Cross- production direction:

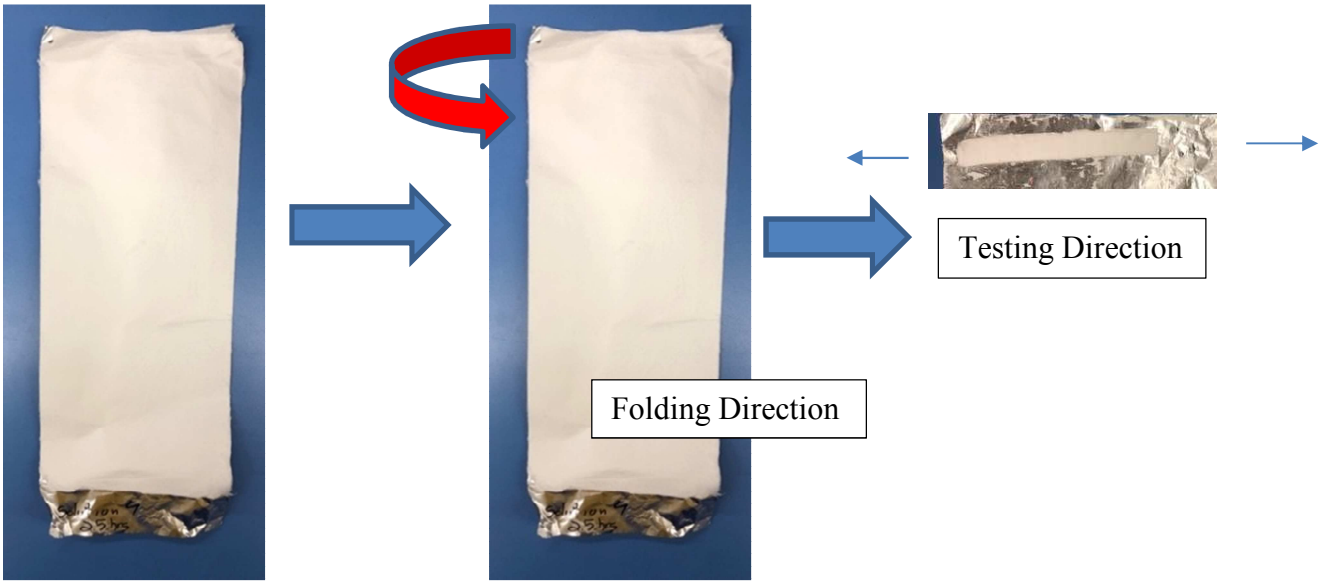

Figure 3.8: *MTS Insight 5 Machine used for the CNF Tensile Strength test.*

Figure 3.9: *Clamp used on the MTS Insight 5 for the Fiber Tensile Strength test.*

Figure 3.10: *Cellulose Acetate Nano-Fiber being tested on the MTS Insight 5 machine.*

3.2.5 Izod Impact Strength Test

The Izod impact strength test is an ASTM standard method of determining the impact resistance of materials like plastics. For this study the Izod test was modified to fulfill the asphalt binder needs. The test procedure was based on the ASTM standard, but it was slightly modified to accommodate the asphalt binder sample preparation and testing. For the test a pendulum is raised to a known and then released. The pendulum swings down hitting the notched asphalt binder sample, breaking it.

For the sample preparation the following steps were followed:

1. Stainless steel mold was built. Its dimensions of the mold were compatible with the testing machine, thickness of 12mm.
2. Asphalt binder was heated in an oven at 165 ^{o}C for 1 hour
3. Cellulose Nanofibers were added to the heated asphalt while still in the oven, the quantity of fibers added depend on the percentage by weight desired.
4. The asphalt binder with the CNF were mixed while still inside the oven using a drilling machine with a whisk for 1.5hours.
5. The final asphalt binder solution was poured inside the molds and rested for 20 minutes in room temperature. It is important to keep in mind that before pouring the asphalt binder inside the molds, it was coated with laser printer paper to avoid the asphalt binder to stick on the mold.
6. With the help of a hot spatula the excess of asphalt was taken away and then kept at room temperature for 1 hour.

7. The molds with the asphalt samples were then cooled down at -14 ºC for 2 hours.
8. The asphalt samples were taken out of the molds and once again cooled down at -14 ºC for 1 hour.
9. With the help of a hot spatula a notch was made in the middle of the asphalt binder sample, following a v-notch mold and then the samples were cooled down for the last time at -14 ºC for 1 hour.
10. The samples were ready to be tested.

The test was conducted based ASTM D256 – Test Method A and it was used a weight of 450g. All the samples were tested at the same temperature. The temperature tested was -11ºC. The following diagram (Figure 3.9) shows the sample preparation for the Izod impact strength test, starting at mold construction until the notch step. The following images (Figure 3.10 and 3.11) show respectively, the machine set up used for the Izod impact strength test and a zoom view of how the sample was attached to the machine prior testing.

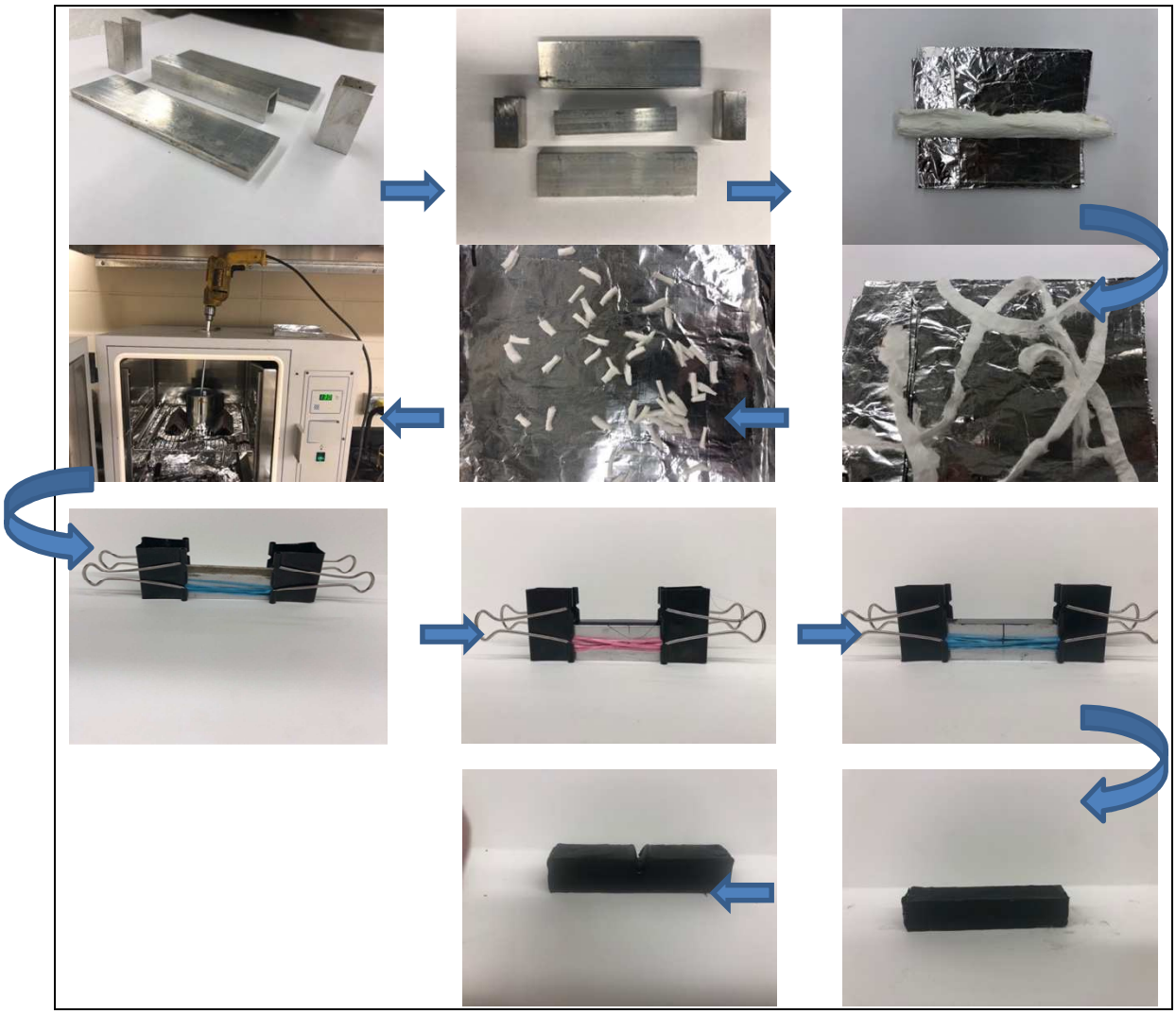

Figure 3.11: *Sample preparation of the Izod impact strength test sample.*

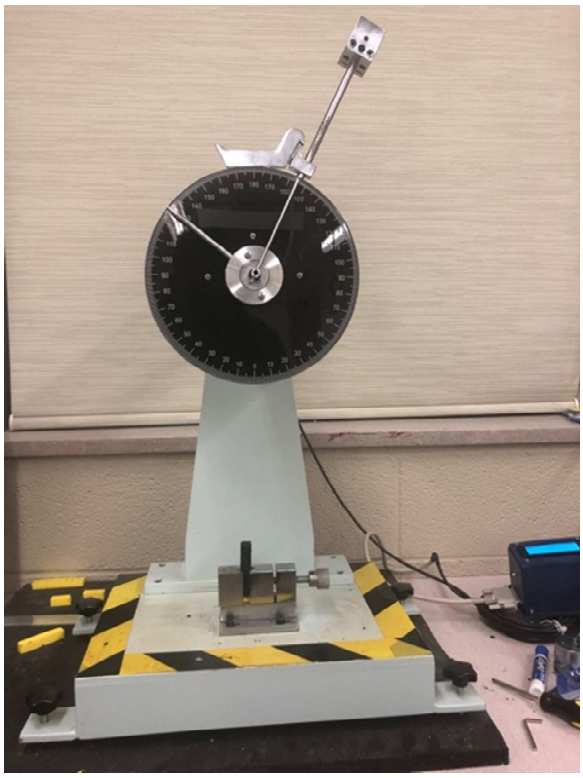

Figure 3.12 *Izod impact strength test set up.*

Figure 3.13: *Zoom view of the Izod impact strength test sample prior being tested.*

3.2.6 Binder Bond Strength Test (BBS)

Adhesive strength between bitumen and aggregate is highly affected by the composition of these two components and by moisture conditions. The Binder Bond Strength Test was used to measure the adhesion between the asphalt binder containing cellulose nanofiber and different aggregates. The test was carried out using a pneumatic adhesion tensile testing instrument (PATTI), which can be seen on Figure 3.12. The aggregates used were quartzite, granite, and gravel. The test will help understand how the asphalt binder behaves when Cellulose Nanofibers are added to it. The nature of the test is to compare the binding adhesive strength of asphalt binder in different aggregates and different conditions when no CNF are added and when different concentrations of CNF are added.

The binder containing Cellulose Nanofiber preparation followed the same procedure as the Izod impact strength test:

1. Asphalt binder was heated in an oven at 165 ^{o}C for 1 hour
2. Cellulose Nanofibers were added to the heated asphalt while still in the oven, the quantity of fibers added depend on the percentage by weight desired.
3. The asphalt binder with the CNF were mixed while still inside the oven using a drilling machine with a whisk for 1.5hours.
4. The asphalt binder containing Cellulose Nanofiber was storage at room temperature.

The BBS sample preparation followed the following steps:

1. The aggregates selected for the test had their surfaces polished and cleaned with distilled water to avoid dust and errors during the test.
2. The asphalt binder was reheated in an oven at 165 ºC for 1 hour.
3. With the help of a hot spatula a thin layer of asphalt was applied on the surface of the testing stub that was fixed in the aggregate right away and kept at room temperature for 30 minutes. For this study, the diameter of the testing stub used was 25mm.
4. Using a spatula, the excess of asphalt binder was scrapped off from the outside of the stub.
5. On this step, the samples are divided into dry condition samples and moisture condition samples. The dry condition samples are kept at room temperature until the moisture condition samples are fully conditioned and ready for testing.

- The following steps only apply for the moisture condition samples.

6. The samples were submerged in a water bath at a temperature of 25°C for 48 hours.
7. Following, the samples were cooled down at -18°C 16 hours.
8. Lastly, the samples were submerged in a water bath at a temperature of 25°C for 4 hours, prior testing.

Both dry condition and moisture condition are tested on the same day following the AASHTO TP-XX-11. Figure 3.13 shows one aggregate sample with individuals BBS samples prior testing. Figure 3.14 shows a zoomed view of one individual BBS sample prior testing. In addition, Figure 3.15 shows the moment when one sample is being testes

using the PATTI machine. The temperature was found to be a major factor affecting the bond strength, based on that both conditions are tested at room temperature, around 25°C ± 0.5°C. The difference between both conditions is that the moisture condition samples were tested while submerged in a water bath at 25°C ± 0.5°C. Tensile strength obtained from the PATTI quantum gold software was used for analysis.

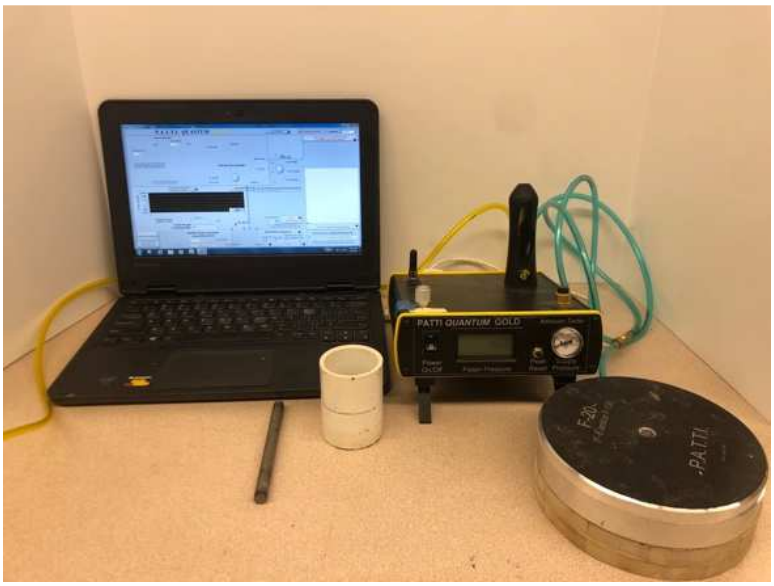

Figure 3.14: *Pneumatic Adhesion Tensile Testing Instrument (PATTI) used to conduct the BBS test.*

Figure 3.15: *View of one aggregate with five samples prior the BBS test.*

Figure 3.16: *Zoomed view of the BBS sample prior testing*

Figure 3.17: *View of one of the granites sample being tested using the PATTI machine.*

3.2.7 Rotational Viscometer Test (RV)

The workability is an important parameter that needs to be evaluated when analyzing asphalt binder. Rotational viscometer test was conducted on unaged asphalt binders using a Brookfield Rotational Viscometer (Figure 3.16) to evaluate the workability during mixing and compaction of the asphalt binder. Three different asphalt binder were tested in three different CNF concentration. The asphalt binder tested were PG 58-28, PG 64-34, and PG 70-28. The concentrations tested were 0% CNF fibers added, 0.3% CNF fibers added, and 0.7% CNF fibers added on the asphalt binder.

Figure 3.18: *Brookfield Rotational Viscometer used for the Rotational Viscometer test.*

The asphalt binder containing Cellulose Nanofiber sample preparation followed the same process as the Izod impact strength test and BBS test:

1. Asphalt binder was heated in an oven at 165 ºC for 1 hour
2. Cellulose Nanofibers were added to the heated asphalt while still in the oven, the quantity of CNF added depend on the percentage by weight desired.
3. The asphalt binder with the CNF were mixed while still inside the oven using a drilling machine with a whisk for 1.5hours.
4. The asphalt binder containing Cellulose Nanofiber was storage at room temperature.

The RV Test followed the following steps:

5. The asphalt binder was heated for 1 hours at 135 ^{o}C.
6. Approximately 11 grams of material was poured inside the testing compartment.

For testing, AASHTOO T316 was followed. A standard cylindrical spindle was submerged in the liquid asphalt binder and was rotated at a constant speed of 20 revolutions/minute (rpm). The torque required for the spindle to maintain a constant rotational speed of 20 rpm was measured and reported as the rotational viscosity. In this study, the rotational viscosities of the binders were determined at 137°C and 167°C.

3.2.8 Semi-Circular Bend Test (SCB)

The Semi-Circular Bend (SCB) Test was used to calculate the fracture energy of asphalt mixtures containing 0%, 0.3%, and 0.7% CNF from a load-displacement curve. For the asphalt mix sample preparation and conditioning ASTM D8044 was followed. The test started at the compaction of the asphalt mix. The asphalt mix were compacted with a height of 120 mm and a diameter of 150 mm (Figure 3.17). For testing the compacted asphalt mix sample needed to be cut into specimens of 57mm thickness (Figure 3.18). A rock saw was used to cut each sample into 4 semi-circle specimens. Following, notches with depth of 25 mm, 32 mm, and 38 mm were saw-cut in the mid span of the semicircular samples using a 1 mm thick diamond blade saw. Figure 3.19 shows one sample with notch depth of 38mm. The SCB sample preparation procedure was similar for the mix containing 0%, 0.3% and 0.7% CNF. For testing an IPC Global Asphalt Standards Tester was used. Figure 3.20 shows the machine set up with the SCB sample on it prior testing.

Figure 3.19: *SCB sample after being compacted at 150mm diameter and 120mm height*

Figure 3.20: *SCB sample after being cut into 57mm thickens samples for the SCB test*

Figure 3.21: *SCB sample after the 38mm notch was cut.*

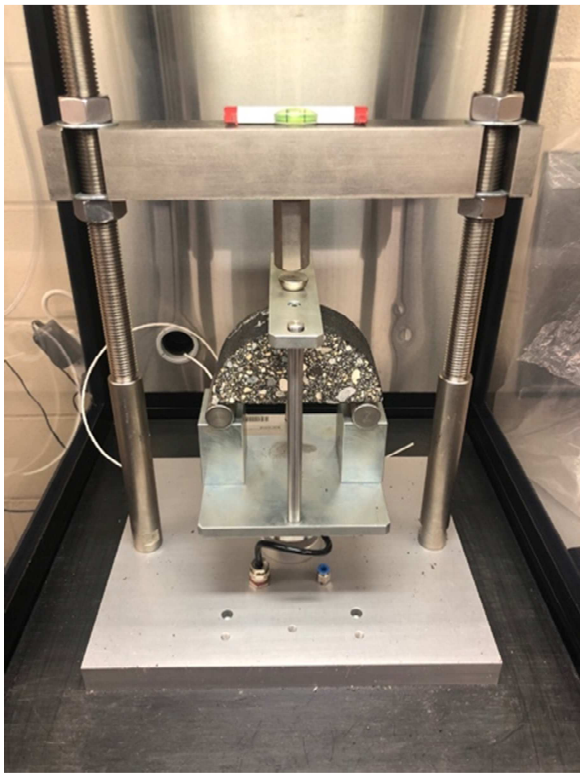

Figure 3.22: *SCB sample on the IPC Global Asphalt Standards Tester prior testing.*

3.2.9 Tensile Strength Ratio Test (TSR)

The Tensile strength Ratio (TSR) Test was used to evaluate the effects of saturation and accelerated water conditioning, with freeze-thaw cycle of the compacted asphalt mix samples. The compaction and testing procedures were followed in accordance with AASHTO T 283 standard.

For the sample preparation the following steps were followed:

1. The asphalt mix was heated up at 165 ºC for 1.5 hours and compacted at a height of 95mm and a diameter of 150mm (Figure 3.21).
2. The samples were kept at room temperature until cooled down.
3. The samples were divided into 2 different categories for testing, the dry condition and the moisture condition.
4. The dry condition samples were kept at room temperature until the moisture condition samples were fully conditioned.

- The following steps only apply for the moisture condition samples.

5. The vacuum saturation was carried on the samples by applying vacuum pressure of 224-660mm Hg while the samples are submerged in the water inside the vacuum chamber (Figure 3.22).
6. The samples were weighted to verify of the saturation is between 70% and 80%. If no, the vacuum saturation is repeated.
7. After obtaining the correct saturation, the samples were wrapped in plastic wrap and put inside an air-sealed bag with 10ml of water.
8. The bag with the samples were transfer to a freezer to cool down at -18°C for 16 hours.

9. Following, the samples are taken out of the bag and submerged in a water bath at 60 ± 1 ºC for 24 hours.
10. Lastly, the samples are submerged in a water bath at 25°C for 2 hours (Figure 3.23).

Following the 2 hours, the specimen was ready to be tested. Both dry conditions samples and moisture conditions samples were tested on the same day, with the minimum time span in between possible. It is important to keep in mind that the moisture samples need to be tested as soon as they were taken out of the water bath. The TSR test was conducted on the conditioned asphalt samples at room temperature in accordance with AASHTO T 283 using an MTS® 810 Material Test System, which can be seen on Figure 3.24.

Figure 3.23: *TSR sample after it was compacted at a height of 95mm and a diameter of 150mm.*

Figure 3.24: *TSR sample being Vacuum saturated inside a vacuum chamber.*

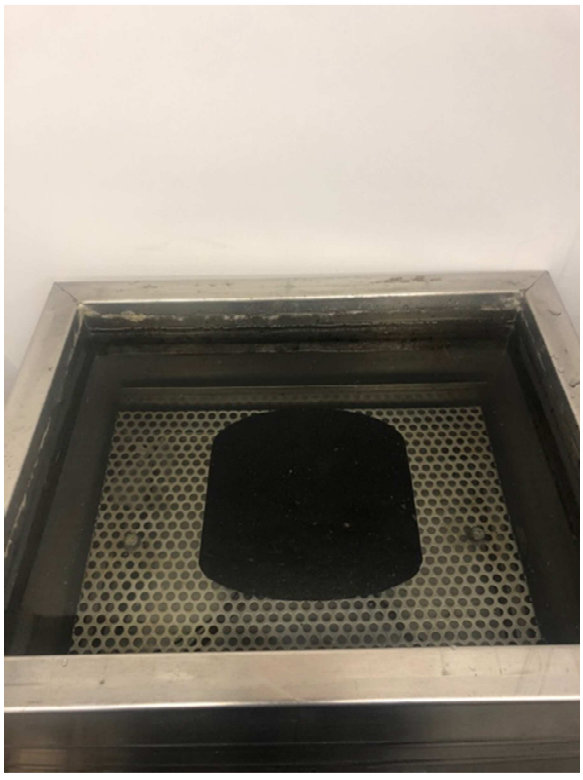

Figure 3.25: *TSR sample being conditioned inside a water bath.*

Figure 3.26: *MTS® 810 Material Test System used to conduct the TSR test.*

3.2.10 Hamburg Wheel Tracking Test (HWT)

Hamburg Wheel Tracking Test (HWT) is a test that evaluates the rutting and stripping potential of the asphalt mix. HWT is used to run simulative test that measure the asphalt mix qualities by rolling a loaded wheel device repeatedly across a compacted asphalt sample. The performance of the sample is then correlated to actual in-service pavement performance. If the asphalt mix sample undergoes a lot of rutting its performance is less efficient than a pavement that undergoes less rutting. Stripping is the loss of bond between aggregates and asphalt binder. It causes the asphalt mix to decrease its structural support, rutting, and cracking. Three different CNF concentration on asphalt mix samples were tested. The test was used to compare the performance of the asphalt mix when no CNF were added and when different concentration of CNF were added. The asphalt mix

was compacted at a height of 60 mm and a 150mm diameter (Figure 3.25). A small cut was made using a rock saw to fit the asphalt sample inside the mold of the testing machine (Figure 3.26) The HWT Test followed AASHTO T324 criteria and specifications. A Troxler Wheel tracker was used for the test. Figure 3.27 shows the test set up with the samples attached to the machine prior testing.

Figure 3.27: *Hamburg Wheel Tracking sample after being compacted at a height of 60mm and diameter of 150mm.*

Figure 3.28: *Hamburg Wheel tracking sample after being cut to fit in the mold of the HWT testing machine.*

Figure 3.29: *Hamburg Wheel Tracking test set up prior testing with the samples in place.*

CHAPTER FOUR: TEST RESULTS OF CELLULOSE NANOFIBERS

This chapter presents the rotating and static electrospinning CNF production results, as well as, the LSM, SEM, and the tensile strength test results that were conducted on the produced Cellulose Nanofibers. Cellulose Acetate was used for the production of Nanofibers using two different methods. The produced fibers from those different methods were evaluated using LSM, SEM, and tensile strength test to aid on the selection of the optimum method of production and solution for the continuity of the study. A comprehensive analysis of the test results is also presented. Furthermore, the suitability of using one of the electrospinning techniques to produce the optimum CNF was evaluated.

4.1. Rotating Electrospinning Nanofibers

The results from the production of Cellulose Nanofibers using the rotating electrospinning technique are presented on Table 4.1. The results obtained from the produced fibers were evaluated using visual inspection. Five different solutions were used to produce Cellulose Nanofibers. The final product of each solution is illustrated in one of the figures below. Figure 4.1 shows the final product of Solutions 1, while Figure 4.2 shows the final product of Solution 2. Figures 4.3, 4.4, and 4.5 show the final product of Solution 3, 4, and 5, respectively.

Table 4.1*: Key results from the production of Cellulose Nanofibers using rotating electrospinning technique.*

Solution	Key Results
1 (CA and Acetone)	- The produced CNF were dense and evenly spread on the collector plate; - Appeared to have a high thickness; - During the production a few problems were observed. The solution solidified at the tip of the needle, slowing down the production of CNF. The problem was generated by the evaporation rate of acetone.
2 (CA and Acetic Acid)	- The produced CNF were not dense, only a thin layer of CNF was observed; - The CNF were evenly spread on the collector plate; - The amount of CNF produced seemed to be less when compared to other solutions.
3 (CA and Acetic Acid/Water)	- The produced CNF were again not dense, only a thin layer was overserved. - The solution behaved similar to Solution 2, producing less CNF when comparing to others. - A difference between solution 2 and 3 is that the produced CNF for solution 3 are not evenly spread on the collection plate. The CNF are concentrated on the center from the top to bottom of the collector plate.
4 (CA and Acetic Acid/Acetone)	- The produced CNF were dense and evenly spread on the collector plate; - Very similar to the produced CNF using Solution 1. However, the produced CNF using solution 4 appears to have a smaller thickness; - Again, the high evaporation rate of acetone was an issue causing the solution to solidify at the tip of the needle, slowing the process up.
5 (CA and Acetone/Water)	- The produced CNF were inconsistent, visually al samples look different; - A few produced CNF were denser than the others. - A few produced CNF were spread on the center from top to bottom while others were evenly spread on the collector plate. - The thickness of the produced CNF was higher than the others. Almost like a 3D structure was observed; - The evaporation rate of acetone was again a problem. The tip of the needle was getting blocked due to the evaporation of acetone.

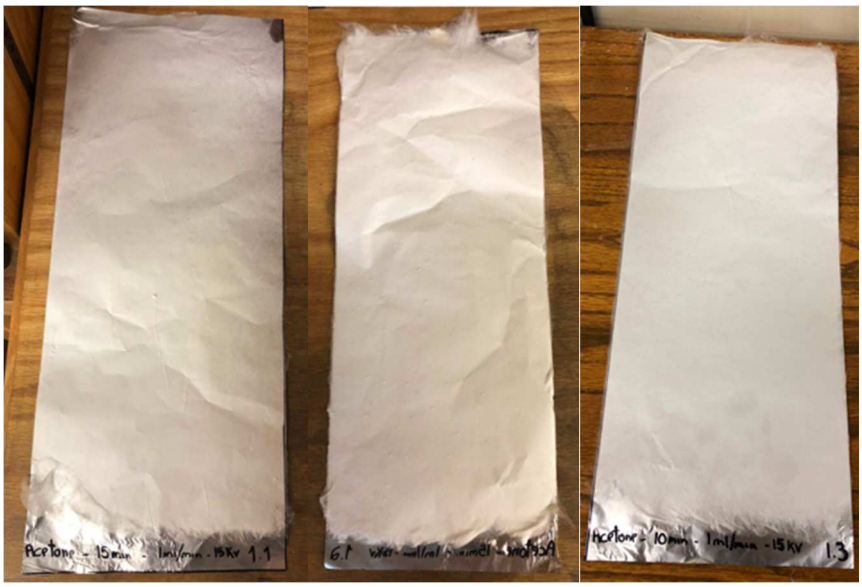

Figure 4.1*:Final results of the CNF produced using solution 1 and rotating electrospinning technique.*

Figure 4.2*: Final results of the CNF produced using solution 2 and rotating electrospinning technique.*

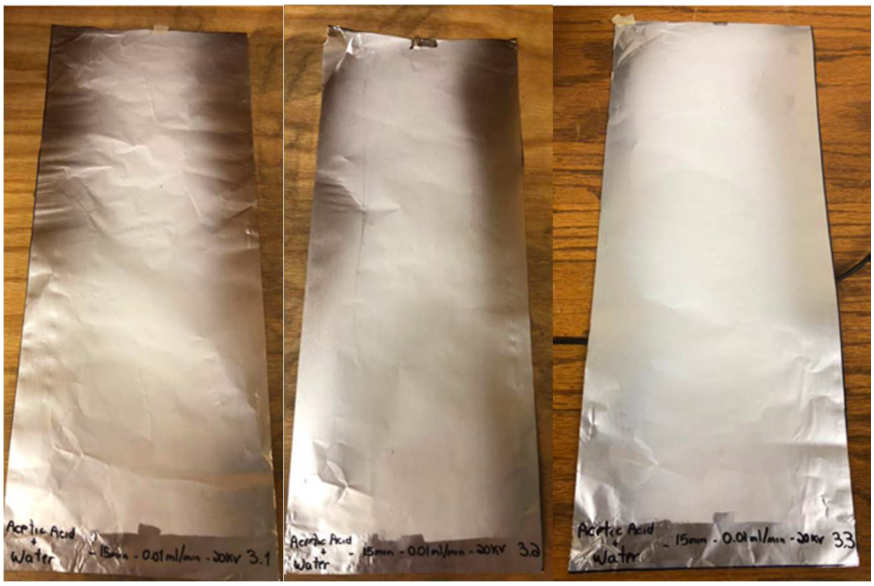

Figure 4.3*: Final results of the CNF produced using solution 3 and rotating electrospinning technique.*

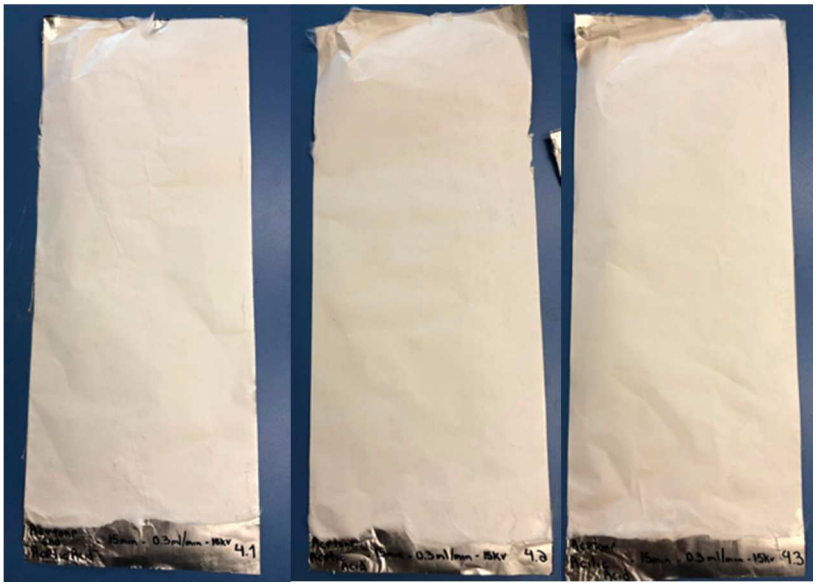

Figure 4.4*: Final results of the CNF produced using solution 4 and rotating electrospinning technique.*

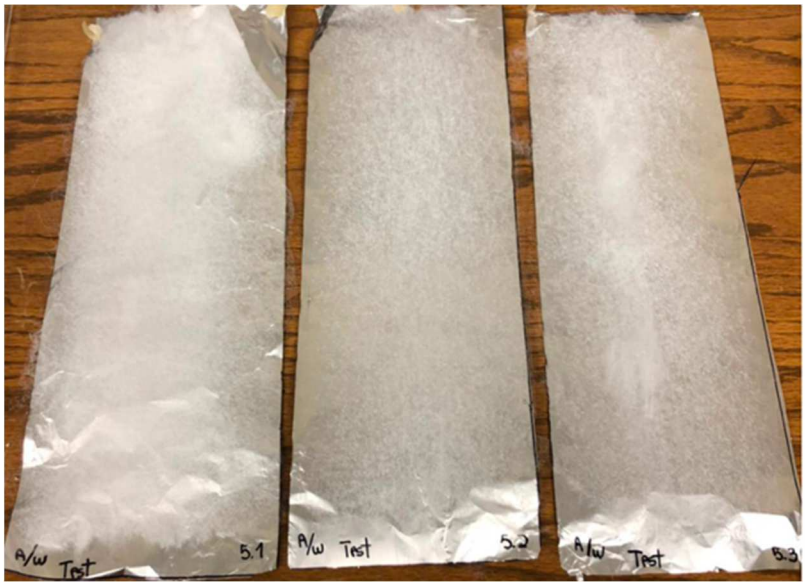

Figure 4.5*: Final results of the CNF produced using solution 5 and rotating electrospinning technique.*

Based only on observation and without any laboratory test, fibers produced with Solution 1 and Solution 4 seems to be the right candidates for the continuity of the study. That is due to the easiness of production and final result. The process of production with Solution 1 and 4 showed to have the least problems with the high evaporation rate of the acetone. The final product of these two solutions showed to have a higher density and thickness when compared to the other produced fibers. However, to fully evaluate the produced fibers and choose the optimum solution and technique, laboratory tests need to be done.

4.2. Static Electrospinning Nano-Fibers

The results from the production of Cellulose Nanofibers using the static electrospinning technique are presented on Table 4.2. The results obtained from the produced CNF were evaluated using visual inspection. Overall, the results from the static electrospinning were very similar to the results from rotating electrospinning. Once again, five different solutions were used to produce fibers. The final product of each solution is illustrated in

one of the figures below. Figure 4.6 shows the final product of Solutions 1, while Figure 4.7 shows the final product of Solution 2. Figures 4.8, 4.9, and 4.10 show the final product of Solution 3, 4, and 5, respectively.

Table 4.2: *Key results from the production of Cellulose Nanofibers using static electrospinning technique.*

Solution	**Key Results**
1 (CA and Acetone)	- The produced CNF showed to have a high density and it was concentrated on the center of the collector plate; - The produced CNF showed to have a high thickness; - Due to the high evaporation rate of acetone, the tip of the needle was getting blocked.
2 (CA and Acetic Acid)	- The produced CNF showed to be not dense, only a thin layer of fibers was observed. - The thickness of the produced CNF was very small. - The CNF were produced only on the center of the collection plate. A small area of produced fibers was observed; - No problems with the production was observed.
3 (CA and Acetic Acid/Water)	- The produced CNF were once again found only on the center of the collector plate. - The density and thickness of the produced CNF showed to be average. It was observed that the density was similar to solution 1 but the thickness was similar to solution 2. - A problem was observed during the production. The solution was too liquid and due to that some drops of the solution fell on the collector without being electrospun.
4 (CA and Acetic Acid/Acetone)	- The produced CNF were found evenly spread on the collector plate, which differs Solution 4 from the others. - The density and thickness were found to be high, similar to solution 1. - Once again, the high evaporation rate of the acetone was a problem;
5 (CA and Acetone/Water)	- The Solution 5 produced a different type of CNF. It is possible to see that for solutions 5 the CNF were more like a 3D structure; - The produced CNF were not consistent throughout the process; - The CNF were found to be produced only on the center of the collector plate. - The thickness and density of the produced CNF were observed to be higher than the other solutions. - The high evaporation rate of acetone was again a problem. The tip of the needle was getting blocked due to the evaporation of acetone

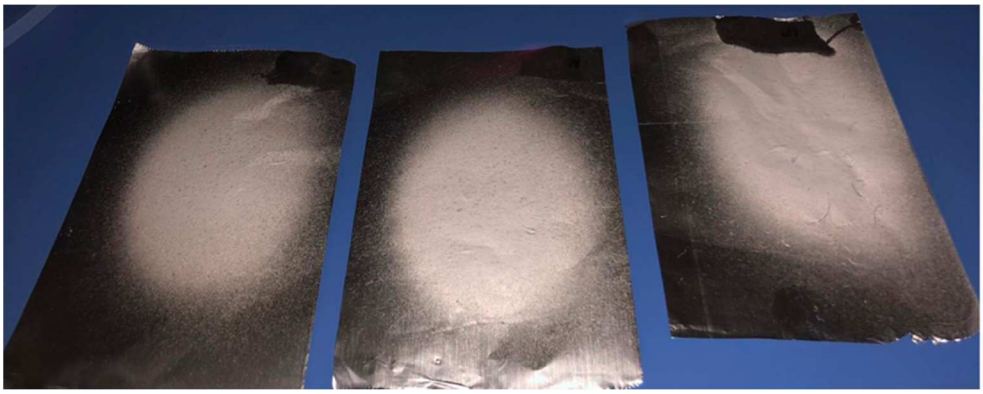

Figure 4.6*: Final results of the CNF produced using solution 1 and static electrospinning technique.*

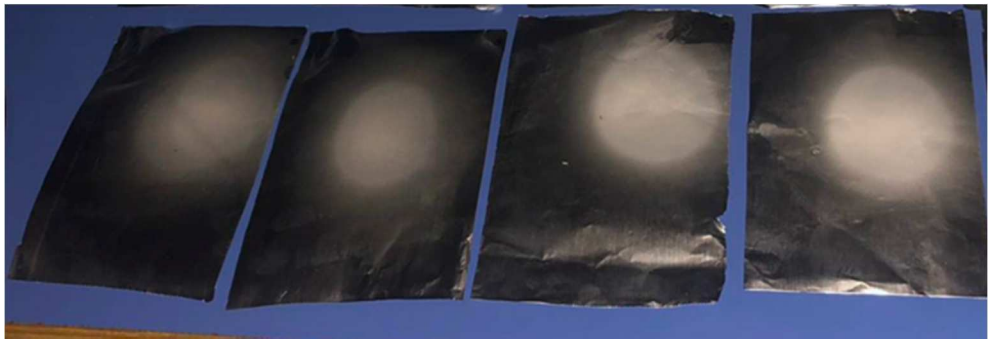

Figure 4.7*: Final results of the CNF produced using solution 2 and static electrospinning technique.*

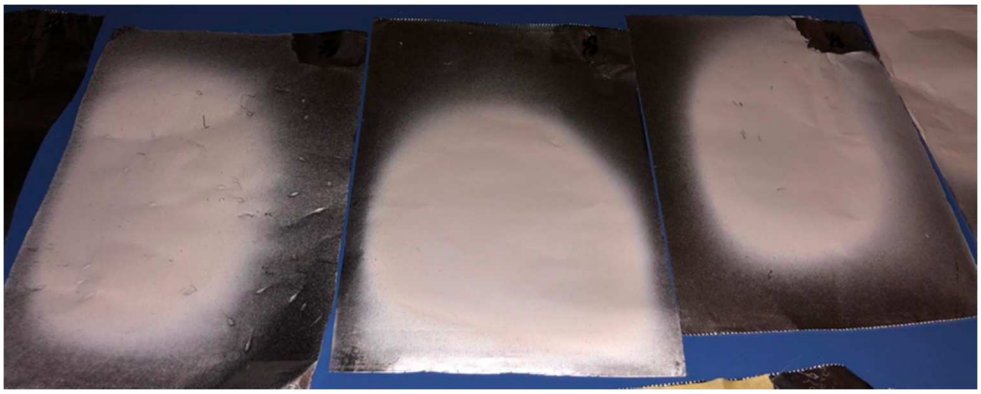

Figure 4.8*: Final results of the CNF produced using solution 3 and static electrospinning technique.*

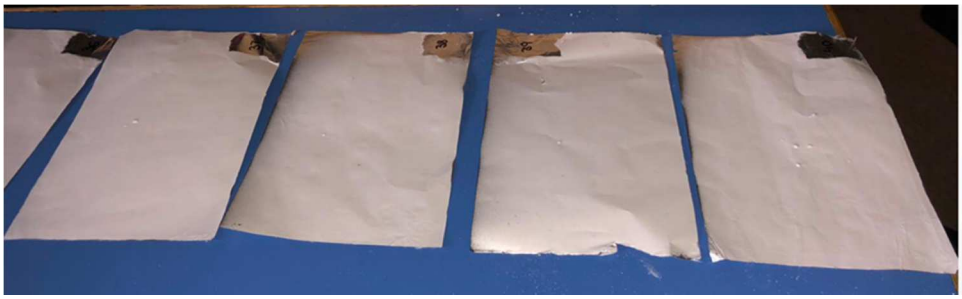

Figure 4.9*: Final results of the CNF produced using solution 4 and static electrospinning technique.*

Figure 4.10*: Final results of the CNF produced using solution 5 and static electrospinning technique.*

Based only on observation and without any laboratory test, CNF produced with Solution 1,4, and 5 seems to be candidates for the continuity of the study. That is due to the easiness of production and final result. The process of production with Solution 1,4, and 5 showed to not have any major problems only a few setbacks due to the high evaporation rate of the acetone. The final product of these three solutions showed to have a higher density and thickness when compared to the other produced CNF. For the static electrospinning, Solution 5 was observed to have the highest thickness and uniquely structure, meaning that it could possibly the best solution for production the CNF for the continuity of the study. However, to fully evaluate the produced Cellulose Nanofibers and choose the optimum solution and technique, laboratory tests need to be done.

4.3. Laser Scan Microscopy (LSM)

Laser Scan Microscopy was used to analyze the roughness and orientation of the produced Cellulose Nanofibers. The resulting LSM images are presented on the figures below. Figures 4-11 shows the LSM image of the fibers produced from solution 1. Figures 4.12, 4.13, and 4.14 show the LSM images of the fibers produced from solution 2,3, and 4, respectively. All the figures are a result of the static electrospinning. Due to the high roughness of the samples produced from solution 5, Laser Scan Microscopy was not able to capture any image.

Figure 4.11*: LSM Image from Cellulose Nanofibers produced with Solution 1.*

Figure 4.12*: LSM Image from Cellulose Nanofibers produced with Solution 2.*

Figure 4.13*: LSM Image from Cellulose Nanofibers produced with Solution 3.*

Figure 4.14*: LSM Image from Cellulose Nanofibers produced with Solution 4.*

From the resultant images of the Laser Scanning Microscopy it was found that produced fibers with Solution 1 (Cellulose Acetate + Acetone) were rougher than the other ones. That can be observed when comparing the Figure 4.11 with the others. In Figure 4.11 it is possible to see some white spots, which correspond to spaces between the top and the bottom layer of the fibers. The space observed on Figure 4.11 suggests that the produced fibers with solution 1 is the rougher that the others tested fibers. LSM captures images based on the top layer and the bottom layer, so if the distance between top and bottom layer is high more white spots will appear on the captured image. If more white spots apper on the capture image means that the sample is rougher than one captured image without any white spot. Based on the resultant images for the produced CNF with solution 2,3, and 4 the roughness of the CNF is in some way similar, due to the fact that none white spots where observed on the figures. Based on initial observation of produced CNF with solution 5, it appeared to be rougher than any other produced CNF. That could be proved through the LSM. The fact that no image was captured from the produced CNF using Solution 5

proved that the solution CNF was rougher than all the other ones. No image was captured due to the high quantity of white spots on the screen, the distance between the top layer and the bottom layer of the CNF was high that overcome the scope of the Laser scanning Microscopy.

From the resultant images of the Laser Scanning Microscopy was also found that the entanglement from all the produced fibers were similar. No solution allowed the CNF to be produced in any sort of alignment. All the figures above showed that the CNF were electrospun in a random alignment, not following any pattern. Based on the results obtained from the LSM images it is safe to suggest that the produced CNF using solution 5 would present a similar result if the capture of the image was possible.

Overall, the LSM test allowed to verify the roughness and entanglement of the produced CNF. Solution 1 and 5 was found to be the rougher ones. Solution 1 (Cellulose Acetate + Acetone) was found to be the rougher one, within the tested ones, based on the captured images and Solution 5 (Cellulose Acetate + Acetone/Water) was found to be rougher due to the fact that the LSM could not capture its picture due to the high distance from top to bottom layer of the produced fiber. Regarding the entanglement, it was found that all the tested CNF had the same pattern of entanglement. The CNF were found to be electrospun in a random pattern, not following any alignment. Based on that, produced CNF using solution 5 were assumed to have the same random pattern than the tested CNF.

4.4. Scanning Electron Microscopy (SEM)

The morphology and the diameter of the electrospun Cellulose Nanofibers was observed using SEM. The resultant image for produced Cellulose Nanofiber from Solution

1 is shown in Figure 4-15. For produced CNF from Solution 2 the resultant images from SEM are shown in Figure 4-16. In addition, Figures 4-17 show the resultant images from SEM of produced CNF from Solution 3. Now, for produced cellulose nanofiber from solution 4 the resultant images from the SEM are illustrated in Figure 4-18. Lastly, the resultant images from the produced CNF from Solution 5, is shown in Figures 4-19. For the calculation of the average diameter of the produced fibers an image analyzer software was used. ImagePro was the software used for the analyze of the CNF diameter. The diameter ranges, as well as the average diameter from the different produced fibers are presented on Table 4.3.

Table 4.3*: Diameter ranges and Average diameter for the produced Cellulose Nanofibers using different solutions.*

Solution	Minimum Value of Diameter (µm)	Maximum Value of Diameter (µm)	Average Diameter (µm)
1 - CA and acetone	0.142	0.631	0.387
2 - CA and acetic acid	0.08	0.300	0.190
3 - CA and acetic acid/water	0.100	0.398	0.249
4 - CA and acetic acid/ acetone	0.251	0.501	0.330
5 - CA and acetone/water	1.0	2.512	1.756

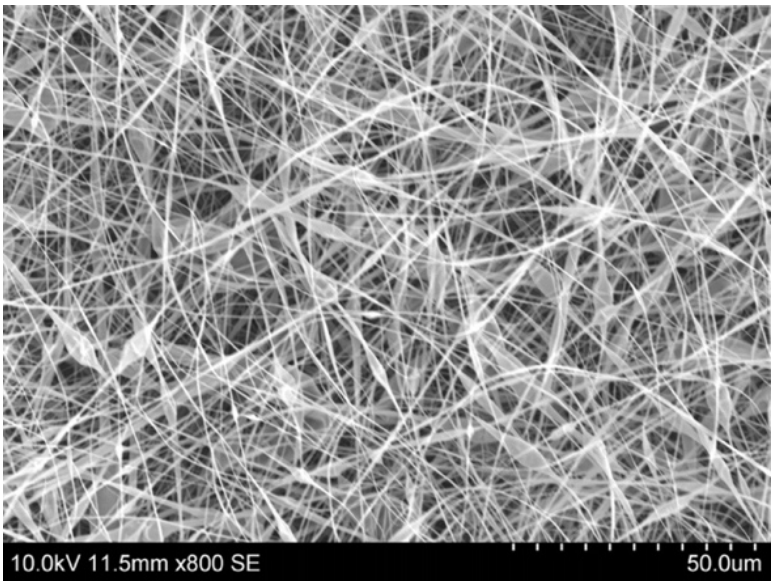

Figure 4.15*: SEM image from the produced CNF using Solution 1.*

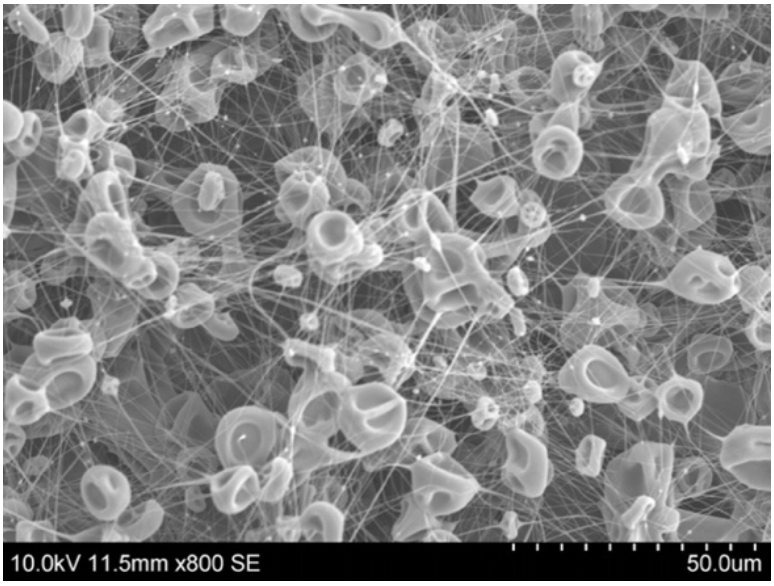

Figure 4.16*: SEM image from the produced CNF using Solution 2.*

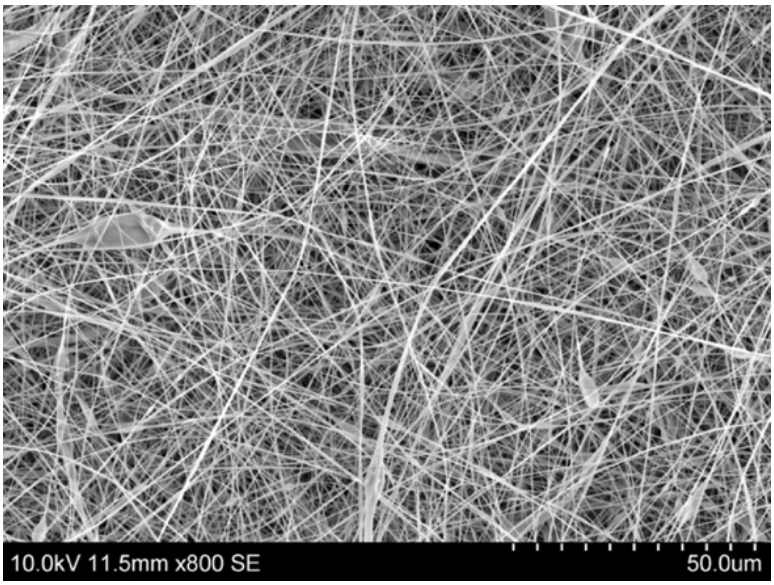

Figure 4.17*: SEM image from the produced CNF using Solution 3.*

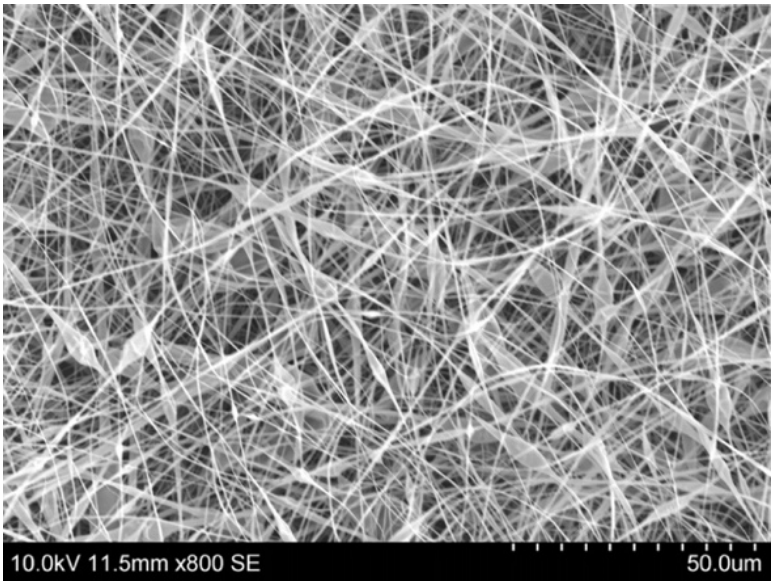

Figure 4.18*: SEM image from the produced CNF using Solution 4.*

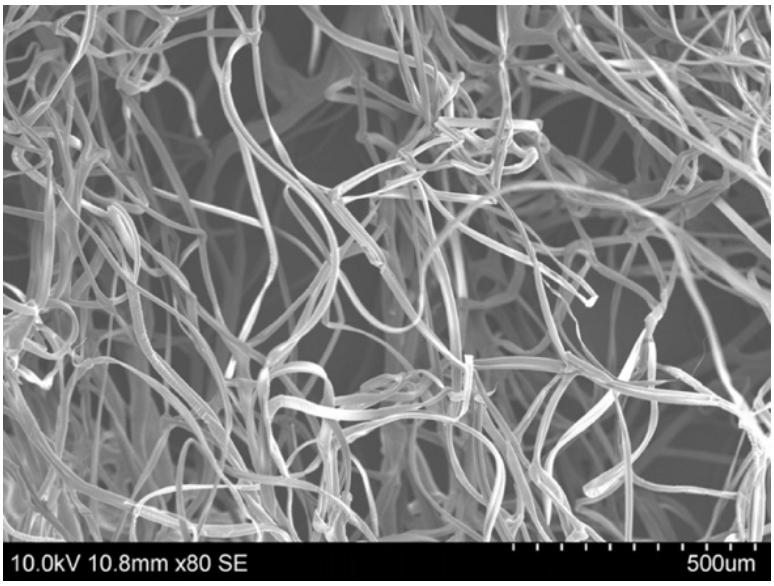

Figure 4.19*: SEM image from the produced CNF using Solution 5.*

The resultant figures from the SEM showed that all the produced CNF, independent of the solution used, were electrospun in a random orientation, there are no alignment within the fibers. The Figures 4.15, 4.16, 4.17, 4.18, and 4.19 showed that, in respect to the entanglement, all the solution resulted on a similar result, which is no specific fiber orientation. Similar results were also found using the LSM.

From the resultant SEM images, it was possible to observe that the produced fibers using Solution 2 (Cellulose Acetate + Acetic Acid) are different than the other ones. The difference is due to the fact that the within the fibers it is possible to see some globules of solution without being electrospun. This could be da result of the incapacity of the solution to be blended together, meaning that the solution was not able to properly electrospun CNF. The fact that the solution was incapable of mixing could explain why the produced fibers using Solution 2 were observed to be very thin and not dense. From the SEM images and previous observations, the Solution 2 was discarded as a possible candidate for the continuity of the study. Regarding the others SEM images, very few globules are observed,

but without interfering on the electrospun of the CNF. The globules could be explained by a problem when the solution was being mixed. The globules problem can be solved by the addition of more time on the solution mixing.

From Table 4.3 it was found that the produced CNF with Solution 5 had the highest average diameter, which was previously assumed based on the production observations. It was found that the average diameter of solution 5 CNF was 1.756μm, which is 353.7% higher than Solution 1 CNF (0.387μm), 824.2% higher than Solution 2 CNF (0.190μm), 605.2% higher than Solution 3 CNF, and 432.1% higher than Solution 4 CNF. From the SEM images and Table 4.3 it is evident that the produced fibers from Solution 5 are thicker than the other ones. The high average diameter of the CNF could mean that it could withstand a higher tensile force. However, that can only be proved after a Fiber Tensile Test been done.

Overall, based on observations and tests the produced CNF using Solution 2 and 3 can be discarded as future possibilities for the continuity of the study. Both of the CNF produced using these solutions were observed to have low roughness, low production quantity, low density, low diameter and specially for Solution 2 low electrospun rate. However, to fully discard the solutions from the study the fiber tensile strength test was done. So far from all the observations and tests done fibers produced with Solution 1, 4 and 5 are the best options from the continuity of the study.

4.5. Tensile Strength Test

The CNF tensile strength test was used to measure the maximum load the produced Cellulose Nanofiber could withstand. From each solution used for CNF production, two

samples of each were used for the test. The average value from the two tested CNF was used for evaluation. The results from the CNF tensile test are presented on Tables 4-4 and 4-5. Table 4-4 show the results from the tested samples that were produced using the rotating electrospinning technique while Table 4.5 shows the results from the tested samples that were produced using the static electrospinning technique.

Table 4.4*: CNF Tensile Strength test results from rotating electrospinning.*

Rotating Electrospinning					
Solution	**Specimen**	**Production Direction**		**Cross-Production Direction**	
		Tensile Strength (N)	**Average Tensile Strength (N)**	**Tensile Strength (N)**	**Average Tensile Strength (N)**
1	1	7.9	7.75	9.3	8.30
	2	7.6		7.3	
2	1	0.4	0.35	5.3	3.75
	2	0.3		2.2	
3	1	N/A	N/A	N/A	N/A
	2	N/A		N/A	
4	1	5	5.35	6.8	6.7
	2	5.7		6.6	
5	1	2.3	2.45	2.5	1.9
	2	2.6		1.3	

Table 4.5*: CNF Tensile Strength test results from static electrospinning.*

Static Electrospinning					
Solution	**Specimen**	**Production Direction**		**Cross-Production Direction**	
		Tensile Strength (N)	**Average Tensile Strength (N)**	**Tensile Strength (N)**	**Average Tensile Strength (N)**
1	1	8.7	7.45	3.7	3.85
	2	6.2		4	
2	1	N/A	N/A	N/A	N/A
	2	N/A		N/A	
3	1	N/A	N/A	N/A	N/A
	2	N/A		N/A	
4	1	3.9	4.15	3.4	3.9
	2	4.4		4.4	
5	1	6.8	8.6	7.8	9.05
	2	10.4		10.3	

Only four types of rotating electrospun CNF were tested and only three types of static electrospun CNF were tested. Produced CNF using Solution 3 (Cellulose Acetate + Acetic acid/water) from rotating and static electrospinning were not able to be tested due to the fact that the CNF could not be extracted from the collector place. The produced CNF were extremely thin and not dense enough to be able to be extracted for tensile testing. The same happened for CNF produced using Solution 2 (Cellulose Acetate + Acetic Acid) from static electrospinning. Based on that these CNF could be assumed to have low tensile strength, which is not desired for the continuity of the study.

From Table 4.4 (CNF Tensile Strength test results from rotating electrospinning) it is evident that, for both production direction and cross-production direction average tensile strength for Solution 1 (Cellulose Acetate + Acetone) CNF are higher than all the other tested CNF. For production direction, it was found that the average tensile strength for Solution 1 CNF was 7.75N, which is 2114.3% higher than the average tensile strength of Solution 2 CNF (0.35N), 44.9% higher than the average tensile strength of Solution 4 (Cellulose Acetate + Acetic Acid/Acetoner) CNF (5.35N), and 216.3% higher than the average tensile strength of Solution 5 (Cellulose Acetate + Acetone/Water) CNF (2.45N). For cross- production direction, it was found that the average tensile strength for Solution 1 CNF was 8.3N, which is 121.3% higher than the average tensile strength of Solution 2 CNF (3.75N), 23.9% higher than the average tensile strength of Solution 4 CNF (6.7N), and 336.8% higher than the average tensile strength of Solution 5 CNF (1.9N).

From Table 4.5 (CNFTensile Strength test results from static electrospinning) it is evident that, for both production direction and cross-production direction average tensile strength for Solution 5 CNF are higher than all the other tested CNF. For production

direction, it was found that the average tensile strength for Solution 5 CNF was 8.6N, which is 15.4% higher than the average tensile strength of Solution 1 CNF (7.45N) and 107.2% higher than the average tensile strength of Solution 4 CNF (5.35N). For cross- production direction, it was found that the average tensile strength for Solution 5 CNF was 9.05N, which is 135.1% higher than the average tensile strength of Solution 1 CNF (3.85N) and 132.1% higher than the average tensile strength of Solution 4 CNF (3.9N).

It was observed that for the rotating electrospinning technique the produced CNF using Solutions 1,2 and 4 tested at cross-production direction obtained the highest average tensile strength. Based on these results, it can be assumed that the majority of the CNF produced with Solutions 1,2, and 5 were electrospun with a cross-production alignment pattern. On the other hand, for the CNF produced with Solution 5 the average tensile strength value for the production direction is higher than the average tensile strength of the cross-production directions, meaning that for Solution 5 the majority of the CNF were electrospun with a production direction alignment.

In contrast with the results found for the rotating electrospinning Cellulose Nanofibers, it was observed an opposite result for the CNF produced from the static electrospinning. It was observed that the produced CNF from Solution 1 and 4 tested at a production direction obtained the highest average tensile strength. Hence, the majority of the CNF produced had a production direction alignment. On contrary, the CNF produced with Solution 5 had a higher average tensile strength when tested at cross-production direction, meaning that the majority of the CNF produced had a cross-production alignment.

Overall, while some tips regarding the alignment of the Cellulose Nanofibers were found it was not possible to fully establish the alignment of the produced CNF. The rotating electrospinning technique was used with the goal to produce alignment CNF, the idea of a rotating drum while the CNF were being electrospun gave hope to produced alignment fiber. Based on the tests made on the produced CNF the rotating electrospinning technique did not work as planned. So, based on that due to the easiness of production, workability and similarity of results the static electrospinning technique was chosen for the continuity of the study.

The selection of the solution for the production of the CNF for the continuity of the study was made based on the test results gathered, personal experience and visual observation. Based on those criteria the Solution 2, 3, and 4 were discarded. Solution 2 was discarded by the low electrospun rate, low density, low roughness, low average diameter, failure to be extracted from the collector plate, and assumed low tensile strength. The Solution 3 was discarded by similar reasons as Solution 2, it had a low electrospun rate, a low density, low average diameter, low roughness, failure to be extracted from the collector plate and assumed low average tensile strength. Solution 4 had similar characteristics as Solution 1, but it was discarded for not having a high tensile strength. Solution 4 had acceptable morphological characteristics but not as high average tensile strength as solution 1 and solution 5. Solution 1 and Solution 5 had some similar characteristics, both had high density, high production rate and similar entanglement. However, Solution 5 was rougher, had higher average diameter and higher average tensile strength. In other hand, Solution 1 had in its favor the easier of production and uniformity of electrospun CNF. Taking into consideration all the evidences and test results, specially the CNF tensile strength test,

Solution 5 was chosen for the continuity of the study. Once the solution 5 was chosen, CNF were mass produced and extracted at a cross-production direction for the laboratory tests on modify asphalt binder and mix. Cellulose Acetate + Acetone/water (Aka. Solution 5) together as static electrospinning were used to electrospun Cellulose Nanofibers for the continuity of the study.

CHAPTER FIVE: TEST RESULTS OF ASPHALT BINDER

This chapter presents the Izod impact strength test, BBS, and RV test results conducted on asphalt binders containing Cellulose Nanofiber and asphalt binder without Cellulose Nanofiber. Three different asphalt binders were tested, namely PG58-28, PG64-34, and PG70-28. Each asphalt binder was tested four times, one being without any CNF, the other three times with different concentration of Cellulose Nanofibers. A comprehensive analysis of the test results is also presented. Furthermore, the suitability of using Cellulose Nanofibers as additives in asphalt binders was evaluated.

5.1. Rotational Viscometer test

Figures 5.1, 5.2 and 5.3 present the results of the rotational viscosity test conducted on the unaged unmodified (0% CNF), and unaged modified (0.3% CNF and 0.7% CNF) on PG 58-28, PG 64-34 and PG 70-28 binders, respectively. The test results presented on the figures 5.1, 5.2, and 5.3 are based on the temperatures on which quantity of CNF were tested. From the Figures 5.1,5.2, and 5.3, it is evident that the viscosity of all the three tested asphalt binders reduced with the increasing temperatures, regardless of the quantity of CNF added. The viscosity of PG 58-28 with 0%, 0.3%, and 0.7% CNF asphalt binder were found to be 0.308 Pa-s, 0.413 Pa-s, and 0.625 Pa-s, respectively at 137°C, and it decreases to 0.125 Pa-s (59% reduction), 0.15 Pa-s (64% reduction), and 0.218 Pa-s (65% reduction), respectively at 167°C. The viscosity of PG 64-34 with 0%, 0.3%, and 0.7% CNF asphalt binder were found to be 0.867 Pa-s, 0.979 Pa-s, and 1.179 Pa-s, respectively at 137°C, and it decreases to 0.304 Pa-s (65% reduction), 0.321 Pa-s (67% reduction), and 0.383 Pa-s (68% reduction), respectively at 167°C. The viscosity of PG 70-28 with 0%, 0.3%, and 0.7% CNF asphalt binder were found to be 1.175 Pa-s, 1.45 Pa-s, and 1.716 Pa-

s, respectively at 137°C, and it decreases to 0.404 Pa-s (66% reduction), 0.666 Pa-s (54% reduction), and 0.836 Pa-s (51% reduction), respectively at 167°C. Also, comparing 5.1, 5.2, and 5.3 reveals that the viscosities of the PG 70-28 binder are higher than those measured for the PG 58-28 and PG 64-34 binders, regardless the quantity of CNF, as expected. The viscosity of PG 70-28 with 0% CNF at 137°C was found to be 74% higher than PG 58-28 with 0% CNF added and 26% higher than PG 64-34 with 0% CNF added. The viscosity of PG 70-28 with 0.3% CNF at 137°C was found to be 72% higher than PG 58-28 with 0.3% CNF added and 32% higher than PG 64-34 with 0.3% CNF added. The viscosity of PG 70-28 with 0.7% CNF at 137°C was found to be 64% higher than PG 58-28 with 0.7% CNF added and 31% higher than PG 64-34 with 0% CNF added. The viscosity of PG 70-28 with 0% CNF at 167°C was found to be 69% higher than PG 58-28 with 0% CNF added and 25% higher than PG 64-34 with 0% CNF added. The viscosity of PG 70-28 with 0.3% CNF at 167°C was found to be 77% higher than PG 58-28 with 0.3% CNF added and 52% higher than PG 64-34 with 0.3% CNF added. The viscosity of PG 70-28 with 0.7% CNF at 167°C was found to be 74% higher than PG 58-28 with 0.7% CNF added and 54% higher than PG 64-34 with 0% CNF added.

Furthermore, the viscosities of the PG 58-28 binder were found to vary from 0.308 to 0.625 Pa-s at 137 °C and from 0.125 to 0.218 Pa-s at 167 °C, while the viscosities of the PG 64-34 and PG 70-28 binder were found to vary from 0.867 to 1.179 Pa-s and 1.175 to 1.716 Pa-s respectively at 137 °C and from 0.304 to 0.383 Pa-s and 0.404 to 0.836 Pa-s respectively at 167 °C. PG 58-28 exhibited the lowest and PG 70-28 exhibited the highest viscosity values. Therefore, it can be concluded that the PG 70-28 binder is expected to require more compaction efforts in the field, while PG 58-28 is expected to require less

compaction efforts in the field. Also, it can be concluded that the addition of CNF resulted in higher viscosity values, meaning that the higher the quantity of added CNF more compaction efforts are required in the field. These observations were found to be consistent with the findings reported in previous studies (Lu and Isacsson, 1997; Xiao et al., 2003). As reported by Xiao et al. (2003) the behavior of viscosity of all the asphalt binders are generally affected by polymer type, asphalt source and test temperature. The high viscosity observed for the polymer modified binders are a due to the strong interaction between the polymer particles in the asphalt binder.

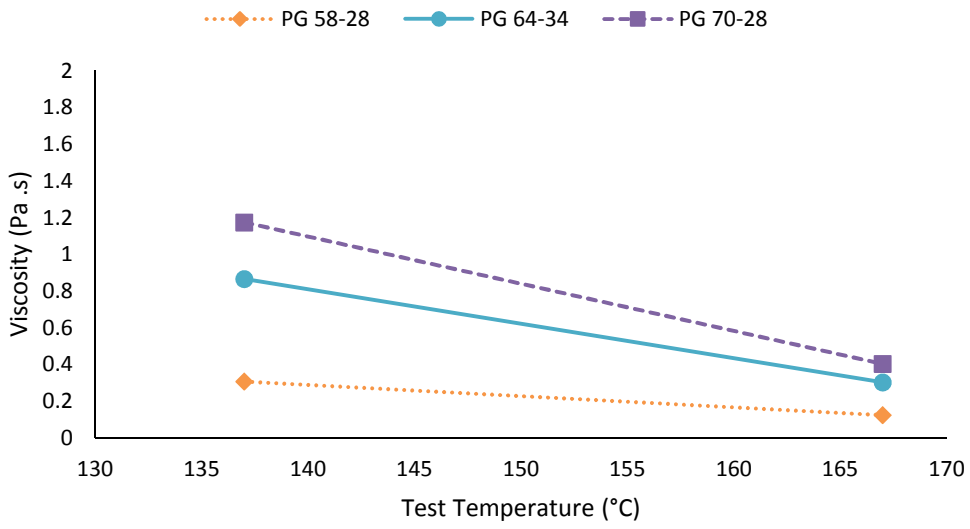

Figure 5.1*: Variation of viscosity with temperature for not CNF modified PG 58-28, PG 64-34, and PG70-28 asphalt binders*

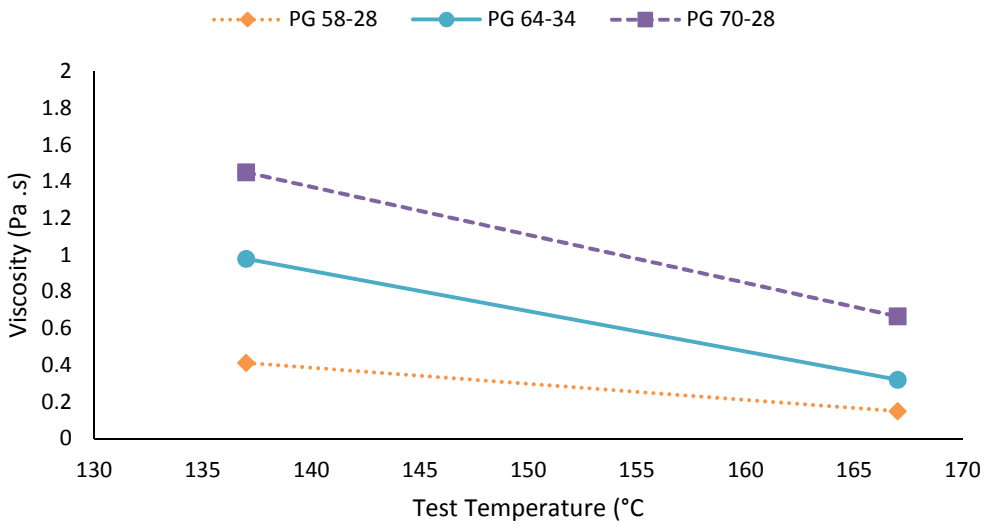

Figure 5.2*: Variation of viscosity with temperature for 0.3% CNF Nanofibers modified PG 58-28, PG 64-34, and PG70-28 asphalt binders.*

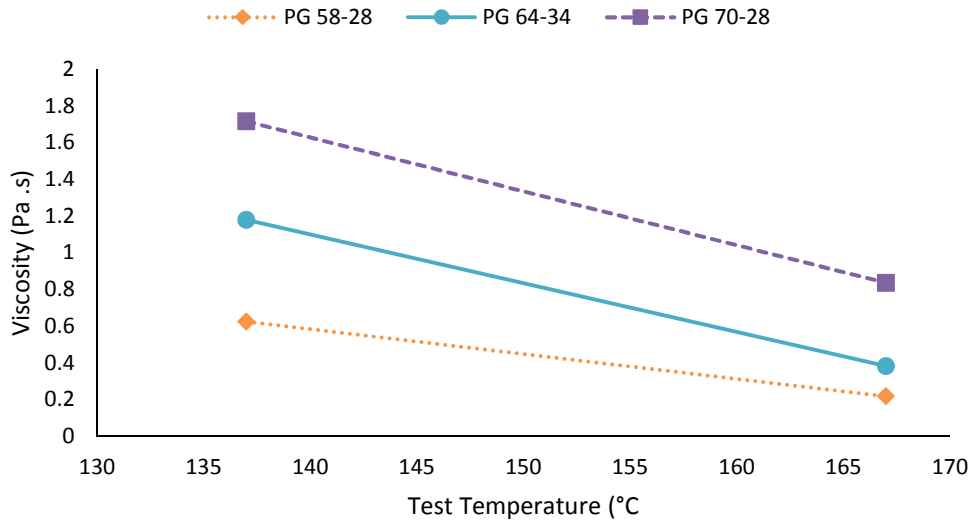

Figure 5.3*: Variation of viscosity with temperature for 0.7% CNF Nanofibers modified PG 58-28, PG 64-34, and PG70-28 asphalt binders.*

Figures 5.4, 5.5 and 5.6 present the results of the rotational viscosity test conducted on PG 58-28, PG 64-34 and PG 70-28 binders, respectively. The figures show the effect of

the Cellulose Nanofibers on the viscosity value for each tested asphalt binder. From the Figures 5.4,5.5, and 5.6, it is evident that the viscosity of all the three asphalt binders tested increased with the increasing percentage of added CNF. For PG 58-28 the viscosity increased from 0.308 Pa-s at 0% CNF to 0.413 Pa-s (34% increase) at 0.3% CNF and to 0.625 Pa-s (103%) at 0.7% CNF at 137°C, while for 167°C the viscosity of PG 58-28 increased from 0.125 Pa-s at 0% CNF to 0.15 Pa-s (20% increase) at 0.3% CNF and to 0.218 Pa-s (74% increase) for 0.7% CNF. For PG 64-34 the viscosity increased from 0.867 Pa-s at 0% fibers to 0.979 Pa-s (13% increase) at 0.3% CNF and to 1.179 Pa-s (36%) at 0.7% CNF at 137°C, while for 167°C the viscosity of PG 64-34 increased from 0.304 Pa-s at 0% CNF to 0.321 Pa-s (6% increase) at 0.3% CNF and to 0.383 Pa-s (36% increase) for 0.7% CNF. For PG 70-28 the viscosity increased from 1.175 Pa-s at 0% CNF to 1.45 Pa-s (23% increase) at 0.3% CNF and to 1.716 Pa-s (46%) at 0.7% CNF at 137°C, while for 167°C the viscosity of PG 64-34 increased from 0.404 Pa-s at 0% CNF to 0.666 Pa-s (65% increase) at 0.3% CNF and to 0.836 Pa-s (107% increase) for 0.7% CNF. Based on the results it is possible to conclude that the quantity of added CNF into the asphalt binder have an impact on the viscosity value. The addition of 0.3% and 0.7% of Cellulose Nanofibers increase the viscosity of all the three testes binder. The higher viscosity could be explained as a result of a strong interaction between the natural polymer particles in the binder and by the polymer structure used to modify the asphalt binders (Xiao et al. (2014) and Lu and Isacsson (1997)).

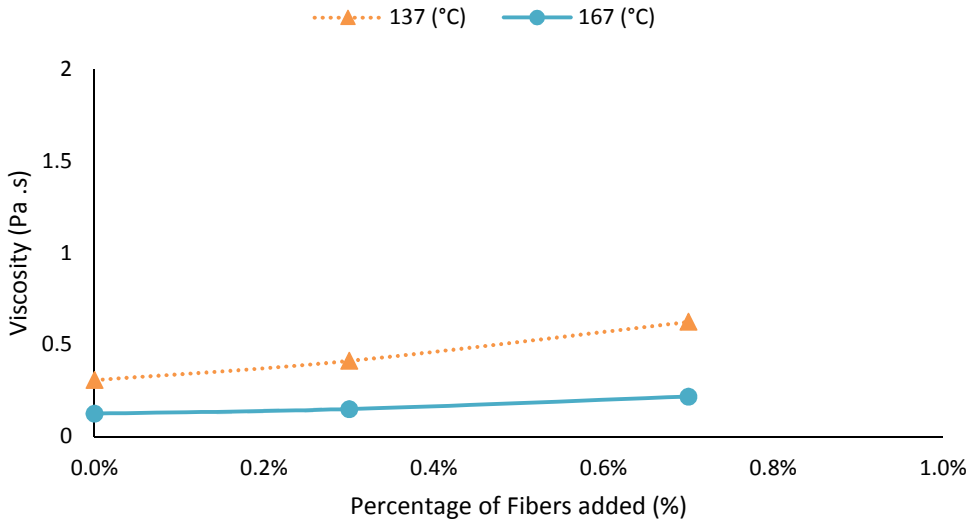

Figure 5.4: Variation of viscosity with percentage of added CNF for PG 58-28 asphalt binders.

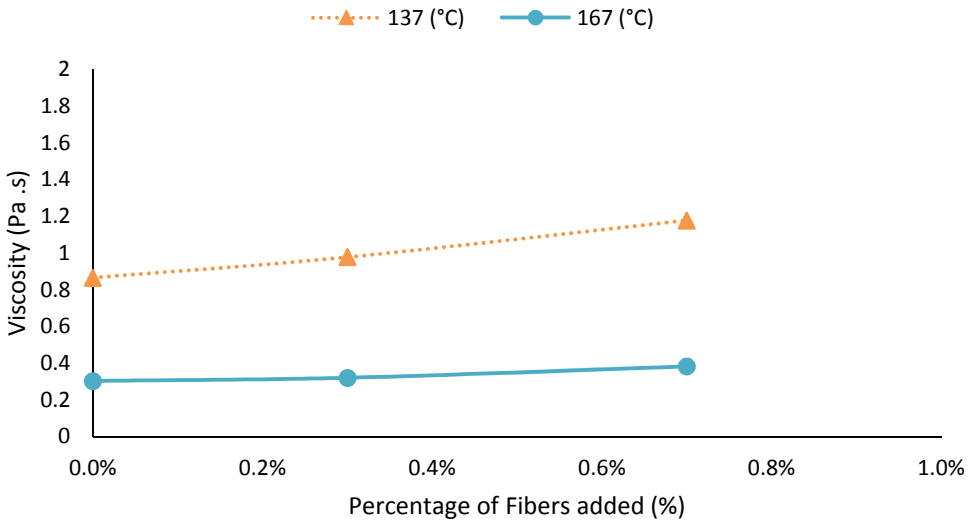

Figure 5.5: Variation of viscosity with percentage of added CNF for PG 64-34 asphalt binders.

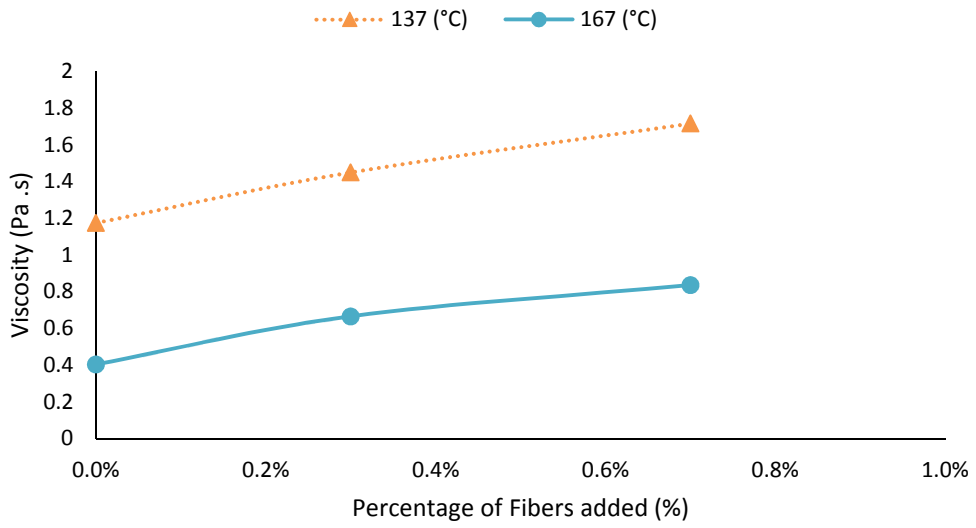

Figure 5.6: Variation of viscosity with percentage of added CNF for PG 70-28 asphalt binders.

5.2. Binder Bonding Strength test

The BBS tests were conducted on asphalt binder-aggregate samples which consisted of three types of asphalt binders, namely PG 58-28, PG 64-34, and PG 70-28 and three types of aggregates, namely granite, quartzite and gravel. Each of the tested binder was tested for three different composition, each binder was modified with 0%, 0.3%, and 0.7% CNF. The BBS tests were conducted on both moisture-conditioned and unconditioned samples.

Table 5.1 and Figure 5.7, 5.8, and 5.9 present a summary of the average bond tensile strength (ABTS) values obtained by conducting BBS tests on granite samples prepared with asphalt binders (PG 58-28, PG 64-34, and PG 70-28) without any CNF and those blended with 0.3% CNF and 0.7% CNF with and without moisture conditioning. Also, the BBS ratios calculated by dividing the ABTS values of moisture-conditioned samples to dry-conditioned ones. In addition, the failure modes, namely adhesive and cohesive, along

with the standard deviation (SD) and coefficient of variation (COV) values for BBS tests are presented in Table 5.1. Figure 5.10 shows the examples of failure mode determination.

Table 5.6: *Binder bond strength test results for various asphalt binders with granite.*

Granite										
Binder Type	**Additive**	**Dry -conditioned**				**Moisture Conditioned**				
		ABTS (kPa)	SD (%)	COV (%)	Failure Type (visual)	ABTS (kPa)	SD (%)	COV (%)	Failure Type (visual)	BBS Ratio (Wet/Dry)
PG 58-28	Neat (0%)	139.1	9.2	6.6	99% Cohesive	107.0	13.2	12.3	96% Cohesive	0.77
	0.3 % CNF	106.5	4.1	3.8	98% Cohesive	106.9	2.5	2.4	79% Cohesive	1.00
	0.7 % CNF	124.7	4.7	3.8	92% Cohesive	114.8	3.4	3.0	88% Cohesive	0.92
PG 64-34	Neat (0%)	62.9	6.4	10.2	97% Cohesive	54.4	2.7	4.9	85% Cohesive	0.87
	0.3 % CNF	74.7	7.8	10.4	96% Cohesive	56.9	1.8	3.2	79% Cohesive	0.76
	0.7 % CNF	106.7	7.3	6.9	99% Cohesive	88.9	9.4	10.6	70% Cohesive	0.83
PG 70-28	Neat (0%)	126.4	6.9	5.5	94% Cohesive	92.2	16.1	17.4	79% Adhesive	0.73
	0.3 % CNF	126.5	8.6	6.8	98% Cohesive	76.2	18.3	24.1	78% Adhesive	0.60
	0.7 % CNF	139.2	57.6	41.4	97% Cohesive	112.5	6.5	5.8	70% Cohesive	0.81

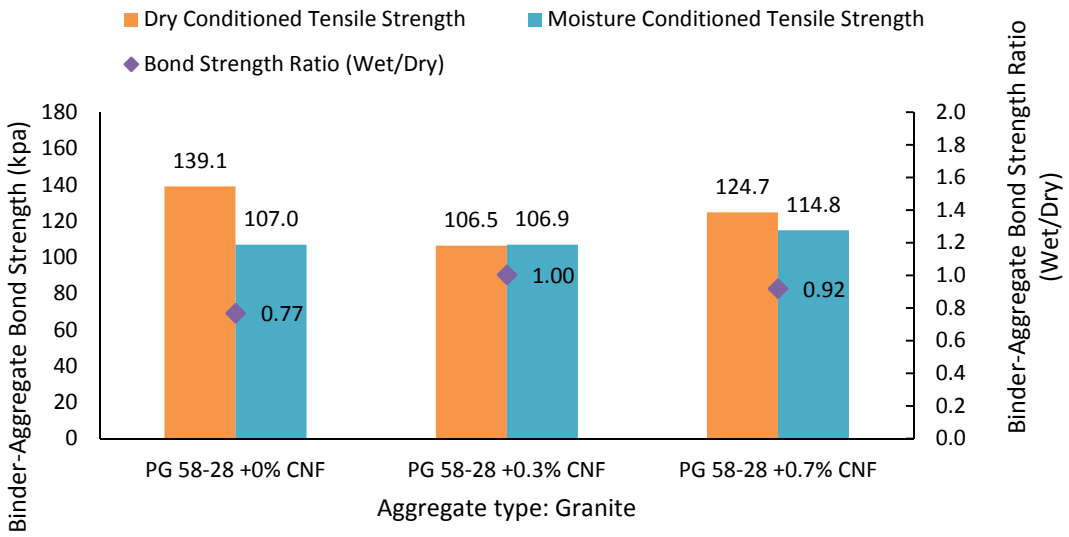

Figure 5.7: *Average bond- strength and BBS ratio for PG 58-28 on granite.*

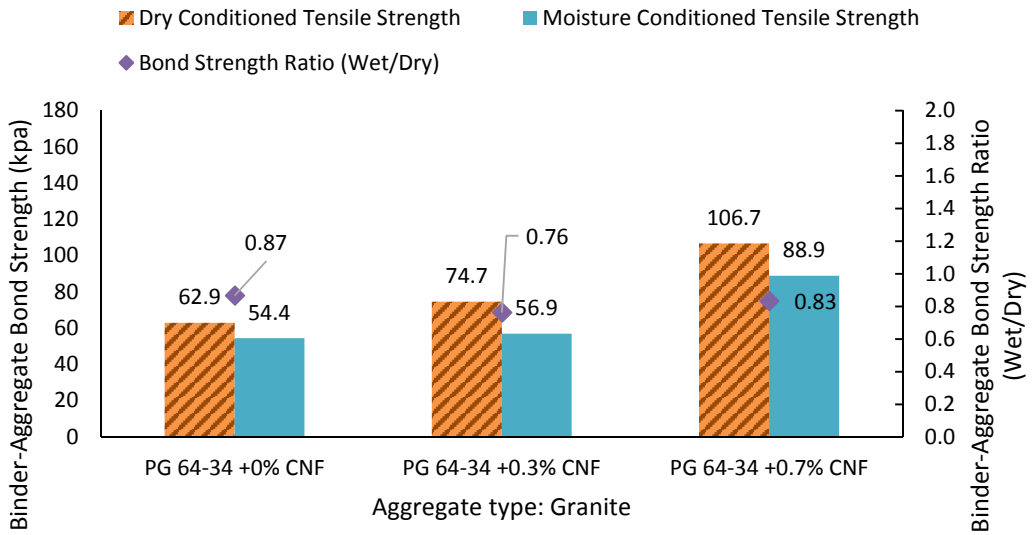

Figure 5.8*: Average bond- strength and BBS ratio for PG 64-34 on granite.*

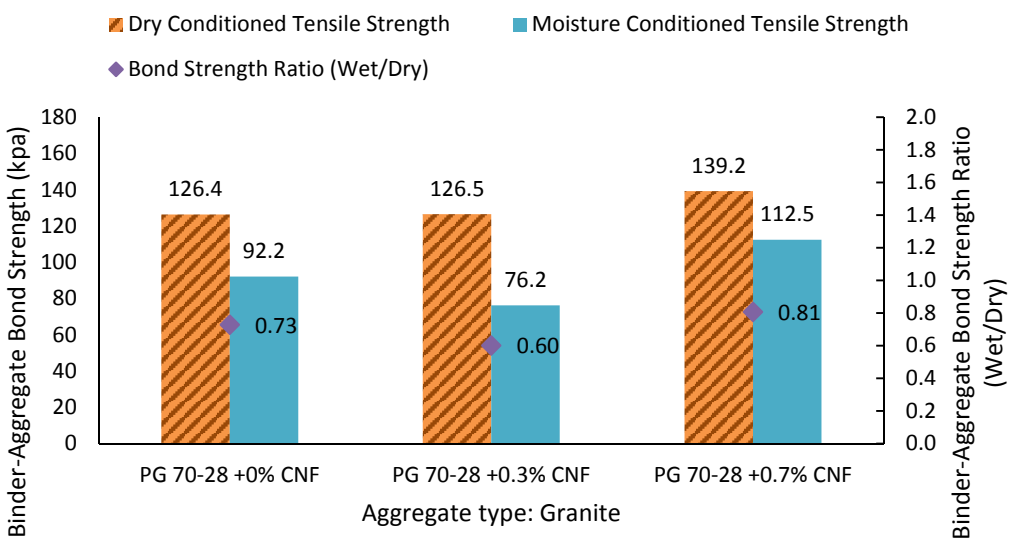

Figure 5.9: *Average bond- strength and BBS ratio for PG 70-28 on granite.*

From Table 5.1and Figures 5.7 it is evident that the dry conditioned average bond tensile strength of the neat PG 58-28 binder with granite (139.1 kPa) decreased (23.4% and 10.3%) as a result of addition of 0.3% and 0.7% Cellulose Nanofibers to the bend. Also, from Table 5.1 and Figure 5.7, it is evident that the moisture conditioned average bond tensile strength of the neat PG 58-28 binder with granite (107 kPa) remained almost unchanged (0.01% decrease) and increased (7.3%) as a result of addition of 0.3% and 0.7% CNF to the bend. In other words, the addition of Cellulose Nanofiber to the bend affected negatively the dry conditioned average bond tensile strength of the binder. Also, it did not significantly affect the adhesion of PG 58-28 binder to granite after moisture conditioning.

From Table 5.1and Figure 5.8 it is evident that the dry conditioned average bond tensile strength of the neat PG 64-34 binder with granite (62.9 kPa) increased (18.8% and 69.6%) as a result of addition of 0.3% and 0.7% Cellulose Nanofibers to the bend. Also, from Table 5.1 and Figure 5.8, it is evident that the moisture conditioned average bond tensile strength of the neat PG 56-34 binder with granite (54.4 kPa) increased (4.6% and 63.4%) as a result

of addition of 0.3% and 0.7% CNF to the bend. In other words, the addition of Cellulose Nanofiber to the bend significantly affected the adhesion of PG 58-28 binder to granite after dry and moisture conditioning.

From Table 5.1and Figure 5.9 it is evident that the dry conditioned average bond tensile strength of the neat PG 70-28 binder with granite (126.4 kPa) remained almost unchanged (0.08% increase) and increased (10.1%) as a result of addition of 0.3% and 0.7% CNF to the bend. Also, from Table 5.1 and Figure 5.9, it is evident that the moisture conditioned average bond tensile strength of the neat PG 70-28 binder with granite (92.2 kPa) decreased (17.4%) and increased (22%) as a result of addition of 0.3% and 0.7% CNF to the bend. In other words, the addition of Cellulose Nanofiber to the bend did not significantly affect the adhesion of PG 58-28 binder to granite after dry conditioning. Regarding the moisture conditioned, the addition of CNF affected negatively the ABTS when 0.3% CNF were added and affected positively the ABTS when 0.7% CNF were added.

In order to compare the effect of moisture-conditioning on the ABTS values, a parameter, namely binder bond strength (BBS) ratio was calculated by dividing the moisture conditioned ABTS to the dry conditioned ABTS for each asphalt binder blend-aggregate system tested herein. The BBS ratio is desirable to be higher in order to represent a mix with a better resistance to moisture induced damage. From Table 5.1 and Figure 5.7 it was found that the BBS ratio of neat PG 58-28 asphalt binder with granite (0.77) increased (29.9% and 19.5%) when of 0.3% and 0.7% CNF where added to the bend. From the Table 5.1 and Figure 5.8 it was found that the BBS ratio of neat PG 64-34 asphalt binder with granite (0.87) decreased (12.6% and 4.6%) when of 0.3% and 0.7% CNF where added to the bend. From Table 5.1 and Figure 5.9 it was found that the BBS ratio of neat PG 70-

28 asphalt binder with granite (0.73) decreased (17.8%) and increased (11%) when of 0.3% and 0.7% CNF where added to the bend.

It is important to notice that the failure mode was recorded based on the visual observation of the pictures taken from the failure surface after the BBS test. Figure 5.10 shows an example of adhesive failure and cohesive failure. On the left side of the picture is an example of an adhesive failure, when the asphalt binder fails to adhere to the aggregate. On the other hand, on the right side of the picture is the cohesive failure, when the asphalt binder fails in a cohesive way between the aggregate and the testing stub. From Table 5.1, the failure for all blends of the dry conditioned (PG 58-28, PG 64-34, and PG 70-28) binder-granite samples were found to be cohesive. Similarly, the failure mode for all blends of all the moisture conditions (PG58-28, PG64-34, and PG 70-28) binder-granite samples, excluding PG 70-28 0%CNF and PG 70-28 0.3% CNF, were also found to be cohesive. Enthought, the failure mode after moisture conditioned were found to be cohesive, the moisture conditioning had a detrimental effect on the adhesion of binder and aggregate. The percentages of cohesive failure decreases when comparing dry conditioned to moisture conditioned. For PG 70-28 0% CNF and PG 70-28 0.3% CNF the effects of the moisture had a bigger impact on the failure mode. For these two sets of test the failure mode went from cohesive (dry conditioned) to adhesive (moisture conditioned).

Figure 5.10*: Example of adhesive failure (left) and cohesive failure (right) in BBS test.*

Table 5.2 and Figure 5.11, 5.12, and 5.13 present a summary of the average bond-strength (ABS) values obtained by conducting BBS tests on quartzite samples prepared with asphalt binders (PG 58-28, PG 64-34, and PG 70-28) without any CNF and those blended with 0.3% CNF and 0.7% CNF with dry conditioned and moisture conditioning. Also, the BBS ratios calculated by dividing the ABS values of moisture-conditioned samples to those of dry ones. In addition, the failure modes, namely adhesive and cohesive, along with the standard deviation (SD) and coefficient of variation (COV) values for BBS tests are presented in Table 5.2.

Table 5 7*: Binder bond strength test results for various asphalt binders with granite.*

Quartzite										
Binder Type	Additive	Unconditioned				Moisture Conditioned				
		ABS (kPa)	SD (%)	COV (%)	Failure Type (visual)	ABS (kPa)	SD (%)	COV (%)	Failure Type (visual)	BBS Ratio (Wet/Dry)
PG 58-28	Neat (0%)	133.7	12.3	9.2	98% Cohesive	177.3	4.6	2.6	89% Cohesive	1.33
	0.3% CNF	115.9	7.9	6.8	98% Cohesive	144.0	2.3	1.6	88% Cohesive	1.24
	0.7% CNF	99.5	18.3	18.4	98% Cohesive	160.6	3.6	2.2	62% Cohesive	1.62
PG 64-34	Neat (0%)	60.0	7.5	12.5	96% Cohesive	56.2	5.5	9.7	96% Cohesive	0.94
	0.3% CNF	66.1	2.9	4.4	96% Cohesive	83.8	31.8	38.0	94% Cohesive	1.27
	0.7% CNF	105.0	43.1	41.0	97% Cohesive	133.5	50.7	38.0	94% Cohesive	1.27
PG 70-28	Neat (0%)	114.0	7.4	6.5	91% Cohesive	148.4	56.4	38.0	54% Cohesive	1.30
	0.3% CNF	104.6	3.5	3.4	95% Cohesive	121.0	10.8	8.9	92% Cohesive	1.16
	0.7% CNF	124.2	6.6	5.3	98% Cohesive	172.3	65.9	38.2	95% Cohesive	1.39

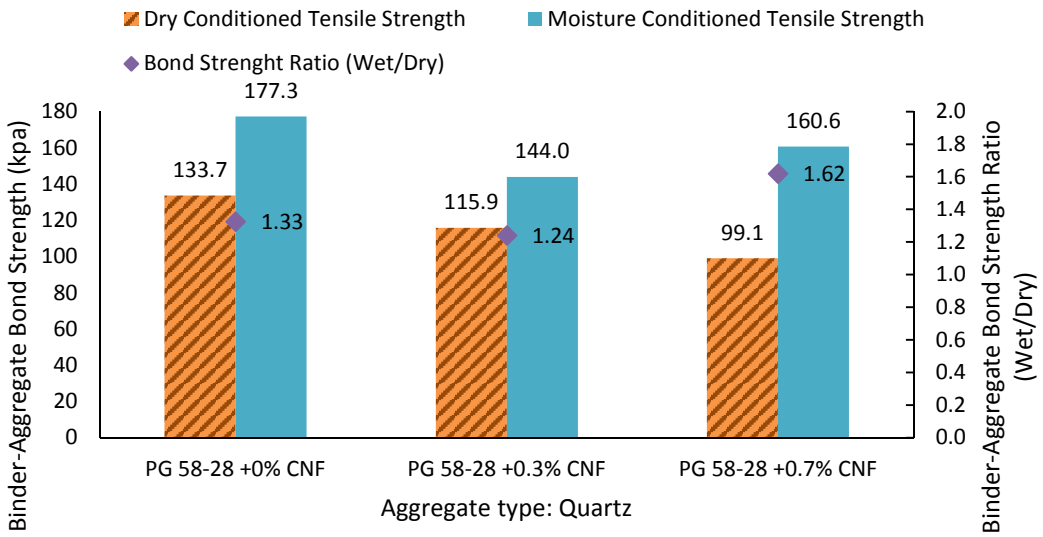

Figure 5.11: *Average bond- strength and BBS ratio for PG 58-28 on quartzite.*

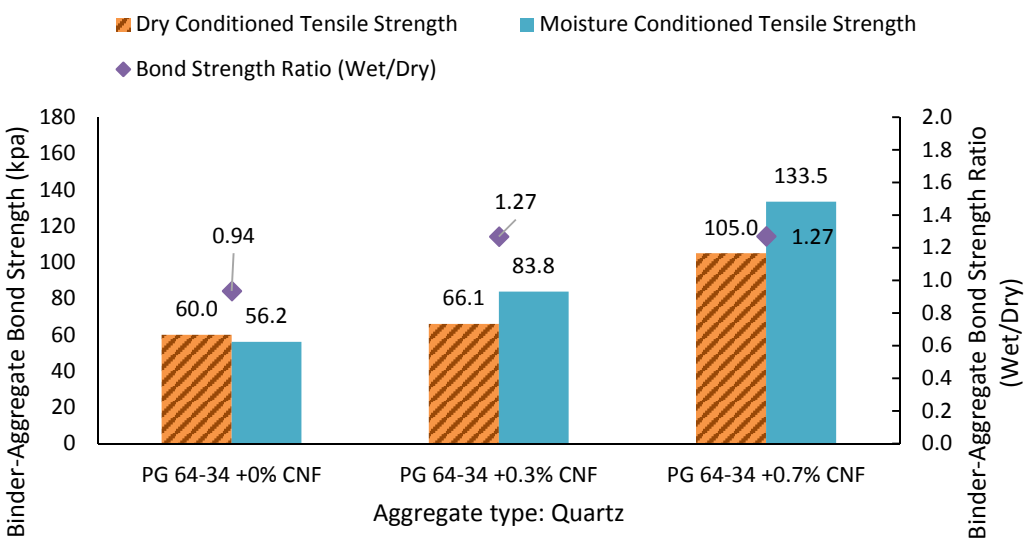

Figure 5.12*: Average bond- strength and BBS ratio for PG 64-34 on quartzite.*

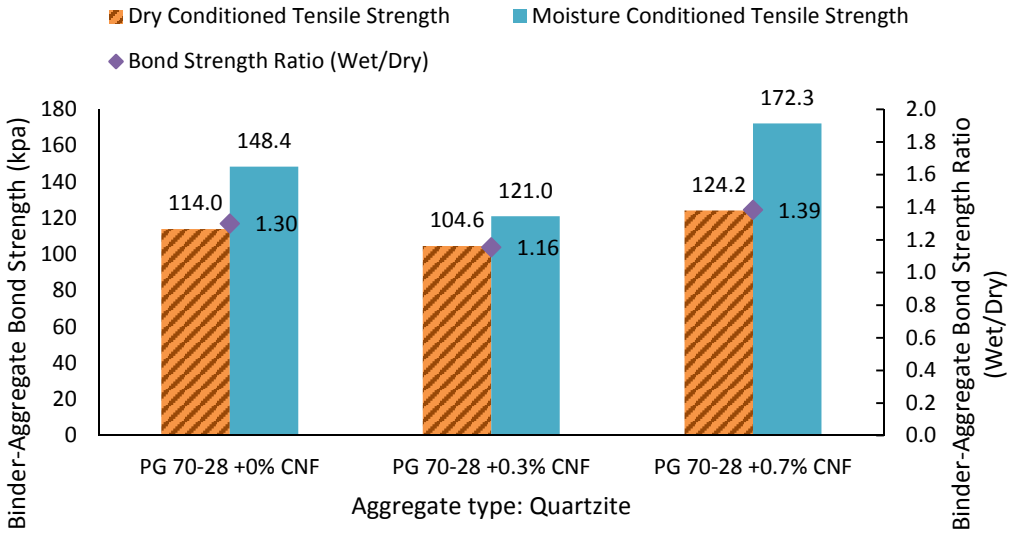

Figure 5.13: *Average bond- strength and BBS ratio for PG 70-28 on quartzite.*

From Table 5.2 and Figure 5.11 it is evident that the dry conditioned average bond tensile strength of the neat PG 58-28 binder with granite (133.7 kPa) decreased (13.3% and 25.6%) as a result of addition of 0.3% and 0.7% Cellulose Nanofibers to the bend. Also, from Table 5.2 and Figure 5.11, it is evident that the moisture conditioned average bond tensile strength of the neat PG 58-28 binder with granite (177.3 kPa) also decreased (18.8%

and 9.8%) as a result of addition of 0.3% and 0.7% CNF to the bend. In other words, the addition of Cellulose Nanofiber to the bend affected negatively both dry and moisture conditioned average bond tensile strength of the binder.

From Table 5.2and Figure 5.12 it is evident that the dry conditioned average bond tensile strength of the neat PG 64-34 binder with granite (60.0 kPa) increased (10.2% and 75%) as a result of addition of 0.3% and 0.7% CNF to the bend. Also, from Table 5.2 and Figure 5.11, it is evident that the moisture conditioned average bond tensile strength of the neat PG 64-34 binder with granite (56.2 kPa) increased (49.1% and 137.5%) as a result of addition of 0.3% and 0.7% CNF to the bend. In other words, the addition of Cellulose Nanofiber to the bend significantly affected the adhesion of PG 58-28 binder to granite after dry and moisture conditioning.

From Table 5.3and Figure 5.13 it is evident that the dry conditioned average bond tensile strength of the neat PG 70-28 binder with granite (114.0 kPa) decreased (8.4%) and increased (8.9%) as a result of addition of 0.3% and 0.7% Cellulose Nanofibers to the bend. Also, from Table 5.2 and Figure 5.13, it is evident that the moisture conditioned average bond tensile strength of the neat PG 70-28 binder with granite (148.4 kPa) decreased (18.5%) and increased (16.1%) as a result of addition of 0.3% and 0.7% CNF to the bend. In other words, the addition of Cellulose Nanofiber to the blend affected negatively the when 0.3% CNF was added both in dry and moisture conditioned. Also, the addition of Cellulose Nanofiber to the blend affected positively the ABTS when 0.7% CNF was added both in dry and moisture conditioned.

From Table 5.2 and Figure 5.11 it was found that the BBS ratio of neat PG 58-28 asphalt binder with granite (1.33) decreased (6.8%) and increased (21.8%) when of 0.3% and 0.7% CNF where added to the bend. From the Table 5.2 and Figure 5.12 it was found that the BBS ratio of neat PG 64-34 asphalt binder with granite (0.94) increased (35.1%) when of 0.3% and 0.7% CNF where added to the bend. From Table 5.2 and Figure 5.13 it was found that the BBS ratio of neat PG 70-28 asphalt binder with granite (1.3) decreased (10.8%) and increased (4.5%) when of 0.3% and 0.7% CNF where added to the bend.

From Table 5.2, the failure for all blends of the dry conditioned (PG 58-28, PG 64-34, and PG 70-28) binder-granite samples were found to be cohesive. Similarly, the failure mode for all blends of all the moisture conditions (PG58-28, PG64-34, and PG 70-28) binder-granite samples, were also found to be cohesive. Enthought, the failure mode after moisture conditioned were found to be cohesive, the moisture conditioning had a detrimental effect on the adhesion of binder and aggregate. The percentages of cohesive failure decreases when comparing dry conditioned to moisture conditioned.

Table 5.3 and Figure 5.14, 5.15, and 5.16 present a summary of the average bond-strength (ABS) values obtained by conducting BBS tests on gravel samples prepared with asphalt binders (PG 58-28, PG 64-34, and PG 70-28) without any CNF and those blended with 0.3% CNF and 0.7% CNF dry conditioned and moisture conditioned. Also, the BBS ratios calculated by dividing the ABS values of moisture-conditioned samples to those of dry conditioned ones. In addition, the failure modes, namely adhesive and cohesive, along with the standard deviation (SD) and coefficient of variation (COV) values for BBS tests are presented in Table 5.3.

Table 5.8: *Binder bond strength test results for various asphalt binders with gravel.*

Gravel										
Binder Type	Additive	Unconditioned				Moisture Conditioned				
		ABS (kPa)	SD (%)	COV (%)	Failure Type (visual)	ABS (kPa)	SD (%)	COV (%)	Failure Type (visual)	BBS Ratio (Wet/Dry)
PG 58-28	Neat (0%)	150.9	9.2	6.1	94% Cohesive	176.0	6.0	3.4	78% Cohesive	1.17
	0.3% CNF	93.4	15.7	16.8	95% Cohesive	108.9	5.9	5.4	85% Cohesive	1.17
	0.7% CNF	90.2	11.2	12.4	84% Cohesive	148.0	4.2	2.8	82% Cohesive	1.64
PG 64-34	Neat (0%)	59.5	3.1	5.3	94% Cohesive	57.2	4.0	7.0	89% Cohesive	0.96
	0.3% CNF	68.3	5.8	8.5	91% Cohesive	80.8	30.7	38.0	96% Cohesive	1.18
	0.7% CNF	116.4	6.7	5.8	99% Cohesive	134.2	6.1	4.5	97% Cohesive	1.15
PG 70-28	Neat (0%)	107.2	3.6	3.3	79% Cohesive	133.4	5.8	4.3	74% Cohesive	1.24
	0.3% CNF	109.8	7.7	7.0	93% Cohesive	143.3	13.8	9.6	86% Cohesive	1.31
	0.7% CNF	125.0	2.2	1.7	96% Cohesive	136.9	5.4	3.9	93% Cohesive	1.10

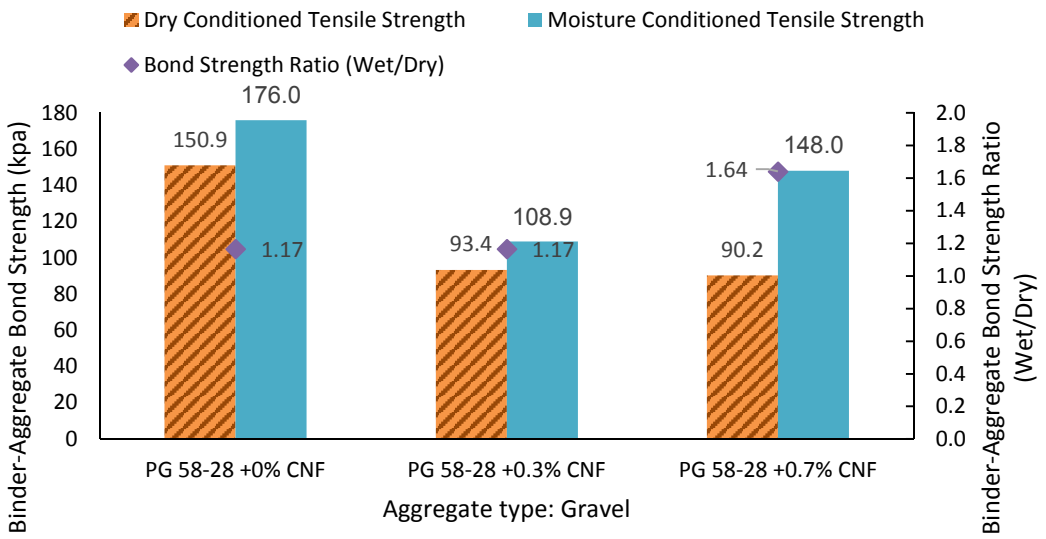

Figure 5.14: *Average bond- strength and BBS ratio for PG 58-28 on quartzite.*

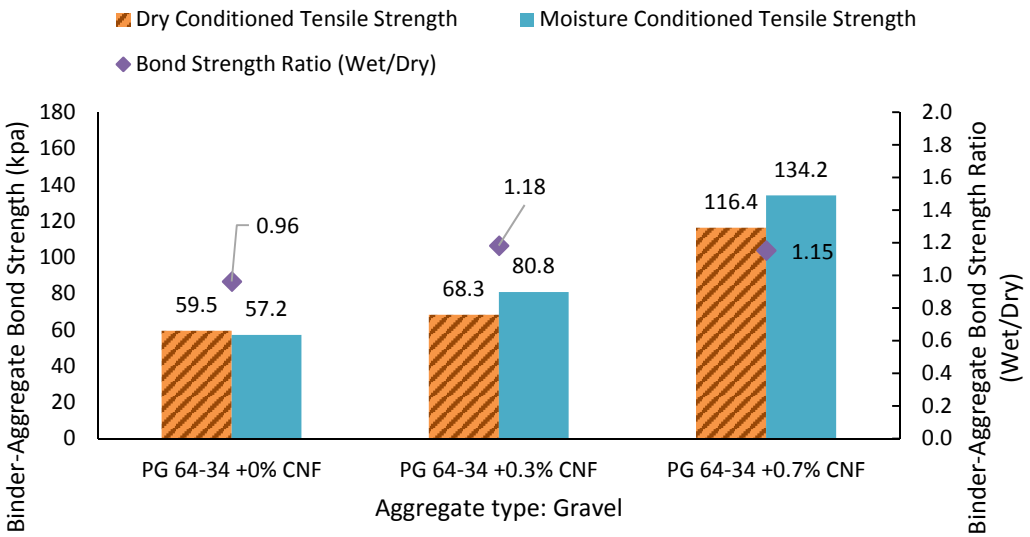

Figure 5.15: *Average bond- strength and BBS ratio for PG 64-34 on quartzite.*

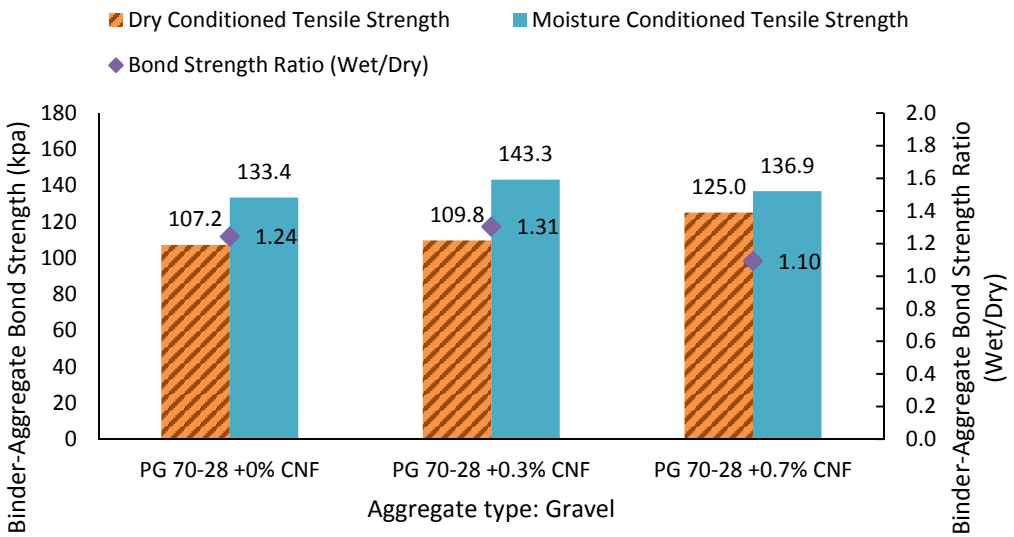

Figure 5.16*: Average bond- strength and BBS ratio for PG 70-28 on quartzite.*

From Table 5.3 and Figure 5.14 it is evident that the dry conditioned average bond tensile strength of the neat PG 58-28 binder with granite (150.9 kPa) decreased (38.1% and 40.2%) as a result of addition of 0.3% and 0.7% Cellulose Nanofibers to the bend. Also, from Table 5.2 and Figure 5.14, it is evident that the moisture conditioned average bond tensile strength of the neat PG 58-28 binder with granite (176.0 kPa) also decreased (38.1%

and 15.9%) as a result of addition of 0.3% and 0.7% CNF to the bend. In other words, the addition of Cellulose Nanofiber to the bend affected negatively both dry and moisture conditioned average bond tensile strength of the binder.

From Table 5.3 and Figure 5.15 it is evident that the dry conditioned average bond tensile strength of the neat PG 64-34 binder with granite (59.5 kPa) increased (14.8% and 95%) as a result of addition of 0.3% and 0.7% Cellulose Nanofibers to the bend. Also, from Table 5.3 and Figure 5.15, it is evident that the moisture conditioned average bond tensile strength of the neat PG 64-34 binder with granite (57.2 kPa) increased (41.3% and 134.6%) as a result of addition of 0.3% and 0.7% CNF to the bend. In other words, the addition of Cellulose nNanofiber to the bend significantly affected the adhesion of PG 58-28 binder to granite after dry and moisture conditioning.

From Table 5.3 and Figure 5.16 it is evident that the dry conditioned average bond tensile strength of the neat PG 70-28 binder with granite (107.2 kPa) increased (2.5% and 16.6%) as a result of addition of 0.3% and 0.7% Cellulose Nanofibers to the bend. Also, from Table 5.3 and Figure 5.16, it is evident that the moisture conditioned average bond tensile strength of the neat PG 70-28 binder with granite (133.4 kPa) increased (7.4% and 2.6%) as a result of addition of 0.3% and 0.7% CNF to the bend. In other words, the addition of CNF to the bend significantly affected the adhesion of PG 58-28 binder to granite after dry and moisture conditioning.

From Table 5.3 and Figure 5.14 it was found that the BBS ratio of neat PG 58-28 asphalt binder with granite (1.17) remained unchanged and increased (40.2%) when of 0.3% and 0.7% CNF where added to the bend. From the Table 5.3 and Figure 5.15 it was

found that the BBS ratio of neat PG 64-34 asphalt binder with granite (0.96) increased (22.9% and 19.8%) when of 0.3% and 0.7% CNF where added to the bend. From Table 5.3 and Figure 5.16 it was found that the BBS ratio of neat PG 70-28 asphalt binder with granite (1.24) increased (5.6%) and decreased (11.3%) when of 0.3% and 0.7% CNF where added to the bend.

From Table 5.3, the failure for all blends of the dry conditioned (PG 58-28, PG 64-34, and PG 70-28) binder-granite samples were found to be cohesive. Similarly, the failure mode for all blends of all the moisture conditions (PG58-28, PG64-34, and PG 70-28) binder-granite samples, were also found to be cohesive. Enthought, the failure mode after moisture conditioned were found to be cohesive, the moisture conditioning had a detrimental effect on the adhesion of binder and aggregate. The percentages of cohesive failure decreased when comparing dry conditioned to moisture conditioned. The only combination that the cohesive failure did not decrease was for PG 64-34 with 0.3% CNF, the cohesive failure increased from 91% to 96%.

The BBS test results clearly shows that the adhesion of the asphalt binder and aggregates in dry and moisture condition can be affected by the binder type and the aggregate mineralogy. When comparing the BBS ratio of the tested aggregates it was found that quartzite has the largest average value of the BBS ratio. When taking into consideration all the tested combination, it was found that the average BBS ratio value for quartzite was 1.28, which is 5.2% larger than the average BBS ratio value for gravel and 36.7% larger than the average BBS ratio value for granite. When comparing the three tested binder for all the aggregates tested it was found that PG 58-28 had the largest average BBS ratio value. It was found that the average BBS ratio value for PG 58-28 was 1.2, which is 15.7%

larger than PG 64-34 and 11.6% larger than PG 70-28. Based on that, the combination of quartzite and PG 58-28 resulted on a better resistance to moisture-induced damage. Regarding the addition of Cellulose Nanofiber to the asphalt binder, the results showed a promising trend that the Cellulose Nanofibers improved the moisture susceptibility of the asphalt binder. The addition of the CNF to PG 58-58 resulted on the highest BBR ration for each aggregate tested. PG 58-28 with 0.7% CNF was found to have a BBR ratio of 1.62, PG 58-28 with 0.7% CNF was found to have a BBR ratio of 1.64, and PG 58-28 with 0.3% CNF was found to have a BBR ratio of 1.00. These results showed that the addition of Cellulose Nanofiber to the asphalt binder is beneficial to the resistance of the moisture-induced failure of the asphalt.

Adhesion is known to play an important role in determining the durability of a mix in the field (Zhang et al., 2017). The effect of moisture on asphalt is recognized as the major cause of asphalt failure. To maximize adhesion asphalt binder and aggregates need to be chosen based on aggregate minerology, surface texture of aggregate, bitumen chemistry, and the compatibility between bitumen and aggregate (Zhang et al., 2017). Based on the BBS test results, quartzite showed to have a lower moisture absorption than granite and gravel, which resulted in better moisture resistance. The results indicate that the moisture susceptibility of the asphalt binder is strongly dependent on the aggregate chemistry (Xu and Wang, 2016). In addition, the moisture susceptibility of the asphalt could be improved with the addition of Cellulose Nanofibers, improving the asphalt durability.

5.3. Izod Impact Strength Test

Figures 5.17 present the results of the Izod impact strength test conducted on the unaged unmodified (0% CNF), and unaged modified (0.2% CNF, 0.3% CNF 0.5% CNF and 0.7%

CNF) on PG 58-28, PG 64-34 and PG 70-28 binders, respectively. The test results presented on the figures 5.17 are based on the temperature and on the thickness (-11° C and 12mm) which all the combinations of asphalt binder and CNF were tested. From the Figures 5.17, it is evident that the mean impact energy of all the three asphalt binders tested increased with the increasing in quantity of added CNF on the ashalt binder.

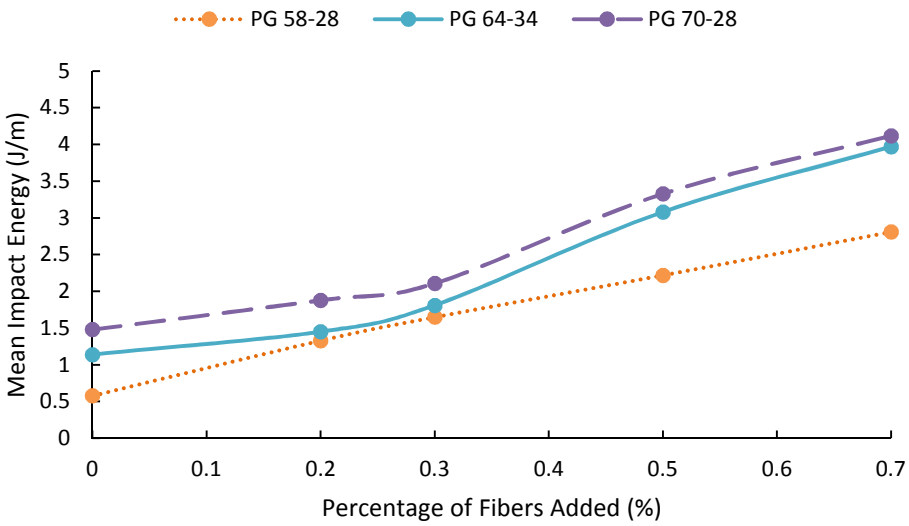

Figure 5.17*: Mean Impact Energy for asphalt binder modified with different concentrations of Cellulose Nanofibers tested at -11°C.*

Figures 5.17 present the results of the Izod impact strength test conducted on PG 58-28, PG 64-34 and PG 70-28 binders, respectively. The figure shows the effect of the CNF on the impact energy value for each tested asphalt binder. From the Figures 5.17, it is evident that the mean impact energy of all the three asphalt binders tested increased with the increasing percentage of added CNF. For PG 58-28 the impact energy increased from 0.58 J/m at 0% CNF to 1.33 J/m (129.3% increase) at 0.2% CNF, to 1.65 J/m (184.5% increase) at 0.3% CNF, to 2.22 J/m (282.8% increase) at 0.5% CNF, and to 2.81 J/m (384.5% increase) at 0.7% CNF. For PG 64-34 the impact energy increased from 1.14 J/m

at 0% CNF to 1.45 J/m (27.2% increase) at 0.2% CNF, to 1.81 J/m (58.8% increase) at 0.3% CNF, to 3.08 J/m (170.2% increase) at 0.5% CNF, and to 3.97 J/m (248.2% increase) at 0.7% CNF. For PG 70-28 the impact energy increased from 1.48 J/m at 0% CNF to 1.88 J/m (27% increase) at 0.2% CNF, to 2.11 J/m (42.6% increase) at 0.3% CNF, to 3.33 J/m (125% increase) at 0.5% CNF, and to 4.12 J/m (178.4% increase) at 0.7% CNF.

Impact strength is the resistance of the material to fracture by a blow, expressed in terms of amount of energy absorbed before fracture. The amount of energy absorbed by an asphalt mix corelates to its fatigue life (Shen et al., 2010). With a higher energy absorption by the asphalt, better will be its fatigue life resistance. A higher absorption of energy the asphalt binder means that the asphalt binder is more flexible and can resist more loading and deformation before failing. It is known that polymer modified asphalt binders (PG 64-34 and PG 58-28) have a higher fatigue life than non-modified asphalt binder (PG 58-28) (Toraldo and Mariani, 2014). The results from Izod impact strength test analysis shows throughout the impact energy values that PG 70-28 and PG 64-34 has a higher fatigue life than PG 58-28.

The mean impact energy results for PG 58-28 shows that the addition of Cellulose Nanofibers could be a replacement of the polymers from PG 64-34 and PG 70-28. The addition of 0.2% CNF on PG 58-28 resulted in an impact energy of 1.33 J/m which is 16.7% higher than the impact energy of the neat PG 64-34. Also, the addition of 0.3% CNF on PG 58-28 resulted in an impact energy of 1.65 J/m which is 11.5% higher than the impact energy of the neat PG 70-28. These results mean that the addition of Cellulose Nanofiber in non-modified asphalt binder could substitute the use of polymers to modify the asphalt binders with the goal to improve their properties. The results showed that a PG

58-28 + 0.2% CNF could behave in a similar way of a neat PG 64-34 and a PG 58-28 +0.3% CNF could behave in a similar way of a neat PG 78-28. These findings add relevant information to the study. However more tests and a deep study on the asphalt binders mixed with Cellulose Nanofiber behaving like polymer modified asphalt binder is necessary to fully conclude the find presented on the study. Although not proved, these findings could represent the beginning of the utilization of an environmentally friendly material to modify the asphalt binder with the goal to improve its properties, such as fatigue life.

CHAPTER SIX: TEST RESULTS OF ASPHALT MIXES

This chapter presents the SCB, TSR, and HWT test results conducted on asphalt mixes that were modified with the addition of Cellulose Nanofibers. Three different asphalt mixes were tested, namely RAP20+0%CNF, RAP20+0.3%CNF, and RAP20+0.7%CNF. Each asphalt binder was tested according to ASTM D8044, AASHTO T283, and AASHTO T324 respectively. A comprehensive analysis of the test results is also presented. Furthermore, the suitability of using CNF as additives in asphalt mixes was evaluated.

6.1. Semi-Circular Bend (SCB) Test Results

The SCB tests were conducted on three asphalt mixes to obtain and compare their cracking resistance through determining the critical strain energy release rate (J_c) for each mix. Also, to determine the effect of the addition of Cellulose Nanofibers on the asphalt mix. According to the test standard followed, ASTM D8044 (ASTM, 2016), the J_c values of 0.5 kJ/m^2 to 0.6 kJ/m^2 are typically the acceptable value for the resistance to cracking for asphalt mixes. Based on that, in order to exhibit a better resistance to cracking a higher strain energy release rate is desirable. Table 6.1 and Figure 6.1 present the critical strain energy release (J_c) values calculated for RAP20+0%CNF, RAP20+0.3%CNF, and RAP20+0.7%CNF.

Table 6.9*:Critical strain energy release rate (J_c) from SCB test.*

Mix	Percent of Fibers Added (%)	Average Sample Thickness (m)	J_c (kJ/m^2)
RAP20 + 0%CNF	0	0.058	0.53
RAP20 + 0.3%CNF	0.3	0.058	0.72
RAP20 + 0.7%CNF	0.7	0.058	0.98

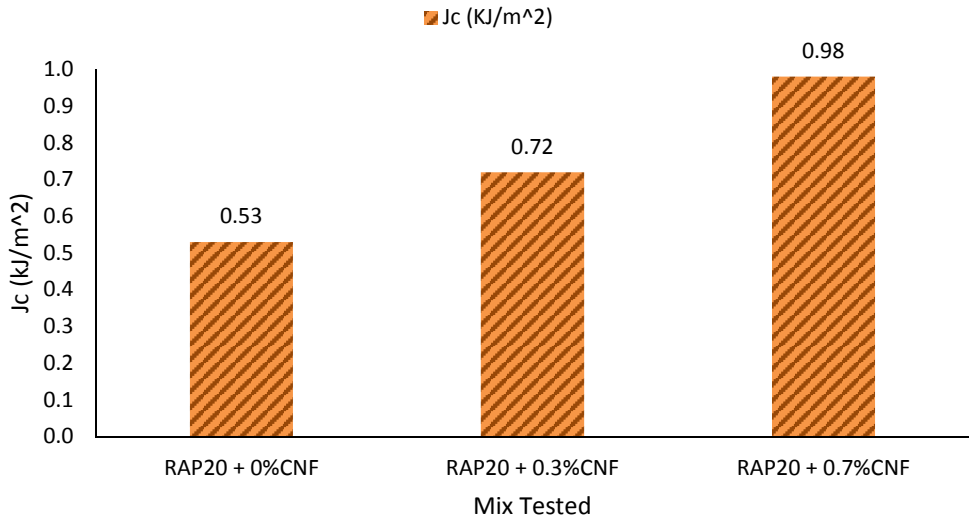

Figure 6.1: *Critical strain energy release rate (J_c) from SCB test.*

From Table 6.1 and Figure 6.1 it is evident that, the critical strain energy rate (J_c) was found to increase by 35.8% when 0.3% CNF was added to the RAP20 mix and by 84.9% when 0.7 CNF was added to the asphalt mix. In other words, the critical strain energy rate increases from 0.53 kJ/m^2 to 0.72 kJ/m^2 and 0.98 kJ/m^2 for RAP20+0.3%CNF and RAP20+0.7%CNF, respectively, meaning that the addition of Cellulose Nanofibers improved the performance of the asphalt mix tested.

The Semi-Circular Bend test is a mechanical test suitable to predict and evaluate the fatigue cracking resistance of an asphalt mix (Barman et al., 2018, Arabani and Ferdowsi, 2009, and Kim et al.,2012). The results for all three asphalt mixes tested are within or higher than the range accepted by the ASTM D8044 (ASTM, 2016), meaning that all tested asphalt mix have an accepted resistance to fatigue cracking. Analyzing the three tested mix the RAP20+0.7%CNF was found to have the higher J_c value. Hence, RAP20+0.7%CNF has a higher fatigue cracking resistance. Overall, the higher the J_c value, the higher the fatigue cracking resistance ((Barman et al., 2018).

6.2. Tensile Strength Ratio (TSR) Test Results

The TSR test was conducted on three asphalt mixes to obtain and compare their resistance to moisture-induced damage through determining the tensile strength ratio for each mix. Also, to determine the effect of the addition of Cellulose Nanofibers on the asphalt mix. The Tensile Strength Ratio values were calculated by dividing the moisture conditions average tensile strength by the unconditioned average tensile strength. According to AASHTO Superpave mix design specification the minimum requirement for TSR is equal or larger than 0.8 (AASHTO, 2012). The TSR and tensile strengths of the three different asphalt mixes (RAP20+0%CNF, RAP20+0.3%CNF, and RAP20+0.7%CNF) tested are presented in Table 6.2 and Figure 6.2.

Table 6.10:*Tensile strength ratio (TSR) test results*

Mix	Percent of Added fibers (%)	Unconditioned Average Tensile Strength (psi)	Conditioned Average Tensile Strength (psi)	Tensile Strength Ratio (TSR)
RAP20+ 0%CNF	0	126.5	108.5	0.86
RAP20 + 0.3%CNF	0.3	138.1	91.8	0.66
RAP20 + 0.7%CNF	0.7	156.3	112.5	0.72

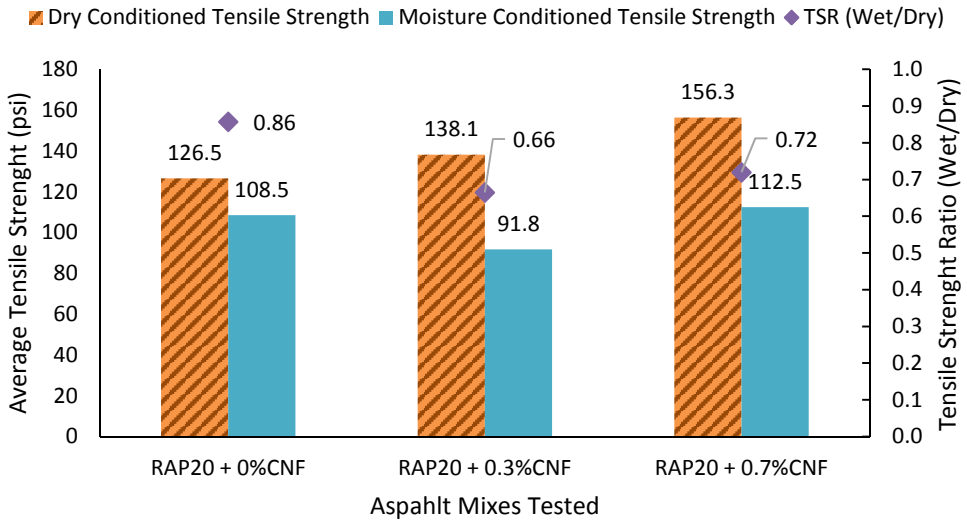

Figure 6.2: *TSR test results for all the tested asphalt mixes.*

From Table 6.2 and Figure 6.2, the average tensile strength values for RAP20+0%CNF, RAP20+0.3%CNF, and RAP20+0.7%CNF were found to be 126.5psi, 138.1psi, and 156.3psi, respectively. The results showed that the addition of 0.3% and 0.7% of CNF to the asphalt mix improve the average tensile strength by 9.2% and 23.6% respectively. After moisture conditioned the average tensile strength values for RAP20+0%CNF, RAP20+0.3%CNF, and RAP20+0.7%CNF were found to be 108.5 psi, 91.8 psi, and 112.5psi, respectively. The results showed that the addition of 0.7% CNF to the asphalt mix improved the average tensile strength value by 3.7%. However, it was found that the addition of 0.3% of CNF decrease the average tensile strength of the asphalt mix by 15.4%.

In order to verify the resistance to moisture-induced damage, the TSR was calculated for all tested asphalt mixes. The ratio calculated indicate the extent of the moisture-induced damage effect of on loss of tensile strength of the mixes. From Figure 6.2, the TSR values for RAP20+0%CNF, RAP20+0.3%CNF, and RAP20+0.7%CNF were

found to be 0.86, 0.66, and 0.72. The results show that the TSR value decrease by 23.3% and 16.3% with the addition of 0.3% CNF and 0.7% CNF respectively. Only the TSR value for RAP20+0%CNF was greater than 0.8, indicating its satisfactory resistance to moisture-induced damage. The other two mixes, RAP20+0.3%CNF, and RAP20+0.7%CNF had a TSR value lower than 0.8, which indicates that they are moisture susceptible.

Overall, the results of the TSR test shows that the addition of Cellulose Nanofibers decreased the TSR ratio, meaning that the mixes RAP20+0.3%CNF, and RAP20+0.7%CNF are more susceptible to moisture-induced damage. However, an important information was found after the TSR test was performed on the asphalt mixes containing Cellulose Nanofiber. The addition of fibers improves the unconditioned tensile strength of the asphalt mixes. It was also found that the addition of 0.7%CNF improved the moisture conditioned tensile strength of the asphalt mixes. Even though, the TSR values decrease the average tensile strength increased. The reason why the TSR values decreased with the addition of cellulose nanofiber is that the unconditioned tensile strength increases in a higher rate than the moisture conditioned tensile strength. Based on the improvement of the tensile strength of the asphalt mixed with the addition of CNF, the asphalt mixes RAP20+0.3%CNF, and RAP20+0.7%CNF could also be considered to have a satisfactory resistance to moisture-induced damage. From the TSR test is not possible to conclude that the addition of fibers improved the performance of the asphalt mix.

6.3. Hamburg Wheel Tracking (HWT) Test Results

The Hamburg Wheel Tracking test was conducted on samples produced for this study, in accordance with AASTHO T324 (AASHTO,2014). The test was conducted on three asphalt mixes (RAP20+0%CNF, RAP20+0.3%CNF, and RAP20+0.7%CNF) to obtain and

compare their rutting susceptibility and moisture-induced damage potential. In this method, two cylindrical samples were cut to fit in the plastic molds of the HWT machine. In this study, the HWT test was conducted on specimens submerged in water at 50°C. The loading cycles consisted of up to 20,000 wheel passes and the rut depth consisted of up to 20mm. Deformations were measured along the length of the wheel path at 11 equally-spaced points. The wheel passes and deformation at the mid-point (Point 6) of the sample was considered for further analysis. From the HWT test results, rut depth, post compaction deformation, creep slope (rate), striping slope, and stripping inflection point (SIP) were determined. Each asphalt mix was tested twice, and the average of the results was used for further evaluation. Figure 6.3 presents the average rut depth with respect to wheel passes for all of the tested asphalt mixes. The rut depths at 1000, 2500, 5000, 7500, 10000, 12500, 15000, 17500, and 20000 passes for RAP20+0%CNF, RAP20+0.3%CNF, and RAP20+0.7%CNF are presented in Table 6.3. Table 6.4 shows the performance parameter of tested asphalt mixes that were obtained from the HWT test.

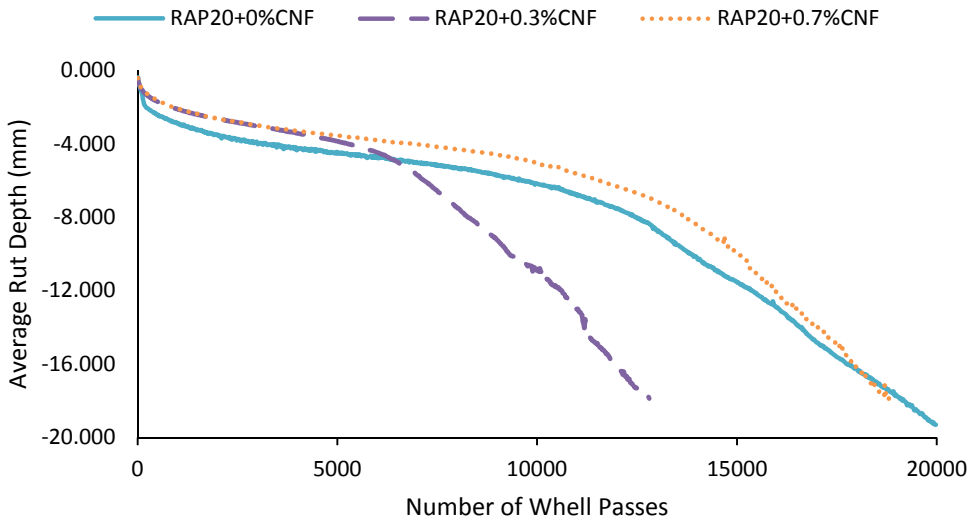

Figure 6.3: *Hamburg Wheel Tracking test results for tested asphalt mixes.*

Table 6.11: *Rut Depths of tested asphalt mixes at different number of passes.*

Tested Asphalt Mix	Wheel Passes						
	1000	4000	8000	10000	12000	16000	20000
RAP 20+0%CNF	2.866	4.352	5.306	6.177	7.521	12.907	19.3
RAP 20+0.3%CNF	2.09	3.413	7.444	10.877	16.004	x	x
RAP 20+0.7%CNF	2.0759	3.2974	4.2872	5.0393	6.3027	12.071	x

Table 6.12: *Performance parameters of tested asphalt mixes obtained from the HWT test results.*

Tested Asphalt Mixes	Performance Parameter obtained from HWT test					
	Post-Compaction (mm)	**Creep Slope (mm/pass)**	**Creep Slope (passes/mm)**	**Stripping Inflection Point**	**Stripping Slope (mm/passes)**	**Stripping Slope (passes/mm)**
RAP 20+0%CNF	2.866	-0.0003	-3333.3	11883	-0.0015	-666.7
RAP 20+0.3%CNF	2.09	-0.0004	-2500.0	6840	-0.0022	-454.5
RAP 20+0.7%CNF	2.0759	-0.003	-333.3	12944	-0.0019	-526.3

The HWT test was conducted on three asphalt mixes to obtain and compare their resistance to moisture-induced damage through determining the rut depth and stripping inflection point for each mix. Figure 6.3 shows the average rut depth with respect to the wheel passes for all of the tested asphalt mixes. The rut depth used for analysis is the average between the mid-point (Point 6) of the two samples tested for all the asphalt mixes. The reason for using the average values for Point 6 is because it will reduce the variance, improve the reliability, and because the maximum deformation is more likely to be in the middle part of specimen (Guo and Prozzi, 2009). The rut depths at 1000, 4000, 8000,

10000, 12000,16000, and 20000 passes are presented on Table 6.3. According to Figure 6.3 and Table 6.3, RAP 20+0%CNF was the only mix that resist to 20000 passes, it was found that the rut depth at 20000 was 19.3mm. The other two mixes (RAP 20+0.3%CNF and RAP 20+0.7%CNF) react the deformation of 20mm before the 20000 passes. In addition, all of the three tested mixes exhibit moisture-induced damage during the test. Therefore, stripping inflection points were observed.

The important performance parameters were determined from the HWT test results and can be found on Table 6.4. The post-compaction deformation is defined as the instantaneous deformation just after the test was started, it simulates the densification of asphalt mix owing to the initial trafficking. The post-compaction rut depth was determined after 1000-wheel passes (Yildirim and Kennedy, 2020). The creep slope is defined as the rut depth per wheel pass in the creep region, which is the rut progression after the post compaction point, representing the rutting due to plastic flow. The stripping slope is defined as the rut depth per wheel pass after the stripping point until the final wheel pass. The striping inflection point (SIP) is used to characterize the moisture-induced damage of the asphalt mix, it determines the point where the moisture start to damage the asphalt mix. For the study purpose, the creep and stripping slopes were defined as the number of passes per unit of rut depth.

The three tested asphalt mixes are compared to examine the effects of the addition of Cellulose Nanofibers on the asphalt mix in the asphalt rut performance. From Figure 6.3 and Table 6.3 is evident that the RAP 20+0.7%CNF exhibited a lower rut depth and a higher stripping inflection point when compared to the other two mixes. The lower rut

depth and higher SIP means that RAP 20+0.7%CNF exhibit a higher resistance to moisture-induced damaged. Analyzing only the rut depth, the addition of CNF to the asphalt mix resulted in a more resistance asphalt. Taking into consideration only the rutting behavior, before any damage due to moisture the Cellulose Nanofiber indeed helped with the rutting resistance of the asphalt. At 4000 passes, RAP 20+0%CNF has a rut depth of 4.532mm with is 21.6% higher than RAP 20+0.3%CNF (3.413mm) and 24.2% higher than RAP 20+0.7%CNF (3.2974). When taking into consideration the resistance to moisture induced damage, the SIP values need to be analyzed. RAP 20+0.7%CNF had a SIP value of 12944 passes which is higher than RAP 20+0%CNF and RAP 20+0.3%CNF, which have a SIP value of 6840 passes (89.2% increase) and 11883 passes (8.9% increase) respectively.

From the HWT test results it was evident that the addition of CNF improves the rutting performance of the asphalt mix. However, it was also evident that the amount of CNF added to the asphalt mix matters. The addition of 0.3% CNF helped with the rut performance, but it exhibits a low SIP value, meaning that is susceptible to moisture induce damage with less passes than the other samples. While the RAP 20+0.3%CNF showed a low moisture induced damage resistance, RAP 20+0.7%CNF showed to perform better in terms of rutting performance and it is more resistant to moisture induced damaged. Overall RAP 20+0.7%CNF is expected to perform better in terms of rutting performance and resistance of moisture induced damage.

The HWT test results raised a question regarding the amount of fibers that need to be added to improve the performance of the asphalt mix. Clearly, the addition of 0.3% CNF

was not enough to improve the performance, it made the performance of the asphalt mix worse. One way to verify if the performance of an asphalt mix with 0.3%CNF was consistently detrimental is to compare the results of HWT with the TSR and the BBS. When comparing all the tests it was positive that the performance of an asphalt mix with 0.3%CNF is tends to be worse than the performance of the same asphalt mix with 0%CNF and much worse than the performance of the same asphalt mix with 0.7% CNF. A few exceptions can be seen when comparing the BBS ratio to the results found after the HWT test and TSR test. The exceptions could be due to the fact that the Cellulose Nanofibers is a material that is very complicate to deal with and due to the high variability when the CNF are being mixed on the asphalt. The addition of only 0.3%CNF on the asphalt binder and asphalt mix could result and internal voids or breakage of interlinks that allow moisture induced damage. On the other hand, the addition of at least 0.7%CNF on asphalt could result in new interlink and less voids, resulting in a better performance of the asphalt. To fully conclude why 0.3%CNF decrease the performance of asphalt and 0.7% CNF improve the performance of asphalt more in depth study and laboratory test are necessary. The goal of the future studies is to analyze what happens internally on the asphalt binder and asphalt mix when Cellulose Nanofibers are added.

CHAPTER SEVEN: CONCLUSION AND RECOMENDATION

7.1. Conclusion

The production through electrospinning technique and addition of Cellulose Nanofiber on asphalt binder and mix with the goal of improving performance characteristics of asphalt binder and mix were evaluated. The experimental plans comprised of production and evaluation of Cellulose Nanofiber, evaluation of asphalt binder modified with 0% CNF, 0.3% CNF, and 0.7% CNF, and evaluation of asphalt mix modified with 0% CNF, 0.3% CNF, and 0.7%CNF.

The evaluation of the electrospun CNF consisted of Laser Scan Microscopy, used to evaluate roughness and entanglement, Scanning Electron microscopy, used to evaluate the morphological characteristics, and Tensile Strength test, used to evaluate the tensile strength of the CNF. Five different types of solutions were evaluated, namely solution 1 (Cellulose Acetate + Acetone), solution 2(Cellulose Acetate + Acetic Acid), solution 3 (Cellulose Acetate + Acetic acid/Water), solution 4 (Cellulose Acetate + Acetic acid/Acetone), and solution 5 (Cellulose Acetate + Acetone/Water). After having their roughness, diameter and tensile strength evaluated, Solution 5 was chosen to be solution used to electrospin the fibers that were added to the asphalt binder and asphalt mix.

Solution 5 showed to be the rougher one, the LSM test could not be done on samples produced with solution 5 due to its roughness, no image was captured because the distance between the top layer and bottom layer of the CNF was higher than the scope of the microscopy.. Solution 5, through analyze of SEM images, showed to have the larger diameter. It was found that the average diameter of Solution 5 was 1.756 μm, which is

353.8% higher than the second largest average diameter (Solution 1, 0.387 μm). Regarding the tensile strength, each solution was tested in two different ways, that was due to the inefficiency of the electrospinning technique (rotating and static electrospinning techniques) to produced alignment fibers. The fibers were tested on production way and cross-production way for both techniques used to produce fibers. Solution 5 was found to have the highest tensile strength when produced with static electrospinning and tested at a cross-production way. Based on the results, Solution 5 was chosen to be used to electrospun the CNF that were used to be added in the asphalt materials. Together with the solution the static electrospinning and cross-production way was chosen for the production of the fibers. The cross-production direction for the static electrospinning is defined as the opposite direction of the collector plate orientation.

The evaluation of Cellulose Nanofibers asphalt binder consisted of Rotational viscometer test, used to evaluate the viscosity of the material, Izod impact strength test, used to evaluate the impact energy release, and Binder Bond Strength test, used to evaluate the adhesion of asphalt binder and aggregate. Three different asphalt binder were used for evaluation, namely PG 58-28, PG 64-34, and PG 70-28. Each of the three asphalt binders were modified with 0%, 0.3%, and 0.7% Cellulose Nanofiber and evaluated. Overall, the CNF altered the performance of the asphalt binder when comparing the neat asphalt binder with the ones containing Cellulose Nanofiber.

Regarding the rotational viscometer test, the viscosity for the three tested binders increased with the increase of added CNF. The results indicate that the asphalt binder gets thicker with the addition of CNF, meaning more compaction efforts are required in the field.

Regarding the Izod impact strength test, the addition of CNF increases the mean impact energy of the asphalt binder for all the tested binders. The amount of energy releases correlates to the fatigue life of the asphalt, meaning that the higher the impact energy the higher is the fatigue life of the pavement. One important finding from the Izod impact strength test was that the addition of Cellulose Nanofibers improved the characteristics of the asphalt binder; one example was that a PG58-28 with 0.2% binder had a similar impact energy as a PG 64-34 without any CNF. A hypothesis is that a non-polymer modified asphalt binder could perform the same as a polymer modified asphalt, depending of the quantity of CNF added to the non-polymer modified asphalt binder.

Regarding the binder bon strength test, it was evident that the adhesion of the asphalt binder and aggregates in dry and moisture condition can be affected by the binder type and the aggregate mineralogy. Based on that the addition of CNF on the asphalt binder was analyzed based on the aggregate type. For Granite, PG 58-28 was found to have the largest BBS ratio, which consists of the ratio between the moisture conditioned samples and the non-conditioned samples. So, when analyzing the addition of CNF for PG 58-28 on granite the BBS ratio increased with the addition of CNF. It was found that the addition of 0.3% CNF resulted in a higher BBS ratio that 0.7% CNF. For Quartzite, PG 58-28 also was found to have the largest BBS ratio. It was found that the addition of 0.3% CNF decreases the BBS ratio while the addition of 0.7% CNF increases the BBS ratio. For Gravel, PG 58-28 was found to have the highest BBS ratio. This time the addition of 0.3% CNF resulted on the same BBS ratio as the neat binder, while the addition of 0.7% CNF increased the BBS ratio. Overall, PG 58-28 was found to have the highest BBS ratio from all the aggregates tested. Also, the highest BBS ratio were obtained when CNF were added.

The evaluation of Cellulose Nanofibers asphalt mix consisted of semi-circular bend test, used for evaluation of cracking resistance through determining the critical strain energy release rate (J_c), tensile strength ratio test, used to evaluate the resistance to moisture-induced damage, and Hamburg wheel tracking test, used to evaluate the resistance to rutting. A mix of asphalt containing HMA mix with a PG 58-28 asphalt binder, mainly quartzite and granite-II aggregates, 20% RAP (RAP20), and with a nominal maximum aggregate size (NMAS) of 12.5mm was used for the study. Three different asphalt mixes were tested, one containing 0% CNF, other containing 0.3% CNF, and another one containing 0.7% CNF.

Regarding the SCB test, the addition of Cellulose Nanofiber on the asphalt mix affected the critical strain energy release rate (J_c). It was found the J_c increased with the increase on the added CNF. RAP 20+0.7% CNF was found to be the higher resistance to fatigue cracking, once the energy released is related to the fatigue life of the asphalt mix.

Regarding the TSR test, it was found that the TSR ratio decreased with the addition of CNF. Even though the TSR ratio decreases it was found that the unconditioned tensile strength increases with the addition of CNF. The higher the amount of CNF the higher was the unconditioned tensile strength of the mix. On the other hand, the moisture tensile strength was found to have a similar result for the RAP20+0.7% CNF but a different one for the RAP20 +0.3%CNF. It was found that the conditioned tensile strength decreased with the addition of 0.3%CNF but increased with the addition of 0.7%CNF. Overall, even though the TSR ratio decrease, it can be considered that the addition of Cellulose Nanofibers on the asphalt mix improved the moisture induced damaged, at least for a minimum of 0.7% CNF.

Regarding the HWT test, it was found that the addition of Cellulose Nanofibers caused the asphalt mix to fail before the 20,000-wheel passes. Only the RAP20+0%CNF achieved the mark of 20,000 passes. When comparing the rut depth at the same point and the stripping point, it was found the RAP20+0.7% CNF had the lowest rut depth and the higher stripping point. That means that the addition of CNF had an effect on the asphalt mix. The results showed that the asphalt was stronger, and more resistant to rutting and moisture damage when 0.7% CNF was added. On the other hand, the results for when 0.3% CNF was added are completely the opposite. Similarly, to the TSR results the addition of 0.3% CNF decrease the resistance to moisture induced damage and, on this case, decrease the stripping point and increase the rutting depth of the asphalt mix. It was found that the RAP20+0.3%CNF was the worst and the RAP20+0.7%CNF was the best asphalt mix, meaning that an optimum amount of Cellulose Nanofibers needs to be added for the asphalt mix to start performing better that a neat asphalt mix.

7.2. Recommendation

A number of recommendations for the future research were made based on the findings and discussion of this study, as follows:

i. It is recommended that a future study evaluate the different methods of electrospinning Cellulose Nanofibers, to optimize the production of CNF and specially to produce align CNF. Cellulose Nanofibers that are produced in a certain alignment could possibly improve even more the performance of the asphalt mix. So far, the production of CNF is limited due to the difficulty of mass production and all the variable that goes to producing CNF using electrospinning technique,

like voltage, distance to collector, concentration of Cellulose and especially which solvent to use.

ii. Following the same though, the solvent is extremely important for the CNF production. It can define the roughness, diameter and tensile strength of the CNF, as was proved on the study. However, all the solvents tested on the study had at least one problem. One example, was the acetone that has a low evaporation temperature, causing the solution to clogs at the tip of the needle causing the interruption of the continuous electrospin of the CNF. Water was a solution for that problems, as well as solvent systems. However even with the water the solution was not continuously electrspoun. Based on that future research is necessary on the solvent field.

iii. One point that needs future research on id the mixture procedure of CNF onto the asphalt mix and asphalt binder. A procedure needs to be estipulate to avoid human intervention. The mixture of the CNF on the asphalt mix was made by hand, which could have made the CNF not evenly dispersed on the asphalt mix. The lack of certain that the CNF are evenly dispersed in the asphalt mix could be avoided if a procedure is estipulate for that. Mixing CNF by hand could cause the results to be dependent on the person who performed the mixture.

iv. Future binder evaluation studies are necessary to evaluate if a non-polymer modified binder could perform the same way a polymer modified asphalt binder only by the addition of Cellulose Nanofibers. The results for the Izod impact strength test showed that the addition of CNF on asphalt binder made it in some

way comparable to another asphalt binder. Chemical and morphological analyze needs to be done to fully prove the hypothesis presented on this study.

v. One important finding on the study was the fact that the addition of 0.3% CNF made the asphalt mix and most of the time the asphalt binder to be more susceptible to moisture induced damage than a neat asphalt mix and asphalt binder. In depth study on the chemical reaction of the Cellulose Nanofiber with the asphalt binder and mix is necessary to understand why that happened. It is unknow why that happened from the tests performed on this study. The tests performed on this study had similar results regarding the decrease in moisture induced damage when 0.3% CNF was added. However, the tested failed to answer why that could be happening.

vi. Based on the fact that 0.3% CNF decreases the moisture induced resistance of the asphalt mix and binder and 0.7% CNF increased the moisture induced damage of the asphalt mix and binder teste. Future studies are necessary to determine the optimum amount of Cellulose Nanofiber that need to be added for the asphalt mix start performing better.

REFERENCES

AASHTO. (2012). Superpave Volumetric Mix Design. American Association of State Highway and Transportation Officials, Washington, DC, USA.

AASHTO T 283 (2010). Standard Method of Test for Resistance of Compacted Asphalt Mixtures to Moisture-Induced Damage. American Association of State Highway and Transportation Officials, Washington, D.C.

AASHTO T 316 (2013). Standard Method of Test for Viscosity Determination of Asphalt Binder Using Rotational Viscometer. American Association of State Highway and Transportation Officials, Washington, D.C.

AASHTO T 324 (2014). Standard Method of Test for Hamburg Wheel-Track Testing of Compacted Hot Mix Asphalt (HMA). American Association of State Highway and Transportation Officials, Washington, D.C.

AASHTO TP 105 (2013). Standard Method of Test for Determining the Fracture Energy of Asphalt Mixtures Using the Semicircular Bend Geometry (SCB). American Association of State Highway and Transportation Officials, Washington, D.C.

AASHTO TP XX (2011). Standard Method of Test for Determining Asphalt Binder Bond Strength by Means of the Bitumen Bond Strength (BBS)Test. American Association of State Highway and Transportation Officials, Washington, D.C.

Ahmad, J., Yusoff, N. I. M., Hainin, M. R., Rahman, M. Y. A., & Hossain, M. (2014). Investigation into hot-mix asphalt moisture-induced damage under tropical climatic

conditions. *Construction and Building Materials*, *50*, 567–576. doi: 10.1016/j.conbuildmat.2013.10.017

Airey, G. D. (2004). Fundamental Binder and Practical Mixture Evaluation of Polymer Modified Bituminous Materials. *International Journal of Pavement Engineering*, *5*(3), 137–151. doi: 10.1080/10298430412331314146

Anderson, D. A. (1994). *Binder Characterization and Evaluation*. Washington, DC: Strategic Highway Research Program, National Research Council.

Arabani, M., & Ferdowsi, B. (2009). Evaluating the Semi-Circular Bending Test for HMA Mixtures. *IJE Transactions A: Basics*, *22*(1), 47–58.

ASTM. (2016). D 8044-16 Standard Test Method for Evaluation of Asphalt Mixture Cracking Resistance using the Semi-Circular Bend Test (SCB) at Intermediate Temperatures1. In ASTM International, 100 Barr Harbor Drive, PO Box C700, West Conshohocken, PA

ASTM. (2018). D 256-18 Standard Test Methods for Determining the Izod Pendulum Impact Resistance of Plastics. In ASTM International, 100 Barr Harbor Drive, PO Box C700, West Conshohocken, PA

Barman, M., Ghabchi, R., Singh, D., Zaman, M., & Commuri, S. (2018). An alternative analysis of indirect tensile test results for evaluating fatigue characteristics of asphalt mixes. *Construction and Building Materials*, *166*, 204–213. doi: 10.1016/j.conbuildmat.2018.01.049

Becker, Y., Méndez, M. P., & Rodríguez, Y. (2001). Polymer Modified Asphalt. *Vision Tecnologica*, *9*(1), 39–50.

Bernier, A., Zofka, A., & Yut, I. (2012). Laboratory evaluation of rutting susceptibility of polymer-modified asphalt mixtures containing recycled pavements. *Construction and Building Materials*, *31*, 58–66. doi: 10.1016/j.conbuildmat.2011.12.094

Chen, J.-S., Liao, M.-C., & Tsai, H.-H. (2002). Evaluation and optimization of the engineering properties of polymer-modified asphalt. *Practical Failure Analysis*, *2*(3), 75–83. doi: 10.1007/bf02719194

Chen, X., & Huang, B. (2008). Evaluation of moisture damage in hot mix asphalt using simple performance and superpave indirect tensile tests. *Construction and Building Materials*, *22*(9), 1950–1962. doi: 10.1016/j.conbuildmat.2007.07.014

Colbert, B., & You, Z. (2012). The properties of asphalt binder blended with variable quantities of recycled asphalt using short term and long term aging simulations. *Construction and Building Materials*, *26*(1), 552–557. doi: 10.1016/j.conbuildmat.2011.06.057

Collins, J. H., Bouldin, M. G., Gelles, R., & Berker, A. (1991). *Interpretation of dynamic mechanical test data for paving grade asphalt cements*. St. Paul, MN: Association of Asphalt Paving Technologists.

Cong, P., Zhang, Y., & Liu, N. (2016). Investigation of the properties of asphalt mixtures incorporating reclaimed SBS modified asphalt pavement. *Construction and Building Materials*, *113*, 334–340. doi: 10.1016/j.conbuildmat.2016.03.059

Daniel, J. S., Pochily, J. L., & Boisvert, D. M. (2010). Can More Reclaimed Asphalt Pavement be Added? *Transportation Research Record: Journal of the Transportation Research Board*, *2180*(1), 19–29. doi: 10.3141/2180-03

El-Latief, R. A. E. A. (2018). Asphalt Modified with Biomaterials as Eco-Friendly and Sustainable Modifiers. *Modified Asphalt*. doi: 10.5772/intechopen.76832

Elseifi, M. A., Flintsch, G. W., & Al-Qadi, I. L. (2003). Quantitative Effect of Elastomeric Modification on Binder Performance at Intermediate and High Temperatures. *Journal of Materials in Civil Engineering*, *15*(1), 32–40. doi: 10.1061/(asce)0899-1561(2003)15:1(32)

Fakhri, M., & Hosseini, S. A. (2017). Laboratory evaluation of rutting and moisture damage resistance of glass fiber modified warm mix asphalt incorporating high RAP proportion. *Construction and Building Materials*, *134*, 626–640. doi: 10.1016/j.conbuildmat.2016.12.168

Fischer, S., Thümmler, K., Volkert, B., Hettrich, K., Schmidt, I., & Fischer, K. (2008). Properties and Applications of Cellulose Acetate. *Macromolecular Symposia*, *262*(1), 89–96. doi: 10.1002/masy.200850210

Frey, M. W. (2008). Electrospinning Cellulose and Cellulose Derivatives. *Polymer Reviews*, *48*(2), 378–391. doi: 10.1080/15583720802022281

Ghabchi, R., Singh, D., & Zaman, M. (2014). Evaluation of moisture susceptibility of asphalt mixes containing RAP and different types of aggregates and asphalt binders using the

surface free energy method. *Construction and Building Materials*, *73*, 479–489. doi: 10.1016/j.conbuildmat.2014.09.042

Ghabchi, R., Singh, D., & Zaman, M. (2015). Laboratory evaluation of stiffness, low-temperature cracking, rutting, moisture damage, and fatigue performance of WMA mixes. *Road Materials and Pavement Design*, *16*(2), 334–357. doi: 10.1080/14680629.2014.1000943

Ghabchi, R., Singh, D., Zaman, M., & Hossain, Z. (2015). Laboratory characterisation of asphalt mixes containing RAP and RAS. *International Journal of Pavement Engineering*, *17*(9), 829–846. doi: 10.1080/10298436.2015.1022778

Ghabchi, R., Barman, M., Singh, D., Zaman, M., & Mubaraki, M. A. (2016). Comparison of laboratory performance of asphalt mixes containing different proportions of RAS and RAP. *Construction and Building Materials*, *124*, 343–351. doi: 10.1016/j.conbuildmat.2016.07.029

Gong, W., Tao, M., Mallick, R. B., & El-Korchi, T. (2012). Investigation of Moisture Susceptibility of Warm-Mix Asphalt Mixes through Laboratory Mechanical Testing. *Transportation Research Record: Journal of the Transportation Research Board*, *2295*(1), 27–34. doi: 10.3141/2295-04

Guo, R., & Prozzi, J. A. (2009). A Statistical Analysis of Hamburg Wheel Tracking Device Testing Results. *Road Materials and Pavement Design*, *10*(SI), 327–335. doi: 10.3166/rmpd.10hs.327-335

Han, S. O., Youk, J. H., Min, K. D., Kang, Y. O., & Park, W. H. (2008). Electrospinning of cellulose acetate nanofibers using a mixed solvent of acetic acid/water: Effects of solvent composition on the fiber diameter. *Materials Letters*, *62*(4-5), 759–762. doi: 10.1016/j.matlet.2007.06.059

Hansen, K. R., and Copeland, A. (2013). Annual Asphalt Pavement Industry Survey on Recycled Material and Warm-Mix Asphalt Usage: 2009–2012. *No. IS-138*, *National Asphalt Pavement Association*, 5100 Forbes Blvd., Lanham, MD 20706.

Hong, F., Chen, D.-H., & Mikhail, M. M. (2010). Long-Term Performance Evaluation of Recycled Asphalt Pavement Results from Texas. *Transportation Research Record: Journal of the Transportation Research Board*, *2180*(1), 58–66. doi: 10.3141/2180-07

Huang, B., Shu, X., Dong, Q., & Shen, J. (2010). Laboratory Evaluation of Moisture Susceptibility of Hot-Mix Asphalt Containing Cementitious Fillers. *Journal of Materials in Civil Engineering*, *22*(7), 667–673. doi: 10.1061/(asce)mt.1943-5533.0000064

Joel Co., Scanning Electron Microscope (SEM) Products, *JEOL Ltd.*, www.jeol.co.jp/en/products/list_sem.html; Last Accessed: May 22, 2020.

Kakar, M. R., Hamzah, M. O., & Valentin, J. (2015). A review on moisture damages of hot and warm mix asphalt and related investigations. *Journal of Cleaner Production*, *99*, 39–58. doi: 10.1016/j.jclepro.2015.03.028

Khattak, M. J., Khattab, A., & Rizvi, H. R. (2011). Mechanistic Characteristics of Asphalt Binder and Asphalt Matrix Modified with Nano-Fibers. *Geo-Frontiers 2011*. doi: 10.1061/41165(397)492

Khattak, M. J., Khattab, A., Rizvi, H. R., & Zhang, P. (2012). The impact of carbon nano-fiber modification on asphalt binder rheology. *Construction and Building Materials*, *30*, 257–264. doi: 10.1016/j.conbuildmat.2011.12.022

Kim, M., Mohammad, L. N., Challa, H., & Elseifi, M. A. (2015). A simplified performance-based specification for asphalt pavements. *Road Materials and Pavement Design*, *16*(sup2), 168–196. doi: 10.1080/14680629.2015.1077005

Kim, S., Sholar, G. A., Byron, T., and Kim, J. (2009). Performance of Polymer- Modified Asphalt Mix with Reclaimed Asphalt Pavement.*Transportation Research Record: Journal of the Transportation Research Board, 2126(1),* 109-114.

Kim, Y.-R. (2011). Cohesive zone model to predict fracture in bituminous materials and asphaltic pavements: state-of-the-art review. *International Journal of Pavement Engineering*, *12*(4), 343–356. doi: 10.1080/10298436.2011.575138

Kim, Y.-R., Zhang, J., & Ban, H. (2012). Moisture damage characterization of warm-mix asphalt mixtures based on laboratory-field evaluation. *Construction and Building Materials*, *31*, 204–211. doi: 10.1016/j.conbuildmat.2011.12.085

Kumar, P., Mehndiratta, H. C., & Singh, K. L. (2010). Comparative Study of Rheological Behavior of Modified Binders for High-Temperature Areas. *Journal of Materials in Civil Engineering*, *22*(10), 978–984. doi: 10.1061/(asce)mt.1943-5533.0000099

Li, D., & Xia, Y. (2004). Electrospinning of Nanofibers: Reinventing the Wheel? *Advanced Materials*, *16*(14), 1151–1170. doi: 10.1002/adma.200400719

Li, R., Xiao, F., Amirkhanian, S., You, Z., & Huang, J. (2017). Developments of nano materials and technologies on asphalt materials – A review. *Construction and Building Materials*, *143*, 633–648. doi: 10.1016/j.conbuildmat.2017.03.158

Liu, H., & Hsieh, Y.-L. (2002). Ultrafine fibrous cellulose membranes from electrospinning of cellulose acetate. *Journal of Polymer Science Part B: Polymer Physics*, *40*(18), 2119–2129. doi: 10.1002/polb.10261

Lu, X., & Isacsson, U. (1997). Influence of styrene-butadiene-styrene polymer modification on bitumen viscosity. *Fuel*, *76*(14-15), 1353–1359. doi: 10.1016/s0016-2361(97)00144-0

Moghadas Nejad, F., Aflaki, E., & Mohammadi, M. A. (2010). Fatigue behavior of SMA and HMA mixtures. *Construction and Building Materials*, *24*(7), 1158–1165. doi: 10.1016/j.conbuildmat.2009.12.025

Mohammad, L. N., Kim, M., & Elseifi, M. (2012, 2012//). Characterization of Asphalt Mixture's Fracture Resistance Using the Semi-Circular Bending (SCB) Test. *Paper presented at the 7th RILEM International Conference on Cracking in Pavements*, Dordrecht.

Moraes, R., Velasquez, R., & Bahia, H. U. (2011). Measuring the Effect of Moisture on Asphalt–Aggregate Bond with the Bitumen Bond Strength Test. *Transportation Research Record: Journal of the Transportation Research Board*, *2209*(1), 70–81. doi: 10.3141/2209-09

Nikon instruments Inc., Nikon Develops Enhanced C2 plus Confocal Microscope." *Nikon Instruments Inc.*, www.microscope.healthcare.nikon.com/about/news/nikon-develops-enhanced-c2-plus-confocal-microscope; Last accessed: May 22, 2020.

Ozer, H., Al-Qadi, I. L., Lambros, J., El-Khatib, A., Singhvi, P., & Doll, B. (2016). Development of the fracture-based flexibility index for asphalt concrete cracking potential using modified semi-circle bending test parameters. *Construction and Building Materials*, *115*, 390–401. doi: 10.1016/j.conbuildmat.2016.03.144

Read, J., & Whiteoak, D. (2003). *Shell Bitumen Handbook* (5th ed.). London: Thomas Telford Publishing.

Reyes-Ortiz, O., Berardinelli, E., Alvarez, A., Carvajal-Muñoz, J., & Fuentes, L. (2012). Evaluation of Hot Mix Asphalt Mixtures with Replacement of Aggregates by Reclaimed Asphalt Pavement (RAP) Material. *Procedia - Social and Behavioral Sciences*, *53*, 379–388. doi: 10.1016/j.sbspro.2012.09.889

Sargand, S. M., and Kim, S. S. (2001). Performance Evaluation of Polymer Modified and Unmodified Superpave Mixes. In *Second International Symposium on Maintenance and Rehabilitation of Pavements and Technological Control*, Auburn, AL.

Shen, S., Chiu, H.-M., & Huang, H. (2010). Characterization of Fatigue and Healing in Asphalt Binders. *Journal of Materials in Civil Engineering*, *22*(9), 846–852. doi: 10.1061/(asce)mt.1943-5533.0000080

Singh, D., Chitragar, S. F., & Ashish, P. K. (2017). Comparison of moisture and fracture damage resistance of hot and warm asphalt mixes containing reclaimed pavement

materials. *Construction and Building Materials*, *157*, 1145–1153. doi: 10.1016/j.conbuildmat.2017.09.176

Smit, E., Bűttner, U., & Sanderson, R. D. (2005). Continuous yarns from electrospun fibers. *Polymer*, *46*(8), 2419–2423. doi: 10.1016/j.polymer.2005.02.002

Son, W. K., Youk, J. H., Lee, T. S., & Park, W. H. (2003). Electrospinning of ultrafine cellulose acetate fibers: Studies of a new solvent system and deacetylation of ultrafine cellulose acetate fibers. *Journal of Polymer Science Part B: Polymer Physics*, *42*(1), 5–11. doi: 10.1002/polb.10668

Subbiah, T., Bhat, G. S., Tock, R. W., Parameswaran, S., & Ramkumar, S. S. (2005). Electrospinning of nanofibers. *Journal of Applied Polymer Science*, *96*(2), 557–569. doi: 10.1002/app.21481

Toraldo, E., & Mariani, E. (2014). Effects of polymer additives on bituminous mixtures. *Construction and Building Materials*, *65*, 38–42. doi: 10.1016/j.conbuildmat.2014.04.108

Tungprapa, S., Puangparn, T., Weerasombut, M., Jangchud, I., Fakum, P., Semongkhol, S., … Supaphol, P. (2007). Electrospun cellulose acetate fibers: effect of solvent system on morphology and fiber diameter. *Cellulose*, *14*(6), 563–575. doi: 10.1007/s10570-007-9113-4

Wen, H., Bhusal, S., & Wen, B. (2013). Laboratory Evaluation of Waste Cooking Oil-Based Bioasphalt as an Alternative Binder for Hot Mix Asphalt. *Journal of Materials in Civil Engineering*, *25*(10), 1432–1437. doi: 10.1061/(asce)mt.1943-5533.0000713

Wen, H., Wu, S., Mohammad, L. N., Zhang, W., Shen, S., & Faheem, A. (2016). Long-Term Field Rutting and Moisture Susceptibility Performance of Warm-Mix Asphalt Pavement. *Transportation Research Record: Journal of the Transportation Research Board*, *2575*(1), 103–112. doi: 10.3141/2575-11

West, R., Kvasnak, A., Tran, N., Powell, B., & Turner, P. (2009). Testing of Moderate and High Reclaimed Asphalt Pavement Content Mixes. *Transportation Research Record: Journal of the Transportation Research Board*, *2126*(1), 100–108. doi: 10.3141/2126-12

Xiao, F., Jordan, J., & Amirkhanian, S. N. (2009). Laboratory Investigation of Moisture Damage in Warm-Mix Asphalt Containing Moist Aggregate. *Transportation Research Record: Journal of the Transportation Research Board*, *2126*(1), 115–124. doi: 10.3141/2126-14

Xiao, F., Amirkhanian, S., Wang, H., & Hao, P. (2014). Rheological property investigations for polymer and polyphosphoric acid modified asphalt binders at high temperatures. *Construction and Building Materials*, *64*, 316–323. doi: 10.1016/j.conbuildmat.2014.04.082

Xu, G., & Wang, H. (2016). Study of cohesion and adhesion properties of asphalt concrete with molecular dynamics simulation. *Computational Materials Science*, *112*, 161–169. doi: 10.1016/j.commatsci.2015.10.024

Yang, X., You, Z., & Dai, Q. (2013). Performance Evaluation of Asphalt Binder Modified by Bio-Oil Generated from Waste Wood Resources. *International Journal of Pavement Research and Technology*, *6*(4), 431–439.

Yildirim, Y. (2007). Polymer modified asphalt binders. *Construction and Building Materials*, *21*(1), 66–72. doi: 10.1016/j.conbuildmat.2005.07.007

Zhang, J., Airey, G. D., Grenfell, J., & Apeagyei, A. K. (2017). Moisture damage evaluation of aggregate–bitumen bonds with the respect of moisture absorption, tensile strength and failure surface. *Road Materials and Pavement Design*, *18*(4), 833–848. doi: 10.1080/14680629.2017.1286441